DISSERTATION

submitted to the

Combined Faculties for the Natural Sciences and for Mathematics

of the Ruperto-Carola University of Heidelberg, Germany

for the degree of

Doctor of Natural Sciences

presented by

Dipl.-Ing. (BA) Franziska Faulstich, M.Sc.

born in Bad Salzungen

Oral examination:

……..

Generation and evaluation of chimeric particles consisting of HPV16 L1 and $p16^{INK4a}$ for second generation HPV vaccines

Referees:

Prof. Dr. Martin Müller

Prof. Dr. Magnus von Knebel-Doeberitz

The work described in this thesis was started in January 2011 and completed in March 2014 under the supervision of Prof. Dr. Magnus von Knebel-Doeberitz at the department of Applied Tumor Biology at the Institute of Pathology, University of Heidelberg in cooperation with the German Cancer Research Center (DKFZ), Heidelberg.

Acknowledgements

I owe my most sincere gratitude to Prof. Magnus von Knebel Doeberitz, head of the department of Applied Tumor Biology at the Institute of Pathology, who gave me the possibility to do my PhD project in his group and provided this interesting topic and excellent support to me.

Special thanks go to Prof. Martin Müller, head of the research group Tumorvirus-specific Vaccination Strategies (DKFZ Heidelberg), for being my first referee. His generous help and advice as well as fruitful discussions were essential for the success of this work. In addition, I am grateful to him and his laboratory for providing numerous materials and resources.

I am deeply grateful to my supervisor Dr. Miriam Reuschenbach for her continuous support, encouragement and motivation during research and writing. Her guidance helped me from the initial to the final level of this project.

I would also like to thank the members of my PhD Committee, Prof. Magnus von Knebel-Doeberitz, Prof. Martin Müller and Prof. Dirk Jäger for their time and helpful suggestions in my PhD progress reports.

Many thanks go to Prof. Lutz Gissmann, head of the department Genome Modifications and Carcinogenesis at the DKFZ Heidelberg, for providing the basic vector and discussing the progress of this project with us.

I want to specially thank Prof. Jürgen Kopitz for his always helpful advice, assistance and guidance throughout the protein purification process and Dr. Johannes Gebert for fruitful discussions, especially concerning cloning issues. The experience of both has helped me a lot to find my own way through.

Of course I want to thank my former and current lab members and all those people who spent their time and shared their knowledge for helping me to complete my thesis.

I would like to thank Daniele Viarisio (Genome Modifications and Carcinogenesis, DKFZ Heidelberg) who helped in any way possible with the mouse experiments and sedimentation analysis and it would have been hard to do this without his patient guidance. Also Dr. Lysann Schädlich, Birgit Aengeneyndt (Genome Modifications and Carcinogenesis, DKFZ Heidelberg) and Hanna Seitz (Group Prof. Martin Müller, DKFZ Heidelberg) always answered my questions concerning protein expression and purification and I am greatly thankful that they shared their knowledge and experience with me.

Special thanks go to Dr. Karsten Richter from the Core Facility Electron Microscopy at the DKFZ, who provided all the electron microscopic images and was always willing to look a little bit closer.

I would also like to thank PD Dr. Matthias Kloor from the department of Applied Tumor Biology whose assistance, optimism and professionalism often have been very helpful for me.

Many thanks go to the laboratory staff, especially Marcel and Sigrun, who always supported me with their knowledge and tireless help.

My lunch-fellows and friends Olaf and Patrick additionally inspired me with lively discussions and they always made my days enjoyable and bright.

I wish to extend my warmest thanks to all those who have helped and supported me in any respect during the completion of the project.

I thank Dennis for his loving patience, motivation and encouragement and for always reminding me of the aims I pursue. He was my warming light on cold winter days full of work and he is able to make me laugh and forget the difficulties even in the hard times.

Last but not least, I am heartily thankful to my beloved family who always believes in boundlessly and supports me in all thinkable ways throughout my life.

für Opa

Abstract 1

Zusammenfassung 3

I. Introduction 5

1 Human papillomaviruses 5

1.1 HPV classification and distribution 6

1.2 HPV genome and viral proteins 7

1.2.1 Proteins expressed by early genes E1, E2, E4, E5 and oncogenes E6 and E7 . 7

1.2.2 Structural proteins L1 and L2 8

1.3 Virus life cycle and transforming potential 9

1.4 HPV immunology 11

1.5 Virus like particles and capsomeres 13

2 HPV Vaccination 14

2.1 Prophylactic Vaccines 15

2.2 Therapeutic Vaccines 16

3 $p16^{INK4a}$ as a potential tumor antigen in HPV-associated cancers 17

3.1 Structure and function 18

3.2 Chimeric constructs containing $p16^{INK4a}$ and L1 19

4 Rational and Aims of the project 20

II. Materials and Methods 23

5 Materials 23

5.1 Biological Materials 23

5.1.1 Bacteria 23

5.1.2 Cell lines 24

5.1.3 Animals 24

5.2 Molecular biological materials 24

5.2.1 Plasmids 24

5.2.2 Oligonucleotides 26
5.2.3 Peptides 27
5.2.4 Antibodies 28
5.3 Media and Supplements 29
5.3.1 Bacteria Culture 29
5.3.2 Mammalian cell culture 30
5.4 Material for molecular biological and protein technical methods 31
5.4.1 Preparation, manipulation and analysis of DNA 31
5.4.2 Protein purification 33
5.4.3 Endotoxin detection, quantification and removal 38
5.4.4 Analysis of proteins 38
5.4.5 Electron microscopy 40
5.4.6 Sedimentation analysis 40
5.5 Material for the immunization of mice and analysis of immune response 40
5.5.1 Immunizations 40
5.5.2 ELISA 40
5.5.3 IFNy ELISpot 41
5.6 Chemicals 41
5.7 General materials and consumables 43
5.8 Equipment 44
5.9 Software 45

6 Methods 46

6.1 Manipulation of DNA 46
6.1.1 Purification of plasmid DNA (Mini and Maxi preparation) from E. coli 46
6.1.2 Determination of DNA concentration and purity 46
6.1.3 Enzymatic cleavage of DNA 46
6.1.4 Purification of DNA 47
6.1.5 Precipitation of DNA 47
6.1.6 Dephosphorylation of 5’ends of DNA 47

6.1.7 Analytic and preparative agarose gel electrophoresis 47
6.1.8 Purification of DNA fragments from agarose gels 48
6.1.9 Ligation of DNA fragments 48
6.1.10 Polymerase chain reaction (PCR) 48
6.2 Microbiological methods 50
6.2.1 Culture and storage of bacteria 50
6.2.2 Transformation of bacteria by heat shock 50
6.3 Cultivation and manipulation of eukaryotic cells 51
6.3.1 Cryo-conservation and thawing of eukaryotic cells 51
6.3.2 Determination of cell number and vitality 51
6.3.3 Transfection of mammalian cells 52
6.3.4 Production of Ripa-lysates for protein analysis 53
6.4 Purification and analysis of recombinant proteins 53
6.4.1 Purification of HPV16 L1 capsomeres and chimeric fusion proteins combining HPV16 L1 and $p16^{INK4a}$ from E. coli 53
6.4.2 Purification of $p16^{INK4a}$ from E. coli 55
6.4.3 Explorative protein purification methods 56
6.4.4 Denaturing SDS-polyacrylamide gel electrophoresis (SDS-PAGE) 57
6.4.5 Coomassie-staining of protein gels 57
6.4.6 Silver-staining of protein gels 57
6.4.7 Western blot analysis 57
6.4.8 Determination of protein concentrations 58
6.4.9 Sedimentation analysis 59
6.4.10 Transmission electron microscopy 59
6.4.11 Determination of endotoxin concentrations and endotoxin removal 60
6.4.12 Antigen Capture ELISA 60
6.5 Immunization of mice 60
6.5.1 Immunization by subcutaneous injection 60
6.5.2 Immunization by topical application 61
6.5.3 Blood sampling of immunized mice 61

6.5.4 Splenectomy and preparation of spleen cell suspensions 61
6.6 Analysis of humoral and cellular immune responses 62
6.6.1 VLP-capture ELISA to determine L1-specific antibodies 62
6.6.2 $p16^{INK4a}$ - peptide pool ELISA to determine $p16^{INK4a}$ -specific antibodies 62
6.6.3 Detection of antigen-specific cytotoxic T-lymphocytes by IFNγ-ELISpot 63

III. Results 64

7 Generation and validation of the expression vectors 64
7.1 Cloning of the expression plasmids 65
7.2 Sequence analysis of the generated plasmids 69
7.3 Conclusions 71

8 Protein Expression 72
8.1 Small scale expression - evaluation and optimization 72
8.1.1 Solubility screen 74
8.1.2 Osmosis screen 75
8.2 Large scale expression - protein production 77
8.3 Conclusions 78

9 Protein Purification 79
9.1 Inclusion body purification of HPV16 L1 and chimeric capsomeres 79
9.2 $p16^{INK4a}$ GSTrap purification 81
9.3 GSTrap and SEC purification of soluble fusion proteins 82
9.4 Other purification attempts and separation of the GST-tag 85
9.5 Analysis and removal of endotoxin contaminations in HPV16 L1 protein preparations from E. coli 86
9.6 Structural characterization of chimeric capsomeres 88
9.6.1 Sedimentation analysis 88
9.6.2 Transmission electron microscopy 89
9.6.3 Conformation specific ELISA 90
9.7 Conclusions 90

10 In vivo immunogenicity of the vaccine candidates 91

10.1 Determination of the $p16^{INK4a}$ dose for control groups 91

10.2 Dose-response effect of p16L1 capsomere immunization 92

10.3 Comparison of the different HPV16 L1 - $p16^{INK4a}$ capsomere constructs 95

10.4 Immunogenicity of the HPV16 L1 - $p16^{INK4a}$ capsomeres after single administration 98

10.5 $p16^{INK4a}$-specific T cell reactivity verified with synthetic peptides 100

10.6 Immunogenicity of the HPV16 L1 – $p16^{INK4a}$ capsomeres with co-administration of Montanide adjuvant 101

10.7 Conclusions 103

IV. Discussion 105

11 Generation of chimeric capsomeres consisting of HPV16 L1 and $p16^{INK4a}$ 105

11.1 Production of HPV16 L1 - $p16^{INK4a}$ capsomeres in E. coli 105

11.2 Purification of chimeric capsomeres expressed as inclusion bodies 108

12 Evaluation of the purified chimeric capsomeres 110

12.1 Evaluation of the chimeric capsomeres purified from inclusion bodies 110

12.2 Immunogenicity of the capsomere constructs 111

13 Chimeric HPV16 L1 - $p16^{INK4a}$ capsomeres as a potential vaccine 113

13.1 $p16^{INK4a}$ as an antigen for therapeutic HPV vaccines 113

13.2 HPV16 L1 capsomere conjugation to full length $p16^{INK4a}$ 116

13.3 Evaluation of the prophylactic and therapeutic potential of the chimeric proteins 117

13.4 Future prospects 119

V. References 121

VI. Abbreviations 133

VII. Appendix 136

Abstract

The tumor suppressor p16^{INK4a} is strongly expressed in HPV-transformed precursor lesions and cervical cancer, whereas in normal tissues barely any p16^{INK4a} expression is detectable. It is thus used as a diagnostic marker since several years and it was speculated that targeting p16^{INKa}-overexpressing cells with a therapeutic vaccine could have high benefit for patients suffering from HPV induced neoplasia and cancer.

We designed chimeric capsomeres consisting of full-length p16^{INK4a} and HPV16 L1, the major capsid protein of HPV and antigen of the available prophylactic HPV vaccines, with the aim of using the adjuvant-like effects of L1 particles to potentiate an effective p16^{INK4a} immune response. For this purpose, three constructs were generated to evaluate the antigenic effect of different structural isoforms. The complete p16^{INK4a} encoding cDNA sequence was cloned downstream (pGex-L1ΔN10Δh4ΔC29-p16^{INK4a}) and upstream (pGex-p16^{INK4a}-L1ΔN10Δh4ΔC29) of a modified HPV16 L1 sequence into a pGex-4T-2 expression vector. For the third construct (pGex-L1ΔN10Δh4-p16^{INK4a}-L1ΔC29) the helix 4 region of L1 was replaced by p16^{INK4a}. The proteins were inducible expressed in E. coli. Due to the low solubility of the chimeras, an inclusion body (IB) purification protocol was developed to purify the proteins in high amounts. After IB purification, the proteins were extracted under denaturing conditions with N-Lauroylsarcosine and refolded by dialysis. The capsomere preparations were found to be free of endotoxins after refolding from IBs. The produced particles were then evaluated for their structural properties and the in vivo immunogenicity of the capsomeres was tested in a C57BL/6 mouse model. Besides good stability characteristics, the capsomeres were found to be of rather heterogeneous structure and the immunological comparison of the three different constructs revealed different characteristics. GST-L1ΔN10Δh4-p16^{INK4a}-L1ΔC29 induced highest L1-specific T cell numbers, GST-p16^{INK4a}-L1ΔN10Δh4ΔC29 showed the best antibody response in the VLP-capture ELISA and GST-L1ΔN10Δh4ΔC29-p16^{INK4a} seemed to induce the most efficient anti-p16 humoral immune response. Also the induction of p16-specific T cells could be demonstrated with the GST-L1ΔN10Δh4-p16^{INK4a}-L1ΔC29 construct.

The objective of this thesis was to generate, purify and evaluate a cost-effective second generation therapeutic vaccine based on chimeric capsomeres. The presented vaccine candidates can be cost-efficiently produced in bacteria and purified from inclusion bodies with high yields. The proteins were also found to be stable at room temperature and their immunogenicity was demonstrated in first in vivo mouse experiments. A protein-based vaccine with these properties could have substantial benefit, especially for unindustrialized countries where most of the cervical cancer cases occur. The possibility to generate an effective immune response to p16^{INK4a} further opens new opportunities in the field of cancer

immunotherapy. Not only patients with HPV-associated cancers would benefit from such a vaccine as many other cancers express high levels of $p16^{INK4a}$, too. Also several precancerous neoplasias were shown to elicit increased $p16^{INK4a}$ expression and a $p16^{INK4a}$-directed vaccine might even prevent development of invasive cancer.

Zusammenfassung

Das Tumorsuppressorprotein $p16^{INK4a}$ wird in HPV-transformierten Vorläuferläsionen und Karzinomen stark überexprimiert, wohingegen $p16^{INK4a}$ in normalem Gewebe kaum nachweisbar ist. Aus diesem Grund wird es seit Jahren als diagnostischer Marker verwendet und könnte auch als Ziel eines therapeutischen Impfstoffs hohen Nutzen für Patienten mit HPV-assoziierten Krebserkrankungen und Vorstufen haben.

Im Rahmen dieser Arbeit wurden chimäre Kapsomere rekombinant hergestellt, welche aus der vollständigen Sequenz des humanen Zellzyklusregulators $p16^{INK4a}$ und dem HPV16 Kapsidprotein L1 bestehen. Der L1 Anteil zeichnet sich durch eine bekannte starke Immunogenität aus, die vor einer Infektion mit HPV16 schützen kann und deshalb auch als Antigen in den vorhandenen prophylaktischen Impfstoffen verwendet wird. L1 kann aber auch die Immunantwort gegen andere Antigene verstärken und diese Adjuvansfunktion der Viruskapsomere soll genutzt werden um eine effektive Immunantwort gegen $p16^{INK4a}$ zu generieren. Es wurden 3 Konstrukte getestet, um die antigene Wirkung verschiedener Struktur Isoformen zu vergleichen. Die komplette $p16^{INK4a}$-kodierende cDNA-Sequenz wurde N- und C-terminal einer modifizierten HPV16 L1 Sequenz eingefügt, wobei ein pGex-4T-2 -Expressionsvektor verwendet wurde. Die beiden Klonierungsprodukte pGex-$p16^{INK4a}$-L1ΔN10Δh4ΔC29 und pGex-L1ΔN10Δh4ΔC29-$p16^{INK4a}$ wurden mit einem dritten Konstrukt, pGex-L1ΔN10Δh4-$p16^{INK4a}$-L1ΔC29, ergänzt, für welches die Helix-4 Region von L1 mit der $p16^{INK4a}$-Sequenz ersetzt wurde. Diese Proteine wurden dann in E. coli induzierbar exprimiert. Aufgrund der geringen Löslichkeit der Chimären wurde ein Inclusion Body (IB, Einschlusskörper) Reinigungsprotokoll entwickelt um die Proteine in großen Mengen zu gewinnen. Nach der Reinigung wurden die Proteine unter denaturierenden Bedingungen mit N-Lauroylsarcosin extrahiert und durch Dialyse rückgefaltet. Es wurde festgestellt, dass die Kapsomerpräparate keine Endotoxin-Kontaminationen nach der Gewinnung aus IBs enthalten. Die hergestellten Partikel wurden auf ihre strukturellen Eigenschaften untersucht und ihre in vivo - Immunogenität wurde in einem C57BL/6 Mausmodell getestet. Neben guten Stabilitätseigenschaften weisen die Kapsomere eine eher heterogene Struktur auf und der Vergleich der drei verschiedenen Konstrukte ergab unterschiedliche immunologische Eigenschaften. GST-L1ΔN10Δh4- $p16^{INK4a}$-L1ΔC29 induzierte die höchste Anzahl L1-spezifischer T Zellen; GST-$p16^{INK4a}$-L1ΔN10Δh4ΔC29 zeigte die beste Antikörperantwort im VLP-Capture-ELISA und mit GST-L1ΔN10Δh4ΔC29-$p16^{INK4a}$ wurde die beste humorale anti-$p16^{INK4a}$ Immunantwort erreicht. Auch die Induktion $p16^{INK4a}$ -spezifischer T-Zellen konnte mit dem GST-L1ΔN10Δh4-$p16^{INK4a}$-L1ΔC29 Konstrukt nachgewiesen werden.

Ziel dieser Arbeit war es, einen Capsomer-basierten, kostengünstigen therapeutischen Impfstoff der zweiten Generation herzustellen, zu reinigen und zu evaluieren. Die hier präsentierten Impfstoffkandidaten können kostengünstig in Bakterien hergestellt und aus Inclusion Bodies mit hoher Ausbeute gereinigt werden. Die Proteine sind stabil bei Raumtemperatur und ihre Immunogenität wurde in ersten in vivo Mausexperimenten demonstriert. Ein Impfstoff auf Proteinbasis mit diesen Eigenschaften könnte wesentliche Vorteile haben in der Behandlung von Gebärmutterhalskrebs, besonders in Entwicklungsländern in denen die meisten Fälle auftreten. Die Möglichkeit, eine wirksame Immunantwort gegen $p16^{INK4a}$ zu erzeugen, eröffnet zudem weitere Möglichkeiten im Bereich der Krebs-Immuntherapie. Nicht nur Patienten mit HPV-assoziierten Krebsarten würden von einem solchen Impfstoff profitieren; auch viele andere Krebsarten exprimieren hohe Mengen an $p16^{INK4a}$. Zudem wurde gezeigt, dass verschiedene präkanzeröse Neoplasien erhöhte $p16^{INK4a}$ Level aufweisen und eine Vakzine, die gegen dieses zelluläre Protein gerichtet ist, könnte möglicherweise sogar die Entwicklung invasiver Karzinome verhindern.

I. Introduction

Cancer is a multifaced disease with numerous possibilities of origin. One of these are infectious agents like bacteria, e.g. the bacterium Helicobacter pylori which causes 5.5% of all cancers. Viruses are even more prominent as some play an important role as oncoviruses. Examples are the human papilloma viruses (HPV; cancers of anogenital tract and head and neck region), the hepatitis B and C viruses (HBV, HCV; hepatocellular carcinoma), Epstein-Barr virus (EBV; Burkitt's lymphoma, nasopharynx carcinoma), or the human herpes virus 8 (HHV8; Kaposi's sarcoma) [1]. Especially human papillomaviruses are attributable to almost all cervical cancers and are therefore an important target for global research. First successes were achieved with the release of two prophylactic vaccines but therapeutic intervention for already infected individuals is still challenging.

1 Human papillomaviruses

Infections with human papillomaviruses and the associated risk of cancer development are a major public health burden worldwide. HPVs are commonly transmitted by sexual contact and infect exclusively epithelial cells [2]. If the infection remains persistent due to ineffective clearance by the immune system, both benign papillomas and several types of head and neck tumors and anogenital, particularly cervical carcinoma [3] can develop. The small DNA-viruses have a high prevalence as overall ~ 27 percent of women were tested positive for one or more strains of HPV in a US prevalence study [4]. Especially amongst young women at ages 20 to 24, HPV infections are very common and the prevalence in this age group is typically approx. 20–40 % depending on geographical location [4-6]. The incidence declines with age as infections are often resolved and brought under control by the host immune system [7, 8]. Women who cannot resolve their infection and who maintain persistent active infection for years or decades have an increased rsik to develop cervical intraepithelial neoplasia (CIN) and cancer [7]. Cancer of the cervix is usually slow-growing and may not have symptoms, but premalignant and malignant processes can be found with regular Pap tests (Papanicolau test, a gynecological screening test) [9]. The incidence of invasive cervix carcinomas varies worldwide between 3.6 cases in Finland and 45 cases per 100,000 women in Columbia [10]. In Germany, the frequency of occurrence is declining since introduction of the Pap test in the 1970s/1980s and in 2004 14 cases per 100,000 women were registered. However, cervical intraepithelial neoplasisas are 50- to 100-fold more common and severe precancers of the cervix have an incidence of ~1 percent [11]. Altogether, due to their high prevalence, HPVs are medically very important pathogens.

1.1 HPV classification and distribution

Until now, more than 150 different HPV types could be identified, whereby alpha and beta papillomaviruses (supergroups A and B) represent ~ 90 % of the currently known HPVs [7, 12, 13]. HPVs from the three genera Gamma, Mu and Nu mostly cause cutaneous papillomas and verrucas which do not lead to cancer development [7]. The largest is the alpha group that contains most of the genital / mucosal HPV types. Benign and neoplastic diseases of the anogenital tract include cervical, vaginal, penile and anal cancers [14]. Besides their oncogenic properties in the genital tract, HPVs also infect squamous epithelial tissues in the head and neck region [15]. A subset of squamous cell carcinomas (SCCs) of the head and neck (HNSCC) is HPV-positive and resembles HPV-positive cervical SCC [16, 17]. HPV-associated HNSCCs emerge in the airway mucosa of the oral cavity and oropharynx, but other sites in the head and neck region can also be infected by HPVs, e.g. the nasal sinuses, the eye conjunctiva and ear canals. However, there seems to be an affinity for the oropharynx, especially for the base of the tongue and the tonsils [14, 16]. Furthermore, it was found that viruses from the B supergroup are involved in the development of nonmelanoma skin cancer (NMSC) whereby epidermodysplasia verruciformis (EV) HPV types are most plausibly linked to the development of NMSC [18]. EV is an inherited disease and patients show an increased susceptible to HPVs of the skin [19].

Alpha papillomaviruses are further subdivided into three groups: high risk, low risk and cutaneous. Low-risk HPV types, e.g. HPV 6 and 11, are rarely associated with cervical cancer but are nevertheless medically important as they can cause genital warts. High risk HPVs belonging to the alpha 5, 6, 7 ,9 and 11 species specifically target genital squamous epithelia and are present in almost all cervical cancers [7, 20]. HPV16 is the most prevalent type of the high-risk category in the general population and is responsible for approximately half of all cervical cancers, followed by HPV18 as the second most common HPV type (see figure 1) [7, 14]. In a study performed in the US in 2003/2004 the prevalence of high-risk HPV was 15.2 % among all participating women [4].

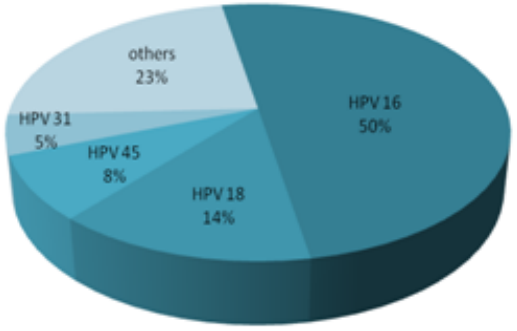

Figure 1: HPV type-specific distribution in cervical cancer. HPV DNA was detected in 93% of the tumors and there was no significant variation in HPV positivity among countries. HPV16 was present in 50% of the specimens, HPV18 in 14%, HPV45 in 8%, and HPV31 in 5%. HPV16 was the predominant type in all countries except Indonesia, where HPV18 was more common. Data obtained from Bosch 1995, Journal of the National Cancer Institute [20].

HPV types 16 and 18 account for approximately 70 percent of all cervical cancer cases worldwide [21], whereby HPV16 is predominantly associated with squamous cell carcinomas appearing at the transformation zone and HPV18 with cancers of the endocervix [13]. The consequences of HPV infection depend on the infecting virus type and site of infection. Further important factors are the regulation of virus persistence, regression and latency. Strategies to reduce the risk of cervical cancer include Pap screening, HPV tests and other biomarkers (e.g. $p16^{INK4a}$ [22]), as well as prevention of HPV infection with vaccines [23]. Whereas the widespread use of these tools has reduced mortality in the industry nations, cervical cancer is still the second leading cause of death among women in developing countries where more than 80 percent of cases occur [1].

1.2 HPV genome and viral proteins

Despite the apparent heterogeneity amongst HPVs, they share some crucial features. Papillomaviruses have a conserved icosahedral capsid architecture [24] with a diameter of 55 nm [25] and contain double-stranded circular DNA. Their genome typically contains about 8000 base pairs (HPV16: 7904 bp) and encodes 8 or 9 ORFs (open reading frames; see figure 2). The encoded genes can be divided into early and late ones depending on their time point of expression during epithelial differentiation.

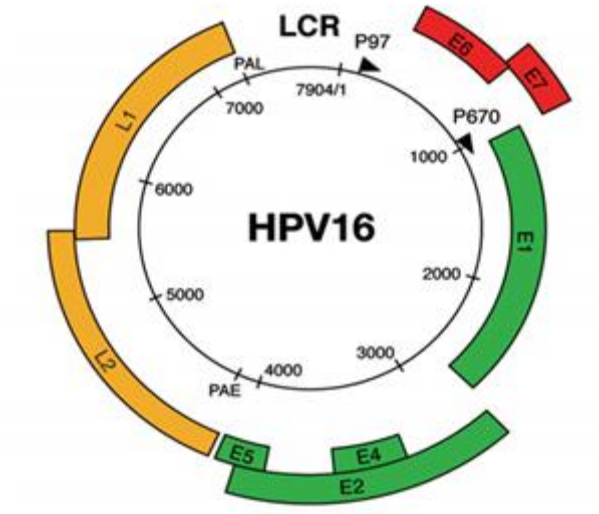

Figure 2: (A) The HPV16 genome (7904 bp) is shown as a black circle with the early (p97) and late (p670) promoters marked by arrows. The six early ORFs E1, E2, E4 and E5 (green) and E6 and E7 (red) are expressed from either p97 or p670 at different stages during epithelial cell differentiation. The late ORFs L1 and L2 (yellow) are located downstream of the early region and are also expressed from p670. The long control region (LCR) also referred to as upstream regulatory region (URR) reaches from base pairs 7156 to 7184. One strand of the double-stranded circular DNA genome encodes all the viral genes. Adapted from Doorbar 2006, Clinical Science [7]

1.2.1 *Proteins expressed by early genes E1, E2, E4, E5 and oncogenes E6 and E7*

All HPVs are epitheliotropic and produce infectious virions in the upper epithelial layers where the p670 promoter is up-regulated, and the viral replication proteins E1, E2, E4 and E5 facilitate viral genome amplification. [2, 7] After infection that requires access to the

basal epithelial layer and invasion to dividing basal cells, probably stem cells [26], the viral genome establishes as a stable episome with low copy number. This process is driven by the expression of E1 and E2 directly after entry into the host cell. The viral replication proteins E1 and E2 are responsible for the regulation of early transcription [27] and have several functions like maintenance of the viral genome in the basal layer. E1 encodes a helicase that contributes to replication and virus load by interacting with the origin of replication, requiring interaction with E2 [2, 28]. E2 also controls the expression of the viral oncogenes E6 and E7 in the lower epithelial layers. E2 binds to the viral DNA, precisely, it has multiple binding sites in the long control region (LCR), leading to its replication and it is also assumed to activate expression of the late genes [29]. E4 is expressed in terminally differentiated keratinocytes [27] and its accumulation at the epithelial surface is thought to improve the release of the virus [7]. E5 is another viral replication protein playing a role in early tumor development but it is not expressed in transformed cells [30].

Concerning E6 and E7 there are functional differences between high and low risk types, whereby the role for the latter, which are generally not associated with malignant neoplasias, is somehow uncertain. In high risk lesions a clear role in cell proliferation is attributable to these oncoproteins [13]. The expression of E6 and E7 is directed by the p97 promoter. Protein E6 (158 aa, ~19 kDa) plays a key role in transcriptional activation and degradation of the cellular tumor antigen p53, thereby deregulates proliferation and leads to impaired apoptosis [31]. E7 (98 aa, ~11 kDa) interacts with the retinoblastoma protein and histone deacetylases. The expression of E6 and E7 in the lower epithelial layers is necessary for entry to S-phase during epithelial differentiation. This provides an environment that is advantageous for viral genome replication and cell proliferation [2]. Both E6 and E7 are accountable for transformation of infected cells. Their function as oncoproteins in the cellular context is described in more detail in 1.3 (Virus life cycle).

1.2.2 *Structural proteins L1 and L2*

The virus capsid is composed of two proteins, L1 and L2 which play important roles in mediating infectivity. The major capsid protein L1 (monomer: see Figure 3) is the primary structural element and has the ability to form pentamers (see Figure 4) which then self-assemble into virus like particles (VLPs, see also 1.5) [25]. L1 consists of 503 amino acids and has a molecular weigth of 56 kDa (HPV16). The minor capsid protein L2 was found to be located in the central internal cavity of the L1 pentamer [32]. It has a size of 473 aa (HPV16) and a molecular weight of 51 kDa. L2 interacts with the viral genome and is essential for the encapsidation process of the viral DNA [33]; it also seems to play a role in infection and immune escape mechanisms of HPV [34]. The natural virus capsid consists of

72 L1 pentamers (360 L1 molecules) and approximately 30 L2 molecules [35]. L1 side chains lining the axial cavity are highly conserved between different HPV types whereby the rim of the L1 pocket is more variable [36].

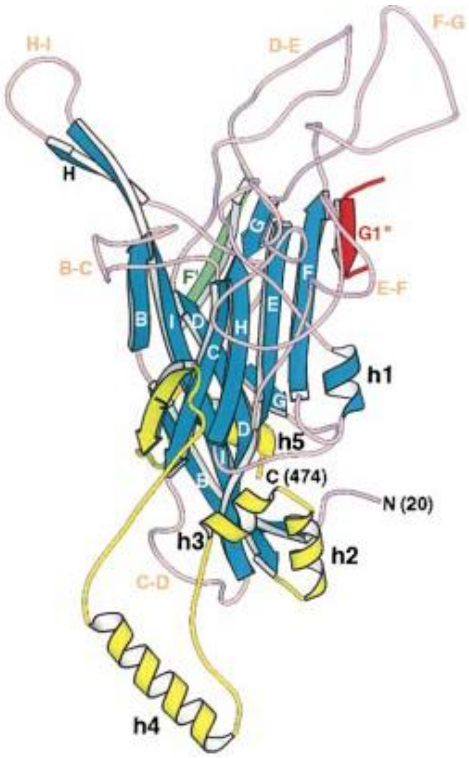

Figure 3: 3D structure of the HPV16 L1 monomer including residues 20-474. β-strands are labeled with capital letters, helices 1-5 are also indicated. helix 4 (h4) (aa 414-431) is essential for VLP assembly. Adapted from Chen et al. 2001, J Mol Biol 307 [37]

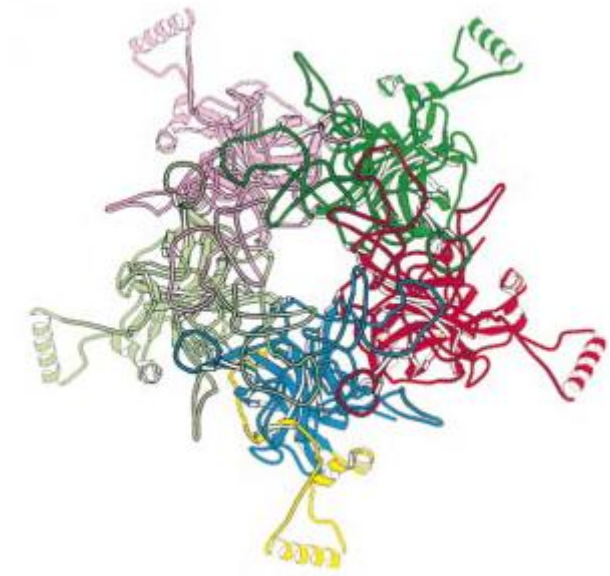

Figure 4: L1 pentamer, viewed along the five-fold axis from outside the particle. Helices 2 and 3 form a groove to which binds h4 of another pentamer via strong hydrophobic contact.
Adapted from Chen et al. 2000, Mol Cell 5 [36]

1.3 Virus life cycle and transforming potential

HPVs display a strong tropism for the basal cell layers at a metaplastic epithelial site of the cervix, the so called transformation zone. This is a ring of mucosa where the glandular epithelium of the endocervix is replaced by squamous epithelium of the ectocervix [38]. Cells close to this squamo-columnar junction have a higher susceptibility for persistent infections wherefrom transformation to malignant cells can occur [13]. Other sites of the body where HPV associated cancers can arise from show similarities as there is also some kind of intersection epithelium like the linea dentata in the anal canal [39] or the uneven reticulated epithelium lining the crypts of the palatine tonsils and the base of the tongue [40, 41] (head and neck squamous cell carcinoma (HNSCC)).

Initially, HPVs bind to the surface of the epithelium or the basement membrane of keratinocytes via the interaction of the major capsid protein L1 with heparan sulfate

proteoglycans [42-44]. Thereby, a role of (micro-) trauma or epithelial wounding and subsequent healing processes is thought to be required as active cell division seems to be necessary for establishing an infection [45-47]. Virus internalization and transfer of the genome to the nucleus is then propagated by changes in the capsid structure [2, 45] but although many studies attempted to elucidate the mechanism of infection, the details of endocytosis are not yet fully understood. It is possible that not only one but various internalization and/or infectious entry pathways exist which may use different cell surface molecules [48] and that this process also depends on the virus type [13]. After internalization the virus is uncoated and entry of the viral genome to the nucleus is facilitated by a complex of L2 and DNA [49, 50].

HPV infection leads to deregulation of the cell cycle whereby high-risk E6 and E7 proteins are crucial for malignant transformation and increased proliferation of suprabasal epithelial cells [7]. In high-risk HPV infected cervical epithelium, cell cycle progression does not depend on external growth factors, but it is stimulated by E7. The transforming activity of E7 is attributable to its interaction with the retinoblastoma (RB) tumor suppressor protein [51]. E7 binds to RB and dissociates the complex between RB and the E2F family of transcription factors. In non-infected cells, the expression of proteins necessary for cell-cycle progression is controlled by RB, which in non-cycling cells associates with E2F and acts as a repressive subunit. In the presence of growth factors, cyclinD/Cdk4/6 is activated, leading to RB phosphorylation and the release of E2F, which drives protein expression. HPV E7 also associates with other proteins involved in cell proliferation, including components of the AP1 transcription complex, enzymes that mediate histone acetylation and the cyclin dependent kinase (Cdk) inhibitors p21 and p27 [7, 52].

A newer study by McLaughlin et al. [53] proposes an alternate mechanism for the E7-mediated $p16^{INK4a}$ overexpression that is independent of pRB-inactivation. They discovered that E7 induces epigenetic reprogramming by activating the histone demethylases KDM6A and KDM6B. These methyl transferases remove the histone H3 lysine 27 trimethyl (H3K27me3) repressive mark from promoters encoding for RB-binding proteins (KDM6A) and $p16^{INK4a}$ (KDM6B). E7 thereby simultaneously inactivates $p16^{INK4A}$ and pRB.

$p16^{INK4a}$ levels rise as HPV-mediated cell proliferation is not dependent on cyclinD/Cdk4/6. In the absence of p16-mediated feedback, the level of p14Arf also rises. p14Arf is encoded by the alternative reading frame of the CDKN2A gene and normally regulates the activity of the MDM (murine double minute) ubiquitin ligase, which maintains p53 at a level below that required for cell cycle arrest and/or apoptosis. Increased p14Arf leads to the inhibition of MDM function and an increasing level of p53 [54-56].

The function of E7 is complemented by the viral E6 protein. E6 associates with the E6AP ubiquitin ligase and mediates p53 degradation. This in turn prevents growth arrest or

apoptosis in response to E7-mediated cell-cycle entry in the upper epithelial layers. [7, 17] The final stage in the papillomavirus productive cycle requires packaging of the replicated genome into infectious particles. Therefore, the capsid proteins L1 and L2 are transported to the nucleus where L1 assembles into capsomeres and L2 contributes to efficient packaging [33] and enhances virus infectivity [57].
Integration of the HPV genome into the host cell chromosome is a critical event in the development of cervical cancer. As infected basal cells migrate towards the epithelial surface, their integration leads to deregulated E6/E7 expression which is critical for the enhanced growth characteristics of cervical cancer cells [2, 7].

1.4 HPV immunology

Most of the cervical HPV infections are cleared as a result of humoral and cell-mediated immune response. However, some infections persist over long periods of time and can progress to cervical intraepithelial neoplasia (CIN) or cancer.
Dendritic cells (DCs) that normally reside in cervical tissue have a unique ability to induce primary immune responses. DCs are antigen-presenting cells (APCs) which capture and transfer information to the cells of the adaptive immune system. They may also be important in immunological tolerance, as well as for the regulation of T cell-mediated immune response. T cells recognize antigens presented on the surface of the major histocompatibility complex (MHC) proteins. In an inflammatory milieu, DCs are activated and up-regulate MHC class I and II molecules, co-stimulatory molecules (CD80 and CD86), and the chemokine receptor-7 (CCR7), and increase the secretion of cytokines. This in turn primes naive CD4+ and CD8+ T cells. Histological examination revealed large infiltrates of T cells in HPV infected epithelium. Natural killer (NK), cytotoxic T lymphocytes (CTL) and additional T cell subsets play important roles in the elimination of virus-infected and tumor cells as they promote their lysis through activation of natural killer group 2 member D (NKG2D) receptors [58]. A successful immune response to HPV infections is characterized by strong, local, cell-mediated immunity that is associated with lesion regression and the generation of serum neutralizing antibodies mostly directed against the L1 capsid protein [59, 60].

Nevertheless, HPVs are very successful pathogens as they induce chronic infections but rarely kill their host. With this strategy they are able to shed large amounts of infectious viruses for transmission to naive individuals [8]. To cause persistent infections, which is the greatest risk factor for the development of HPV associated cervical and other cancers, the virus must escape host immunity. Papillomaviruses have evolved a number of mechanisms to limit the chance of detection by the immune system [7]. One strategy that HPV has evolved to avoid detection is to expose only minimal amount of virus to the immune system

thereby maintaining a very low profile. The virus infects basal cells at low copy number and the expression of oncogenes E6 and E7 is tightly controlled. The viral early proteins are expressed at levels below those required for an effective host immune response [7, 8, 61]. Furthermore, the oncoproteins E6 and E7 interact directly with components of the interferon (IFN) signaling pathways. Interferons are soluble factors that can limit viral infections and activate or attract cells of the immune system including macrophages, neutrophils, DCs and NK cells. The type 1 interferons, IFN-α and IFN-β connect innate and adaptive immunity by activating immature DCs. However, HPV has evolved mechanisms to inhibit interferon synthesis and signaling [8, 61]. Papillomaviruses also modulate antigen presentation. T cells normally recognize infected cells through interactions of their receptors with viral peptides bound to MHC complexes on the surface of infected cells. Dysregulation of the antigen processing machinery results in down-regulation of peptide-MHC complexes and protects infected cells from immune attack. [61, 62] The inhibition of cytokines and chemo-attractants is another escape-mechanism of HPV. Cytokines, chemokines, adhesion molecules and proteases are molecules that direct the migration of cells of the immune system. They elicit local infiltration of inflammatory and immune cells. E6 and E7 proteins of HPV inhibit the production of those immune mediators thus interfering with cytokine patterns and inhibiting DC activation. Further strategies to escape immune surveillance include prevention of apoptosis, inhibition of APC migration, modulation of adherence molecules and molecular mimicry by sequence similarity to human proteins [61]. The HPV productive life cycle itself is an immune evasion strategy as it is coupled to the cellular differentiation cycle of the host [8, 61]. The virus is present during the whole life cycle of the keratinocyte as it infects it as a primitive basal cell and replicates and assembles during cell cycle progression whereby only minimal virus amounts are exposed to the immune system. The Langerhans cell (LC), which is the intraepithelial DC, is the first APC the virus comes into contact with during infection. This professional APC of squamous epithelia should theoretically detect HPV invasion, but evidence indicates that LCs are not activated by the uptake of HPV capsids [8, 63]. In fact, reduced numbers or even absence of Langerhans cells was observed in viral lesions [64]. The cell later dies by natural causes; thus there is no inflammation and the essential signals required for initiation of immune responses are absent [60, 61]. The milieu becomes HPV antigen tolerant [8] as the virus is practically invisible to the host. This is further supported by the non-lytic life cycle of the virus and the resulting lack of pro-inflammatory signals that could activate DCs. HPV antigen-specific effector cells are poorly recruited to the infected area and their activity is down-regulated [8]. Furthermore, viral protein expression and assembly only occurs in the upper epithelial layers and this also restricts the immune system to encounter capsid antigens [59].

Altogether, HPV efficiently evades the innate immune response and delays the activation of the adaptive immune response.

1.5 Virus like particles and capsomeres

A virus like particle (VLP) is the empty capsid of a virus without genetic material inside. VLPs can be produced by genetic engineering and are highly immunogenic: they resemble the native, infectious virions in size and shape and are thereby able to induce high titers of virus-neutralizing antibodies, which provide protection from further virus challenge [65-67]. As described above, the L1 major capsid protein is primarily responsible for virus capsid assembly. After expression in eukaryotic and prokaryotic systems, L1 is able to self-assemble into empty VLPs with similar immunogenicity compared to infectious virions [67]. HPV virions and VLPs usually consist of 72 L1 pentamers [68], also called capsomeres, which are arranged in an T = 7[1] icosahedral architecture with a diameter of 55 nm [25]. VLPs are endocytosed, processed, and presented by APCs to naive T cells [70]. They deliver multiple B and T cell epitopes as immunogens to the MHC class I and class II pathways, thereby extending their utility as self-adjuvanting immunogen delivery systems [71]. Consequently, VLPs can be used as carriers for synthetic or small antigens for the development of subunit vaccines [72]. Especially papillomavirus VLPs are able to induce strong immune responses and allow antigen presentation within a highly organized context as part of the regular array of assembled capsomeres [73, 74]. It was found that the conjugation of mouse self-peptide TNF-α to papilloma VLPs leads to efficient induction of protective auto-antibodies [74]. Also the conjugation of influenza type A M2 protein to HPV VLPs was found to be highly immunogenic and conferred good protection against lethal challenge of influenza virus in mice [72]. This demonstrates that HPV VLP systems can be used as an antigen carrier for developing conjugate vaccines.

Capsomeres represent a potentially lower cost alternative to VLP-based vaccines as they can be produced in large amounts from prokaryotic expression systems and are considered to be more stable at room temperature [75]. Although it was reported that capsomeres are less immunogenic than VLPs [75], another study showed that certain L1 constructs form highly immunogenic capsomeres [76]. The L1 protein was modified in different ways and immunogenicity of the constructs was compared. A construct with an N-terminal deletion of 10 amino acids, named L1ΔN10, proved to be the most immunogenic. L1ΔN10 induced antibody titers equivalent to those generated in response to VLPs [76]. Several other studies present further evidence for the potential of capsomeres as antigen carriers and

[1] T = Triangulation number. T describes size and complexity of an icosahedral capsid (for more details see 69. Caspar DL, Klug A: **Physical principles in the construction of regular viruses.** *Cold Spring HarbSympQuantBiol* 1962, **27:**1-24.)

immune stimulators. Yuan et al. produced a GST-L1 fusion protein in E. coli that formed pentameric capsomeres and was capable of protecting dogs from oral papillomavirus challenge [77]. Rose et al. showed that the capsid-neutralizing antigenic domains are fully conserved in capsomeres and that antisera generated with capsomeres elicit neutralization titers comparable to that of entire VLPs [78]. This was also demonstrated by Fligge et al. with capsomeres of a HPV type 33. When combined with an appropriate adjuvant, capsomeres induce neutralizing antibody titers as high as VLPs do [79].

2 HPV Vaccination

Despite relatively low serum antibody titers, seropositive animals are protected against further viral challenge [80] and passively transferred serum immunoglobulins from immunized to naive animals confer protection from experimental infection [81]. Other experimental studies revealed that immunization with L1 VLPs induces circulating neutralizing antibodies to the L1 capsid protein and thereby offers protection against larger virus amounts [82]. These results provided the background for attempts to develop prophylactic vaccines against human high-risk HPV types based on L1 VLPs [66].

There are diverse vaccination strategies for prevention and treatment of HPV-associated lesions (Figure 5): (I) vaccines for uninfected females to prevent HPV infection/spread, (II) vaccines for the reduction of viral load at the cervical mucosa in females with low-SIL (squamous intraepithelial lesion) and prevention of its progression, (III) vaccines for the treatment of high-SIL, and (IV) immunotherapy for cervical cancer. Currently used HPV vaccines are represented by group I. Possibly, they are able to eliminate persistent HPV infection and if so, they work to suppress HPV infection (II). III and IV are considered to be therapeutic vaccines used for females with disease [83].

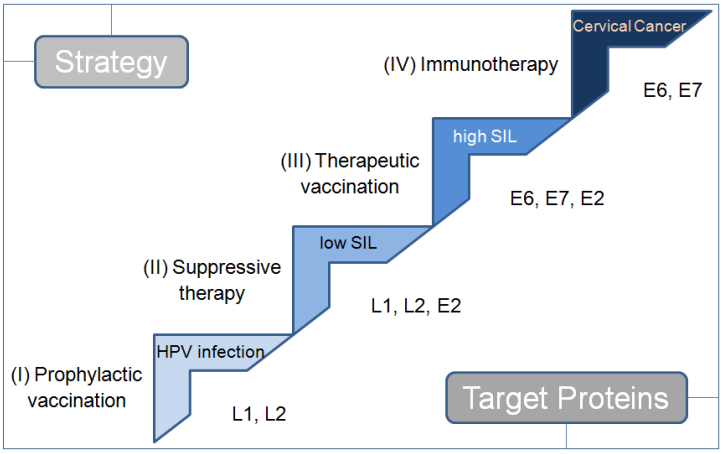

Figure 5: Possible strategies for prophylaxis and treatment of HPV-associated lesions (squamous intra-epithelial lesion, SIL) and the target viral proteins. Modified from: Kawana 2009, Indian J Med Res 130 [83]

2.1 Prophylactic Vaccines

Currently available, prophylactic vaccines contain only two, respectively four, of the HPV types. The bivalent vaccine Cervarix was developed by GlaxoSmithKline and is comprised of a mixture of VLPs derived from the L1 capsid proteins of HPV types 16 and 18 formulated with the AS04[2] adjuvant system [84, 85]. In clinical trials it was found to be safe and protective and it prevents both persistent HPV16/18 infection and the development of low-grade intraepithelial lesions [86]. Gardasil is a quadrivalent vaccine by Merck & Co. protects against the high-risk types 16 and 18 as well as against the low-risk types 6 and 11. With this vaccine, the combined incidence of persistent infection or disease with HPV6, 11, 16, or 18 fell by 90% in the group that received the vaccine compared to the placebo group [87].
Both vaccines were found to be safe, immunogenic, and efficacious in various randomized controlled trials and confer protection against CIN induced by the respective HPV types [60]. For these reasons they are expected to yield significant public health benefits [60].
Exogenously expressed L1 proteins are able to self-assemble into VLPs in vitro thereby providing a potentially effective sub unit vaccine. Currently available HPV L1 VLPs vaccines are produced in yeast or insect cells after inserting the L1 gene into expression vectors. [67, 82] VLPs induce strong humoral and cell-mediated responses. They bind to the cell surface of monocytes, macrophages and DCs resulting in their acute phenotypic activation and production of inflammatory cytokines [88]. It is worth mentioning that the Langerhans cells (LC) do not get activated when incubated with VLP and do not initiate epitope-specific immune responses due to a different endocytosis mechanism [63, 89]. Activated stromal DCs stimulate HPV-specific T-cells [88, 90], but as the virus remains in the epithelium, the probability of encountering stromal DCs is relatively low [8]. Contrary, DCs of the muscle do encounter the highly immunogenic repeat structure of the VLP and the vaccines circumvent viral epithelial evasion strategies since they are delivered by intramuscular injection [8]. DCs migrate to the lymph node and initiate an immune cascade that results in a robust T-cell dependent B-cell response followed by generation of high levels of L1-specific serum neutralizing antibodies and immune memory [8].
Despite these promising perspectives, the neutralizing antibodies generated by HPV L1 VLP vaccines appear to be type-specific and thus only protective against the corresponding virus type [91]. Although there is some evidence for cross-protection against HPV types other than those incorporated in the vaccines [92], it is not clear how and to what extend cross-protection against other types occurs. Current research efforts are directed towards this question. Furthermore, the prophylactic vaccines lack any therapeutic function against

[2] AS04: 3-O-desacyl-40-monophosphoryl lipid A and aluminium hydroxide, a combination of adjuvants used in various vaccine products by GlaxoSmithKline

established HPV infections [93, 94] what could be associated to the fact that the virus capsid proteins are not detectable in high grade dysplasias and cervical carcinomas [95]. Prophylactic vaccines are therefore only effective in women that have not yet encountered HPV infection. This explains the need for developing therapeutic strategies for the control and treatment of existing HPV infections and associated malignancies.

2.2 Therapeutic Vaccines

In contrast to preventive vaccines which induce the generation of neutralizing antibodies [96], therapeutic vaccines aim to initiate a strong cellular immune response, particularly T cell-mediated, to HPV antigens expressed in transformed cells [94]. The patient's own immune response shall be stimulated to recognize and kill cancer cells that express foreign proteins [94]. The most frequently targeted antigens for this purpose are E6 and E7 because they are oncogenic and their overexpression is required for the maintenance of the cancerous phenotype [94]. As T cell-mediated immunity is one of the most crucial components to defend against HPV infections and HPV-associated lesions, effective therapeutic vaccines should generate strong E6/E7-specific T cell-mediated immune responses to the early proteins E6 and E7 [59, 93].

There are various therapeutic HPV vaccines for cervical cancer currently being under clinical investigation. These include live vector-based, peptide or protein-based, nucleic acid-based, and cell-based vaccines targeting the HPV E6 and/or E7 antigens [96]. Ongoing studies show the general applicability of tumor vaccination and prove the correlation of immune and clinical response [97]. So far, the success of therapeutic vaccines is limited [97] although clinical responses could be shown, e.g. in grade 3 vulvar intraepithelial neoplasia (VIN) with a long-peptide E6/E7 peptide [98]. Also a DNA vaccine based on E6 and E7 fragments (ZYC101a) that was tested in a phase 2 trial led to more resolved infections in the vaccine group compared to placebo [99]. Another trial investigated the effect of Imiquimod followed by vaccination with an E6E7L2 fusion protein and reported complete regression in up to 63% of women with VIN grades 2 and 3 whereby the therapeutic effect depended on the differential immune response [100]. Even a live-attenuated vaccine based on E7 secreting Listeria monocytogenes (Lovaxin-C, Lm-LLO-E7) was tested in a phase I trial where relatively safe administration was demonstrated despite the occurrence of severe adverse events in 40% of patients [101, 102].

ProCervix is another therapeutic vaccine candidate developed by Genticel. It is based on the adenylate cyclase vector system derived from *Bordetella pertussis* which targets dendritic cells with high efficiency. The E7 antigen presented within the CyaA context was found to induce T-cell responses in most of the vaccinated HPV 16/18 positive women.

Furthermore, enhanced viral clearance of the infected cervix cells and also more sustained clearance could be shown for the ProCervix (plus Imiqiumod) group [103, 104]. However, this vaccine is designed to prevent progression to cervical dysplasia and cancer before appearance of high grade lesions and therefore is kind of a preventive vaccine for already infected women rather than a therapeutic one for patients.

Altogether, the challenge for therapeutic vaccines is to overcome the immunosuppresion of the host, to create an inflammatory environment in which immature DCs can be activated to present HPV antigens to CTLs and to mount an effective immune response that can eliminate the HPV-infected and transformed cells [59]. As the current vaccines do not appear to be an ultimate strategy, study on new therapeutic HPV vaccines is needed [83]. The development of chimeric vaccines seems to be an appropriate step in this direction [95, 105].

3 $p16^{INK4a}$ as a potential tumor antigen in HPV-associated cancers

The tumor suppressor $p16^{INK4a}$ shows increased expression with worsening grades of cervical intraepithelial neoplasia (CIN) and is strongly overexpressed in HPV induced cervical cancer [106]. Therefore, $p16^{INK4a}$ is considered as a marker for early diagnosis and is routinely used as a highly specific marker for CIN and transforming HPV infections [106-110]. $p16^{INK4a}$ overexpression increases with the severity of cytological/histological abnormality and immunostaining correlates with it [22, 108, 111] as shown in Figure 6.

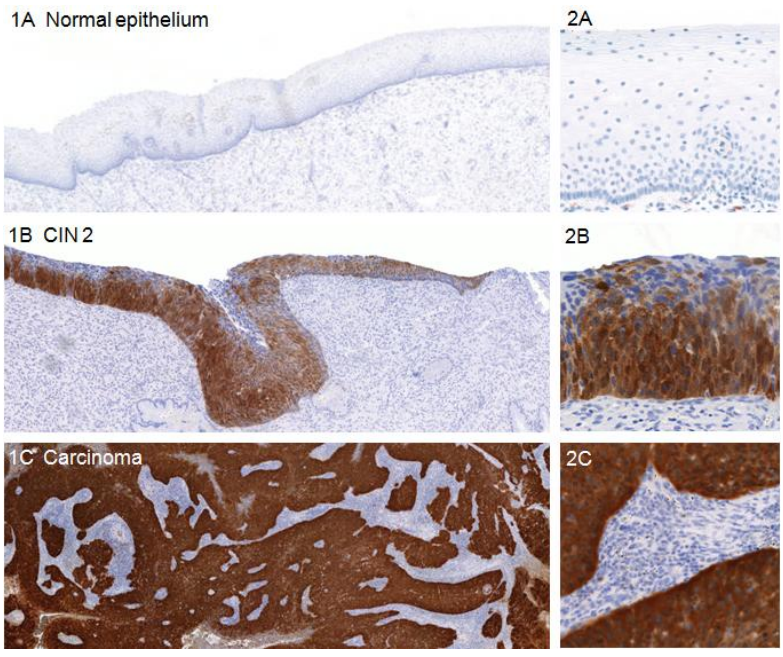

Figure 6: Representative examples of $p16^{INK4a}$ immunohistochemistry. 1: Tissue overview, 2: Enlargement. A: $p16^{INK4a}$ negative normal epithelium, B: $p16^{INK4a}$ positive epithelium of grade II cervical intraepithelial neoplasia (CIN2), C: invasive carcinoma with strong $p16^{INK4a}$ immunoreactivity. (The IHC image was kindly provided by Dr. M. Reuschenbach.)

3.1 Structure and function

$p16^{INK4a}$ is a tumor suppressor protein with a molecular weight of 16 kDa (156 aa). The protein structure shows four contiguous ankyrin repeats (see Figure 7) [112], a protein motif consisting of two alpha helices separated by loops. $p16^{INK4a}$ is encoded by chromosome 9p21 within the INK4a/ARF locus [113]. The INK4 family of CDK inhibitors includes four members with similar biochemical properties: $p15^{INK4b}$, $p16^{INK4a}$, $p18^{INK4c}$ and $p19^{INK4d}$ [114-116]. Mutations and deletions of $p15^{INK4B}$ and $p16^{INK4a}$ are frequently observed in different malignancies and $p16^{INK4a}$ is one of the most direct links between cell cycle control and cancer [117, 118].

Figure 7: Structure of the cyclin-dependent Kinase 4 Inhibitor a ($p16^{INK4a}$) containing 4 helix-turn-helix motifs linked by three loops.
Structure obtained from MMDB [119]: Solution NMR Structure of Tumor Suppressor $p16^{INK4a}$, MMDB ID: 11736

Cyclin-dependent kinases (CDKs) form complexes with cyclins and are thereby activated. The Cyclin-dependent kinase inhibitor 2A, also known as $p16^{INK4a}$, acts as a negative regulator of the proliferation of normal cells by interacting strongly with CDK4 and CDK6. This inhibits their ability to interact with cyclins D and to phosphorylate the retinoblastoma protein (RB). Precisely, $p16^{INK4a}$ expression keeps RB in a hypophosphorylated state what promotes binding of E2F to RB and thereby leads to G1 cell cycle arrest.

HPV oncogene expression and evidence of its deregulation can be monitored through detection of the cellular protein $p16^{INK4a}$ [120] as E6 and E7 disrupt cell cycle checkpoints and affect almost all CDK inhibitors which are linked to the G1 and G2 checkpoints [117]. E7 expression causes an addiction of cervical cancer cell lines to the H3K27 targeting histone lysine demethylase (KDM6B) [53] (see also 1.1.3). E7 triggers oncogene induced stress (OIS), a cell-intrinsic tumor-suppressive mechanism, but on the other hand targets pRB for proteosomal degradation as pRB is a key mediator of OIS. The E7 caused epigenetic de-repression is mediated by $p16^{INK4a}$ that was reported to be an important KDM6B downstream target and its expression is necessary for the survival of E7-expressing cells [121]. Therefore, the role of $p16^{INK4a}$ as a tumor suppressor protein is somehow controversial, at least in HPV16 E7 expressing cells, as its biological activity is more akin to that of an oncogene [121].

E7 inactivates pRB and thereby indirectly induces $p16^{INK4a}$ expression and accumulation [117, 122]. Similarly, the degradation of the tumor suppressor p53 due to elevated E6 levels can also result in upregulation of $p16^{INK4a}$ expression [118]. In summary, the increased $p16^{INK4a}$ expression in HPV-associated tumors can be interpreted as attempt to stop uncontrolled proliferation [123]; but as $p16^{INK4a}$ is released from its negative feedback control by pRB inactivation and KDM6B overexpression, elevated levels of this protein do not lead to cell cycle arrest in tumor cells.

3.2 Chimeric constructs containing $p16^{INK4a}$ and L1

In HPV-transformed precursor lesions and invasive carcinomas the cellular tumor suppressor $p16^{INK4a}$ is strongly overexpressed, whereas in normal tissues barely any $p16^{INK4a}$ expression is detectable. Therefore, $p16^{INK4a}$ is considered to be an interesting target for immunotherapy in patients with HPV-associated cancers. In fact, there is evidence for spontaneous immune responses against $p16^{INK4a}$ since antibodies against $p16^{INK4a}$ can be found in some individuals indicating no complete tolerance against this self-antigen [124]. The first clinical vaccination trial with a p16 peptide in patients with advanced HPV-associated cancers is currently being conducted [125].

In contrast to E6 and E7, HPV L1 decreases gradually according to the severity of cervical neoplasia. $p16^{INK4a}$ expression also increases with infection progression (see Figure 8). Combined expression patterns of $p16^{INK4a}$ and L1 may thus serve as useful biomarkers for the early diagnosis, prognosis and follow-up of cervical dysplastic lesions [126-128].

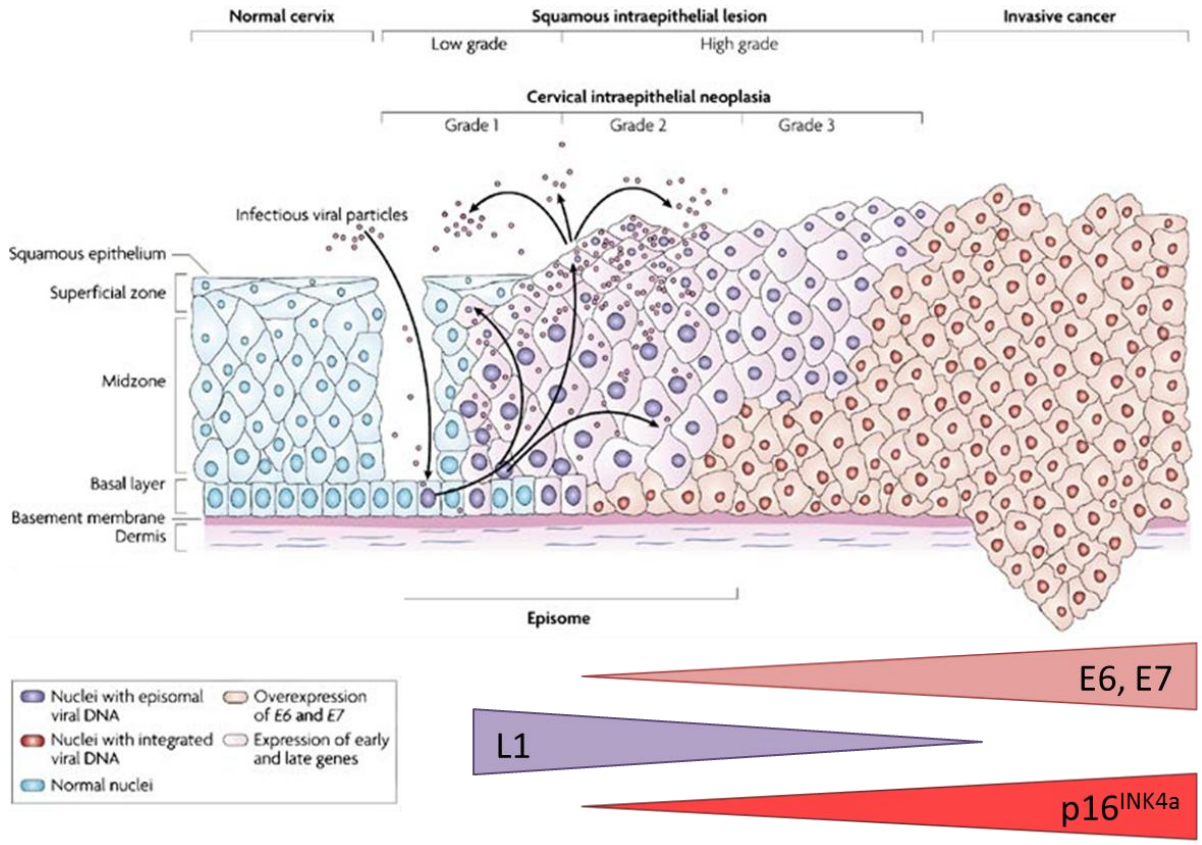

Figure 8: HPV-mediated progression from CIN to invasive cervical carcinoma. HPVs invade the basal membrane through micro abrasions in the epithelial layer. The early genes E1, E2, E4, E5, E6 and E7 are expressed from episomal DNA while the genome is further replicated. The late genes L1 and L2 are expressed in the midzone and superficial zone. Some HPV infections progress to high grade CIN and cervical cancer as the HPV genome becomes integrated into the host chromosomes. This leads to a disruption of E2 and upregulation of oncogene E6 and E7 expression. L1 is barely found in progressing lesions, but $p16^{INK4a}$ expression increases with severity of neoplasia. Modified from Woodman et al. 2007, Nat Rev Cancer 7 [53]

An approach that targets $p16^{INK4a}$ and HPV16 L1 simultaneously could provide a combined prophylactic and therapeutic vaccine with global impact. If it would be possible to raise sufficient and functional immune responses against $p16^{INK4a}$ and thereby guide the immune system to the deregulated malignant cells, a variety of cancers could be treated with such a medicament.

4 Rational and Aims of the project

Despite substantial progress in prophylactic vaccination, there are several challenges left:

- The prophylactic vaccines only induce type-specific immunity and have therefore a negligible prophylactic effect on other HPV types.
- Furthermore they are costly due to the production in mammalian, respectively insect cells.

- A cold chain for transportation is necessary as these vaccines are not stable at room temperature what further increases the cost factor.
- Apart from that it would be necessary to apply prophylactic vaccination widely to achieve an effect for the society and this is hard to accomplish in developing countries, where health systems are problematic, vaccine coverage is poor but need is significant.
- Even screening is not available to all women and mortality and morbidity of HPV-associated malignancies are therefore still high.

This reveals an urgent need for an effective therapeutic HPV vaccine, especially in developing countries.

The objective of this thesis was to generated, purify and evaluate a cost-effective second generation therapeutic vaccine based on chimeric capsomeres as a protein-based vaccine that can be easily produced in bacteria and is stable also when cold-chains are interrupted. This could have substantial benefit, especially for unindustrialized countries.

The tumor suppressor $p16^{INK4a}$ was found to be strongly expressed in CIN and cervical cancer, although its function is abolished in these conditions. It is thus used as a diagnostic marker for several years with high success and targeting $p16^{INKa}$-overexpressing cells with a therapeutic vaccine could have high benefit for patients suffering from HPV induced neoplasia and cancer. This strategy is a promising alternative to currently investigated vaccination attempts based on the induction of an E6 and/or E7-specific immune response. Like the prophylactic vaccines, E6 and E7 based formulations again present the problem of type-specific immunity whereas $p16^{INK4a}$ expression is universal.

To achieve the ambitious aim of developing a therapeutic vaccine the following tasks had to be implemented.

1. Cloning of three different constructs into the bacterial expression system:

   To evaluate the antigenic effect of different structural isoforms three constructs containing L1 and $p16^{INK4a}$ should be generated. Therefore, the complete $p16^{INK4a}$ encoding cDNA sequence will be cloned a) upstream and b) downstream of a modified HPV16 L1 sequence [76] into a pGex-4T-2 expression vector. For the third construct c) the helix 4 region of L1 will be replaced by $p16^{INK4a}$ [129].

2. Expression of the fusion proteins in E. coli:

   The GST-fusion proteins will be expressed in E. coli strains BL21 and Rosetta and the expression characteristics of the fusion proteins will be evaluated in terms of solubility and yield.

3. Purification of bacterial fusion proteins:

   Different purification strategies will be evaluated in consideration of purity, protein structure and yield. Endotoxin removal will be achieved by Triton X-114 phase separation as this method was shown to be suitable for the removal of LPS [130].

4. Evaluation of protein purification and structural characterization:

   Protein expression and purification will be evaluated by Coomassie staining and Western blot analysis. Particle assembly will be verified by electron microscopy, ELISA and sedimentation analysis.

5. Immunological trials:

   The immunogenicity of the chimeric capsomeres will be evaluated in a CL57BL/6 mouse model. Therefore, the animals will be immunized and the humoral and cellular immune response will be measured with ELISA, respectively ELISpot assay.

II. Materials and Methods

5 Materials

5.1 Biological Materials

5.1.1 *Bacteria*

Competent cells:

Table 1: Competent E. coli cells. Resistance, genotype, key features and suppliers are listed.

Strains	Resistance	Genotype and Key Features	Supplier
BL21-T1^{R}	no	F^- ompT $hsdS_B$ (r_B- m_B-) gal dcm tonA • does not contain the *lon* protease. • is also deficient in the outer membrane protease, *OmpT*. • lack of these proteases reduces degradation of heterologous proteins expressed in this strain.	Sigma-Aldrich, Steinheim
Rosetta	Chlor-amphenicol	F^- ompT $hsdS_B$ (r_B- m_B-) gal dcm pRARE (argU, argW, ilex, glyT, leuW, proL) • Express rare tRNAs for AGG, AGA, AUA, CUA, CCC, GGA codons • facilitates expression of genes that encode rare E. coli codons	Novagene (Merck), Darmstadt
Top10	no	F- mcrA Δ(mrr-hsdRMS-mcrBC) Φ80lacZΔM15 Δ lacX74 recA1 araD139 Δ(araleu)7697 galU galK rpsL (StrR) endA1 nupG • *hsdR* for efficient transformation of unmethylated DNA from PCR amplifications • *mcrA* for efficient transformation of methylated DNA from genomic preparations • *lacZM15* for blue/white color screening of recombinant clones • *endA1* for cleaner preparations of DNA and better results in downstream applications due to elimination of non-specific digestion by Endonuclease I • *recA1* for reduced occurrence of non-specific recombination in cloned DNA	Invitrogen, Carlsbad, USA

5.1.2 *Cell lines*

RMA-S a sub-line of the Rauscher-virus-induced lymphoma RBL-5 of C57BL/6 (H-2h) background [131, 132]
Cultivation medium: RPMI (see 5.3.2 for receipt)

TC-1 derived from lung epithelium of C57BL/6 mice, cotransformed with HPV16 E6 and E7 and c-Ha ras oncogenes [133]
Cultivation medium: TC-1 medium (see 5.3.2 for receipt)

C3 C57BL/6 mouse embryo cells transfected with full-length HPV16 genome [134]
Cultivation medium*:* C3-medium (see 5.3.2 for receipt)

2F11 RMA-E7 (HPV-16 E7 WT gene) transfectant [135]
Cultivation medium*:* RPMI (see 5.3.2 for receipt)

Hela cervical cancer cell line of a tumor of a patient named Henrietta Lacks [136]
Cultivation medium: RPMI (see 5.3.2 for receipt)

5.1.3 *Animals*

Female C57BL/6J (H2Db) mice at an age of 7 weeks were specified pathogen-free and kept under pathogen-free conditions in individually ventilated cages at the animal facility of the German Cancer Research Center (DKFZ, Heidelberg, Germany). Mice were purchased from Charles River WIGA Laboratories (Sulzfeld, Germany)

5.2 Molecular biological materials

5.2.1 *Plasmids*

Original vectors

pUC57 common used plasmid cloning vector in E. coli; vector length 2,710 bp; isolated from E. coli strain DH5α (GeneScript, Piscataway, NJ, USA)

pmaxGFP plasmid encoding maxGFP, a green fluorescent protein from the copepod Pontellina plumata, used to test transfection efficiency with fluorescent microscopy (Lonza, Walkersville, MD, USA)

pGex-4T-2 glutathione S-transferase fusion vector with a thrombin protease site to cleave protein from fusion, vestor length 4,970 bp (GE Healthcare, Uppsala, Sweden)

The original pGex-4T-2 vector did not contain a HindIII restriction site. It was introduced in previous trials upstream of the SalI site by PCR. This work was conducted in the division of Genome Modifications and Carcinogenesis (DKFZ Heidelberg, Germany) under supervision of Prof. Lutz Gissmann. The modified pGex-4T-2 vector pGex-L1ΔN10Δ408-431ΔC29-E7 including the HPV16 L1 and E7 genes was kindly provided by Dr. Lysann Schädlich.

Expression plasmids

The following modification key gives an overview of the used abbreviations for the description of expression plasmids

Table 2: Modification key for the generated expression plasmids.

L1	HPV16 L1 gene (wildtype)
ΔN10	deletion of 10 aas at the N-terminus
ΔC29	deletion of 29 aas at the C-terminus
Δh4	deletion of aas 408-431 that comprise the helix 4 region of HPV16 L1
$p16^{INK4a}$	full length cyclin-dependent kinase inhibitor 2A protein (CDKN2A, $p16^{INK4a}$), human

The following pGex plasmids were cloned (BamHI / HindIII) and used for the expression of GST fusion proteins in E. coli during this thesis.

pGex-L1ΔN10Δh4ΔC29: modified HPV16 L1, forms capsomeres
pGex-$p16^{INK4a}$: full length human $p16^{INK4a}$ gene
pGex-L1ΔN10Δh4ΔC29-$p16^{INK4a}$ (construct 1): contains the full-length human $p16^{INK4a}$ gene fused to the C terminus of the modified L1
pGex-$p16^{INK4a}$-L1ΔN10Δh4ΔC29 (construct 2): contains the full-length human $p16^{INK4a}$ gene fused to the N terminus of the modified L1
pGex-L1ΔN10Δh4-$p16^{INK4a}$-L1ΔC29 (construct 3): contains the full-length human $p16^{INK4a}$ gene inserted at the helix 4 position of the modified L1

Plasmid maps for the three chimeric pGex-4T-2 constructs consisting of L1 and $p16^{INK4a}$ can be found in VII (Appendix).

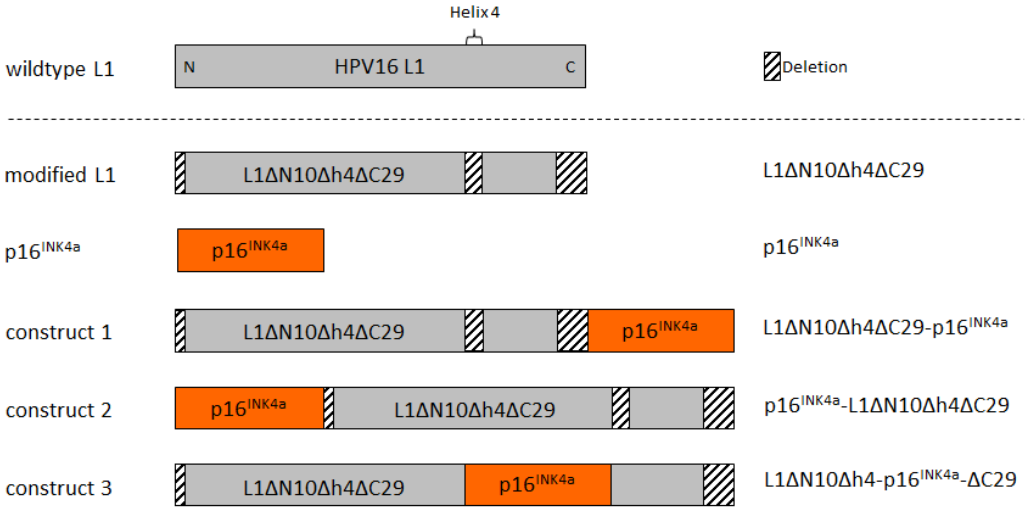

Figure 9: HPV16 L1 - p16^{INK4a} capsomere constructs depicted in cartoon format. The wild-type L1 protein is displayed at the top. Modified L1 and p16^{INK4a} alone were used as controls during immunization studies and were therefore also cloned and expressed in E. coli.

5.2.2 *Oligonucleotides*

Oligonucleotide primers were synthesized by Thermo Scientific (Ulm, Germany). Restriction sites are underlined.

Cloning of pGex-L1ΔN10Δh4ΔC29-p16^{INK4a}

p16_NsiI_forward 5': TTTTATGCATATGGAGCCGGCGGCGGGG

p16_HindIII_reverse 3': TTTTAAGCTTTCAATCGGGGATGTCTGA

for amplification of p16^{INK4a} from Hela cDNA and introduction of restriction sites

Cloning of pGex-p16^{INK4a}-L1ΔN10Δh4ΔC29 with overlap PCR

p16_BamHI_forward 5': TTTTGGATCCATGGAGCCGGCGGCGGGG
for amplification of p16^{INK4a} from Hela cDNA and introduction of BamHI restriction site

p16L1_reverse 3': GACAGGAGGCAAGTAGACATCGGGGATGTCTGAGGG
for amplification of p16^{INK4a} from Hela cDNA and introduction of overlap for combination with L1 insert

p16L1_forward 5': CCCTCAGACATCCCCGATGTCTACTTGCCTCCTGTC
for amplification of L1 DNA (L1ΔN10Δh4ΔC29) from pGex-L1ΔN10Δh4ΔC29-E7

L1_HindIII_reverse 3': TTTTAAGCTTTTAGGCCTTCAATCCTGC
for amplification of L1 DNA (L1ΔN10Δh4ΔC29) from pGex-L1ΔN10Δh4ΔC29-E7 and introduction of HindIII restriction site

p16^{INK4a} insert check primer

p16^{INK4a}_forward 5': CTTCCTGGACACGCTGGT

p16^{INK4a}_reverse 3': GCATGGTTACTGCCTCTGGT

L1 insert check primer

L1d_forward 5': TTTTGAACCATATGGCGACAGCTT

L1d_reverse 3': TTTTATTATTGTGGCCCTGTGCTC

L1-p16 overlap check primer

L1p16_forward 5': CAGTTTCCTTTAGGACGCAAA

L1p16_reverse 3': CATCATCATGACCTGGATCG

p16-L1 overlap check primer

seq_p16L1_reverse 3': TAGGGATGTCCAACTGCAAG

p16^{INK4a}_forward 5': CTTCCTGGACACGCTGGT

Sequencing primer

L1d_forward 5': TTTTGAACCATATGGCGACAGCTT
L1p16_forward 5': CAGTTTCCTTTAGGACGCAAA
p16^{INK4a}_forward 5': CTTCCTGGACACGCTGGT
pGex-4T-2_reverse 3': GGCAGATCGTCAGTCAGTCA
pGex-4T-2_seq 5': GGGCTGGCAAGCCACGTTTGGTG
seq_L1p16_forward 5': CACCTCCAGCACCTAAAGAAG
seq_p16L1_forward 5': TTGAAGCTATCCCACAAATTGA

5.2.3 *Peptides*

Peptides were synthesized by Genaxxon Bioscience GmbH (Ulm, Germany).

HPV16 L1	165-173	AGVDNRECI, H2-Db-restricted CTL epitope of HPV16 L1 [137]	
p16^{INK4a}	1-20	MEPAAGSSMEPSADWLATAA	"1"
p16^{INK4a}	13-32	ADWLATAAARGRVEEVRALL	"2"
p16^{INK4a}	25-44	VEEVRALLEAGALPNAPNSY	"3"
p16^{INK4a}	37-56	LPNAPNSYGRRPIQVMMMGS	"4"

$p16^{INK4a}$	49-68	IQVMMMGSARVAELLLLHGA	“5”
$p16^{INK4a}$	61-80	ELLLLHGAEPNCADPATLTR	“6”
$p16^{INK4a}$	73-92	ADPATLTRPVHDAAREGFLD	“7”
$p16^{INK4a}$	85-104	AAREGFLDTLVVLHRAGARL	“8”
$p16^{INK4a}$	97-116	LHRAGARLDVRDAWGRLPVD	“9”
$p16^{INK4a}$	109-128	AWGRLPVDLAEELGHRDVAR	“10”
$p16^{INK4a}$	121-140	LGHRDVARYLRAAAGGTRGS	“11”
$p16^{INK4a}$	133-152	AAGGTRGSNHARIDAAEGPS	“12”
$p16^{INK4a}$	145-156	IDAAEGPSDIPD	“13”

$p16^{INK4a}$	137-145	TRGSNHARI, H2-Db-restricted CTL epitope of $p16^{INK4a}$
$p16^{INK4a}$	113-121	LPVDLAEEL, H2-Db-restricted CTL epitope of $p16^{INK4a}$
$p16^{INK4a}$	55-63	GSARVAELL, H2-Db-restricted CTL epitope of $p16^{INK4a}$

(these 3 peptides were predicted using the SYFPEITHI epitope prediction algorithm [138].)

$p16^{INK4a}$	37-63	LPNAPNSYGRRPIQVMMMGSARVAEL (“Vicoryx peptide”, [125])

All peptides were delivered lyophilized and dissolved in sterile DMSO at a final concentration of 1 mg/ml or 5 mg/ml. For ELISA (6.6.2) and ELISpot assay (6.6.3), peptide working solutions of 0.5 µg/µl in PBS were prepared.

5.2.4 *Antibodies*

Designation	Specificity	Species	Conc.	Application	Source / Reference
D7D7 -HRP	human $p16^{INK4a}$ (monoclonal)	mouse		WB 1:5000	MTM Laboratories, Heidelberg
E6H4 -HRP	human $p16^{INK4a}$ (monoclonal)	mouse		WB 1:5000	MTM Laboratories, Heidelberg
F-4 (sc-74401)	murine $p16^{INK4a}$ (monoclonal)	mouse	0.2 mg/ml	WB 1:500	Santa Cruz Biotechnology, Heidelberg
MD2H11	HPV16 L1 (monoclonal)	mouse	0.2 mg/ml	WB 1:500	Santa Cruz Biotechnology, Heidelberg
#4543	HPV16 L1 (polyclonal)	rabbit	0.2 µg/ml	ELISA 1:500	Prof. Martin Müller, DKFZ, Heidelberg

#1.3.5.15 (Ritti01)	HPV16 L1 (monoclonal)	mouse		ELISA 1:1000	Prof. Martin Müller, DKFZ, Heidelberg
9A1/2	E. coli GroEl (monoclonal)	mouse	1 mg/ml	WB 1:1000	Abcam, Cambridge, UK
rabbit α-mouse IGG -HRP	mouse (polyclonal)	rabbit	0.8 mg/ml	WB 1:5000 ELISA 1:5000	Thermo Scientific, Rockford, USA
goat α- rabbit IGG-HRP	rabbit (polyclonal)	goat		WB 1:2000	Cell Signaling, Cambrigde, UK
IFNγ (clone R4-6A2)	murine IFNγ (monoclonal)	rat	1 mg/ml	ELISpot (5 µg/ml)	BD Biosciences Pharmingen, Heidelberg
IFNγ biotin-conjugate (clone XMG1.2)	murine IFNγ (monoclonal)	rat	0.5 mg/ml	ELISpot (1 µg/ml)	BD Biosciences Pharmingen, Heidelberg
LS-C15	schistosoma japonicum (polyclonal)	goat	10 mg/ml	CnBr chromatography	Biozol, Eching, Germany
H1JG, clone 7	schistosoma japonicum (monoclonal)	rabbit		ProteinG affinity chromatography	Prof. Martin Müller, DKFZ, Heidelberg

5.3 Media and Supplements

5.3.1 *Bacteria Culture*

LB medium (Luria Bertani):
1 % tryptone
0.5 % yeast extract
1 % NaCl
in aqua bidest.
adjust pH to 7.0 with 5 M NaOH;
sterilized by autoclaving

LB medium for agar plates:
1 % tryptone
0.5 % yeast extract
1 % NaCl
2 % Difco-Bacto-Agar
in aqua bidest.

	adjust pH to 7.0 with 5 M NaOH
	sterilized by autoclaving
	after cooling to 50°C addition of relevant antibiotics
Terrific broth medium	12 g tryptone
Component A:	24 g yeast extract
	4 ml glycerol
	Ad 900 ml aqua bidest.
	sterilized by autoclaving
	Ad 1 L component B before use
Terrific broth medium	23.12 g KH_2PO_4
Component B:	125.41 g K_2HPO_4
	ad 1 L aqua bidest.
	sterilized by autoclaving

Antibiotics

Ampicillin	final conc. 100 µg/ml	Sigma Aldrich, Steinheim, Germany
Chloramphenicol	final conc. 200 µg/ml	Sigma Aldrich, Steinheim, Germany

Chemicals

Sorbitol	Sigma Aldrich, Steinheim, Germany
Betaine	Sigma Aldrich, Steinheim, Germany
IPTG solution 100 mM	40 mg/ml IPTG in aqua bidest.

5.3.2 *Mammalian cell culture*

Trypan Blue solution 0.4%	Sigma Aldrich, Steinheim, Germany

Media

RPMI 1640 liquid with L-Glutamine	PAA Cell Culture Company, Cambridge, UK
	Gibco Life Technologies, Carlsbad, CA, USA
Opti-MEM	Gibco Life Technologies, Carlsbad, CA, USA

Supplements

Penicillin/Streptomycin solution 100 x (5.000 U/ml Pen, 5.000 U/ml Strep)	Gibco Life Technologies, Carlsbad, CA, USA

Fetal Bovine Serum	PAA Cell Culture Company, Cambridge, UK
Geneticin (G418)	Gibco Life Technologies, Carlsbad, CA, USA
L-Glutamine	Sigma Aldrich, Steinheim, Germany
β-mercaptoethanol	Sigma Aldrich, Steinheim, Germany
MEM Non-essential amino-acid solution	Sigma Aldrich, Steinheim, Germany
Sodium pyruvate solution (100 mM)	Sigma Aldrich, Steinheim, Germany
Trypsin (0.25 %)/EDTA	PAA Cell Culture Company, Cambridge, UK

Specific media – recipes

RPMI	RPMI		
	10	%	FCS
	1	%	Penicillin/Streptomycin
	1	%	L-Glutamine
TC-1 medium	RPMI		
	10	%	FCS
	1	%	Penicillin/Streptomycin
	100	µM	β-mercaptoethanol
	0.4	mg/ml	Geneticin
	1	mM	Sodium pyruvate
	1 x MEM Non-essential amino-acid solution		
C3-medium	RPMI		
	10	%	FCS
	1	%	Penicillin/Streptomycin
	2	mM	L-Glutamine
	100	µM	β-mercaptoethanol
	0.1	mg/ml	Kanamycin

5.4 Material for molecular biological and protein technical methods

5.4.1 *Preparation, manipulation and analysis of DNA*

Kits

High pure PCR product purification kit	Roche, Mannheim, Germany
QIAQuick Gel Extraction Kit	Qiagen, Hilden, Germany
QIAGEN Plasmid Mini Kit	Qiagen, Hilden, Germany

QIAGEN Plasmid Maxi Kit	Qiagen, Hilden, Germany
QIAGEN EndoFree Plasmid Maxi Kit	Qiagen, Hilden, Germany

Enzymes

A *Restriction Enzymes*

HindIII HF	New England Biolabs, Frankfurt/M, Germany
BamHI-HF	New England Biolabs, Frankfurt/M, Germany
NsiI	Promega, Medison, USA

B *Polymerases*

Taq DNA Polymerase	Invitrogen, Life Technologies, Carlsbad, USA
HOT FIREPol® DNA Polymerase	Solis Biodyne, Tartu, Estonia

C *Ligation Enzymes*

T4 DNA Ligase	Roche, Mannheim, Germany
Alkaline Phosphatase	Sigma-Aldrich, St. Louis, USA

Chemicals

dNTP Mix (2.5 mM per nucleotide)	Invitrogen, Life Technologies, Carlsbad, USA
DMSO	
$MgCl_2$	Solis Biodyne, Tartu, Estonia
	Invitrogen, Life Technologies, Carlsbad, USA
10 x PCR Buffer	Solis Biodyne, Tartu, Estonia
	Invitrogen, Life Technologies, Carlsbad, USA

DNA marker/ ladder

100 bp DNA ladder	Invitrogen, Life Technologies, Carlsbad, USA
1 kbp ladder	Gibco Life Technologies, Carlsbad, CA, USA

DNA Sequencing GATC, Konstanz, Germany

In-house DNA Sequencing

BigDye® Terminator v3.1 Cycle Sequencing Kit including

- Ready Reaction Mix (RR-Mix)
- BigDye Terminator v1.1/3.1 Sequencing Buffer (5X)

by Applied Biosystems, Life Technologies, USA

Agarose gel electrophoresis

10 x Loading Dye	250 mg bromphenol blue in 33.0 ml 150 mM Tris pH 7.6 60 ml glycerol 7.0 ml aqua bidest add 66.7 ml aqua bidest. to receive 6 x Loading Dye ready for use
10 x TBE Buffer	121.14 g Tris 51.32 g boric acid 3.72 g EDTA ad 1 L with aqua bidest.
Agarose Gel 1%	1 % Agarose (w/v) 0.3 µg/µl Ethidium Bromide in 1 x TBE Buffer

5.4.2 *Protein purification*

Columns and Concentration Filters

Amicon Ultra-15 Centrifugal Filter Units 100kDa	Merck Millipore, Billerica, MA, USA
Amicon Ultra-30 Centrifugal Filter Units 100kDa	Merck Millipore, Billerica, MA, USA
CNBr-Activated Sepharose 4 FF	GE Healthcare, Uppsala, Sweden
Gelfiltration Calibration Kit	GE Healthcare, Uppsala, Sweden
GST Detection Module	GE Healthcare, Uppsala, Sweden
GSTrapTM FF column 1 ml	GE Healthcare, Uppsala, Sweden
GSTrapTM FF column 5 ml	GE Healthcare, Uppsala, Sweden
Protein G Sepharose FF	GE Healthcare, Uppsala, Sweden
Q-Sepharose FF	GE Healthcare, Uppsala, Sweden
Superdex 200 10/300	GE Healthcare, Uppsala, Sweden

Chemicals and Materials

cOmplete® Protease Inhibitor Cocktail (EDTA free)	Roche, Mannheim, Germany
Dialysis Tube Spectra/Por Membrane 3.500	Spectrum, Serva, Heidelberg, Ger
Dithiothreitol (DTT)	Roth, Karlsruhe, Germany

Enzymes:

Thrombin protease	GE Healthcare, Uppsala, Sweden
Lysozyme	Roche, Mannheim, Germany

Buffers and Solutions - Chromatography

Glutathione solution	20 mM Glutathione S reduced in appropriate buffer
Column storage solution	20 % Ethanol

- *GSTrap Affinity Chromatography:*

Buffer L	50 mM Tris 0.2 M NaCl 1 mM EDTA 2 mM DTT pH 8.2
Buffer L_{mod}	50 mM Tris 0.5 M NaCl 1 mM EDTA 5 mM DTT 0.01% Tween80 pH 8.2
Buffer L_{p16}	50 mM Tris 0.1 M NaCl 1 mM EDTA 1 mM DTT pH 8.0
ATP	0.5 M
$MgCl_2$	1 M
Thrombin incubation solution	40 u / ml Buffer L
Column cleaning solution	6 M Guanidinium hydrochloride

- *Ion Exchange Chromatography:*

IEX Buffer	10 mM Tris

	0,1 mM TCEP
	0,05 mM EDTA
	0,01 % Tween80
	pH 8.0

➢ *Protein G Affinity Chromatography*

Buffer L_{p16}	50 mM Tris
	0.1 M NaCl
	1 mM EDTA
	1 mM DTT
	pH 8.2
Buffer 2	50 mM Tris
	0.1 M NaCl
	1 mM EDTA
	1 mM DTT
	20 % (v/v) Glycerol
	pH 8.0
Buffer L_{mod}	50 mM Tris
	0.5 M NaCl
	1 mM EDTA
	5 mM DTT
	0.01 % Tween80
	pH 8.2

➢ *CnBr Affinity Chormatography*

	10 mM Tris
	0.05 mM EDTA
	0.1 mM DTT
	0.045 % (v/v) L-Sarkosine
	pH 8.0
Column cleaning solution	3 M KCl

➢ *Size exclusion chromatography:*

Buffer L_{mod}	50 mM Tris

	0.5 M NaCl
	1 mM EDTA
	5 mM DTT
	0.01 % Tween80
	pH 8.2
Column cleaning solution	20 % EtOH (regular cleaning)

Buffers and Solutions - Inclusion Body Purification

- *Inclusion Body Preparation - Buffers:*

IB Resuspension Buffer	50 mM Tris-HCl
	50 mM NaCl
	0.5 mM EDTA
	1 mM DTT
	5 % Glycerol
	pH 8.0
IB Wash Buffer	50 mM Tris-HCl
	50 mM NaCl
	0.5 mM EDTA
	1 mM DTT
	5 % Glycerol
	1 % Triton X-100
	pH 8.0

- *Denaturing Solutions*:

Urea	4, 6, 8 M in Denaturing Buffer
Guanidinehydrochlorid	7 M in Denaturing Buffer
N-Lauroylsarcosine	3.5 % (v/v)
GuHCl Denaturing Buffer	50 mM Tris
	0.2 M NaCl
	2 mM EDTA
	5 mM DTT
	0.01 % Tween80
	pH 8.0

L-Sarcosine Denaturing Buffer	50 mM Tris
= Urea Denaturing Buffer	0.05 M NaCl
	0.5 mM EDTA
	5 mM DTT
	5 % Glycerol
	pH 8.0

- *Dialysis / Refolding Buffer:*

For protein refolding after denaturing with urea or GuHCl the corresponding denaturing buffers were also used for refolding with step-wise decreasing concentrations of the denaturing agent.

L-Sarcosine Dialyis Buffer	10 mM Tris
	0.05 mM EDTA
	0.1 mM DTT
	0.06 % (v/v) L-Sarcosine
	pH 8.0

Dialysis / Refolding Buffer Screen

50 mM Tris
2 mM DTT

NaCl [M]	Glycerol [%]	NaCl [M] + 10 % Glycerol
0.05	0	0.05
0.1	5	0.1
0.2	10	0.2
0.35	20	

Rapid Dilution Refolding:

Buffer 1	50 mM Tris
	0.05 M NaCl
	0.5 mM EDTA
	5 mM DTT
	5 % (v/v) Glycerol
	pH 8.0
Buffer 2	50 mM Tris
	0.1 M NaCl

	1 mM EDTA
	1 mM DTT
	20 % (v/v) Glycerol
	pH 8.0

5.4.3 *Endotoxin detection, quantification and removal*

QCL-1000 Endpoint Chromogenic LAL Assay	Lonza, Walkersville, MD, USA
LAL Reagent Water	Lonza, Walkersville, MD, USA
LAL reagent grade multi-well plates	Lonza, Walkersville, MD, USA
Triton X-114	Sigma, Steinheim, Germany

5.4.4 *Analysis of proteins*

Standard Solutions

1 x PBS	140 mM NaCl
	2.7 mM KCl
	8.1 mM Na_2HPO_4
	1.5 mM KH_2PO_4
	pH 7.4
PBS-T	0.05 % Tween20
	in 1x PBS
Blocking solution (ELISA)	0.05 % caseine (w/v)
	In PBS-T
1 x TBS	50 mM Tris
	150 mM NaCl
	pH 7.6
TBS-T	0.05 % Tween20
	in 1x TBS
Blocking solution (WB)	5 % milk powder (w/v)
	in TBS-T
Stripping buffer (WB)	33.5 ml aqua bidest.

10 ml SDS 10 %
6.25 ml 0.5 M Tris pH 6.8
350 µl ß-mercaptoethanol

Coomassie G-250 Staining Solution

a) SimplyBlue™ SafeStain

b) Coomassie Staining Solution:

0.02 % Coomassie Brilliant Blue G-250	100 mg
2 % (w/v) phosphoric acid	10 ml
5 % aluminium sulfate	25 g
10 % ethanol (96 %)	50 ml
in aqua bidest.	ad to 500 ml

First of all, aluminium sulfate was dissolved in 250 ml aqua bidest. Then, ethanol was homogenized and subsequently Coomassie Brilliant Blue G-250 was added and dissolved. In a last step, phosphoric acid was added and the solution was filled up with aqua bidest to 500 ml.

Kits

2-D Quant Kit	GE Healthcare, Uppsala, Sweden
SilverQuest™ Silver Staining Kit	Invitrogen, Life Technologies, Carlsbad, USA

SDS-Polyacrylamide gel electrophoresis (SDS-PAGE) and Western Blot

20 x NuPAGE MES SDS Running Buffer
Nitrocellulose Membrane Filter Paper Sandwich 0.45 µm
NuPAGE 10 x Reducing agent
NuPAGE 4 x LDS sample buffer
NuPAGE Novex 4-12% Bis-Tris Gels, 1.0 mm, 12 well and 17 well
X-Cell Blot Module
X-Cell Sure Lock gel chamber
The above listed SDS-PAGE and western blot equipment was all supplied by Invitrogen Life Technologies, Carlsbad, USA.

Power supply Consort E853	Consort, Turnhout, Belgium

Protein Marker:

Precision Plus Protein Standard	Bio-Rad, Munich, Germany
Precision Plus WesternC Standard	Bio-Rad, Munich, Germany

5.4.5 *Electron microscopy*

Carbon-coated copper grid (400 meshes)	Plano, Wetzlar, Germany
CCD-Camera	Proscan, Lagerlechfeld, Germany
Electron microscope EM 912	Zeiss, Jena, Germany
Uranyl acetate solution	1 % uranyl acetate in aqua bidest.
Whatman paper No.10	Schleicher&Schuell, Dassel, Germany

5.4.6 *Sedimentation analysis*

Gradient mixer	kindly provided by Dr. Daniele Viarisio (DKFZ, Heidelberg, Germany)
Ultracentrifugation tubes (14 x 95 mm, PA)	Beckmann, Palo Alto, CA, USA
Refractometer	Schmidt-Haenisch, Berlin, Germany
Sucrose solutions:	5 % Sucrose (w/v) 50 % Sucrose (w/v) in dialysis buffer (5.4.2), sterilized by filtration

5.5 Material for the immunization of mice and analysis of immune response

5.5.1 *Immunizations*

Needles G23	B Braun, Melsungen, Germany
Lancets Solofix	B Braun, Melsungen, Germany
Electric razer	Ermila, Harotec GmbH, Berlin, Germany
Montanide ISA-51 adjuvant	Seppic, Puteaux Cedex, France
Syringes 0.01 - 1 ml Injekt-F	B Braun, Melsungen, Germany
Ear mark pincer KN-292B 2.0	Napox, Natsume Seisakusho, Tokyo, Japan

5.5.2 *ELISA*

F96 Maxisorp Immuno plates	NUNC Fisher Scientific, Denmark
TMB (3,3` 5,5` Tetramethylbenzidine)	Sigma, Steinheim, Germany
1 x PBS	coating buffer
PBS-T 0,05 % Tween20	wash buffer
5 % milk powder (w/v) in PBS-T	blocking buffer (6.6.1)
0.5 % (w/v) caseine in PBS-T	blocking buffer (6.6.2)
1 M H_2SO_4	stop solution

HPV16 VLPs for VLP-capture ELISA (6.6.1) were purified from baculovirus-infected insect cells and kindly provided by Prof. Martin Müller, DKFZ, Germany.

5.5.3 *IFNy ELISpot*

3 x 5 cm metal meshes (0.5 mm mesh size)	DKFZ, Heidelberg, Germany

ACT lysis buffer:	17 mM Tris 160 mM NH_4Cl pH 7.2, sterilized by filtration
PBS-T 0,01 %	0,01 % Tween20 in PBS

Concavalin A	Sigma, Steinheim, Germany
Ionomycin calcium salt	Sigma, Steinheim, Germany
NBT/BCIP, ready-to-use	Sigma, Steinheim, Germany
Multiscreen IP 96 well filter plates MSIPN45	Merck Millipore, Billerica, MA, USA
PMA (Phorbol 12-myristate 13-acetate)	Sigma, Steinheim, Germany
Pokeweed Mitogen	Sigma, Steinheim, Germany
Streptavidin Alkaline Phosphatase	BD Pharmingen, Durham, NC, USA

5.6 Chemicals

Acetic acid 96 %	Merck, Darmstadt, Germany
Agarose	Gibco BRL, Eggenstein, Germany
Albumin from chicken egg white	Sigma-Aldrich, St. Louis, USA
Ammonium persulfate (APS)	Serva, Heidelberg, Germany
Ampicillin	Sigma-Aldrich, St. Louis, USA
Bacto-Agar	Difco Laboratories, Detroit, USA
BCIP-NBT	Sigma-Aldrich, St. Louis, USA
Betaine	Sigma-Aldrich, St. Louis, USA
Boric acid	Merck, Darmstadt, Germany
Bovine serum albumin (BSA)	Sigma-Aldrich, St. Louis, USA
Bradford reagent *Dye Reagent Concentrate*	Bio-Rad, Munich, Germany
Bromphenol blue	Serva, Heidelberg, Germany
Coomassie Brilliant Blue	Sigma-Aldrich, St. Louis, USA

Developer for photographic processing	Adefo-Chemie, Dietzenbach
Dimethylsulfoxide (DMSO)	Merck, Darmstadt, Germany
D-Sorbitol >98%	Sigma-Aldrich, St. Louis, USA
Ethanol p.a.	Merck, Darmstadt, Germany
Ethidium bromide	Sigma-Aldrich, St. Louis, USA
Ethylenediaminetetraacetate (EDTA)	Merck, Darmstadt, Germany
Fixer for photographic processing	Adefo-Chemie, Dietzenbach
Formaldehyde 37 %	Roth, Karlsruhe, Germany
Glacial acetic acid	Serva, Heidelberg, Germany
Glutathione	Sigma-Aldrich, St. Louis, USA
Glycerol 86 %	Roth, Karlsruhe, Germany
Hydrochloric acid 37 %	Roth, Karlsruhe, Germany
Imidazole	Roth, Karsruhe, Germany
Isopropyl β-D-1-thiogalactopyranoside (IPTG)	Sigma-Aldrich, St. Louis, USA
Luminol reagent (ECL)	Santa Cruz, Santa Cruz, USA
Mercaptoethanol	Merck, Darmstadt, Germany
Methanol	Merck, Darmstadt, Germany
Milk powder	Roth, Karlsruhe, Germany
N-Lauroylsarcosine sodium salt solution	Sigma-Aldrich, St. Louis, USA
p-Nitrophenylphosphate	Sigma-Aldrich, St. Louis, USA
Ponceau red solution	Sigma-Aldrich, St. Louis, USA
Potassium dihydrogen phosphate	Gerbu Biochemicals, Gaiberg, Germany
RIPA Buffer	Sigma-Aldrich, St. Louis, USA
Roti-Quant	Roth, Karlsruhe, Germany
Sodium acetate	Merck, Darmstadt, Germany
Sodium carbonate	Merck, Darmstadt, Germany
Sodium chloride	AppliChem, Darmstadt, Germany
Sodium dihydrogen phosphate dihydrate	J.T. Baker, Deventer, Netherlands
Sodium dihydrogenphosphate monohydrate	J.T.Baker, Deventer, Netherlands
Sodium hydrogene carbonate	Merck, Darmstadt, Germany
Sodium hydroxide (NaOH)	Roth, Karlsruhe, Germany
Sodium dodecyl sulfate (SDS)	Roth, Karlsruhe, Germany
Sulfuric acid (H_2SO_4)	Roth, Karlsruhe, Germany
Tetramethylethylenediamine (TEMED)	Serva, Heidelberg, Germany
Tris-(hydroxymethyl)aminomethane	Roth, Karlsruhe, Germany
Triton-X100	Sigma-Aldrich, St. Louis, USA
Tryptone	Difco, Detroit, USA

Tween20	Calbiochem, Merck, Darmstadt, Germany
Tween80	Sigma-Aldrich, St. Louis, USA
Yeast extract	Difco Laboratories, Detroit, USA

5.7 General materials and consumables

10 ml incubation tubes (bacteria)	Greiner, Frickenhausen, Germany
50 ml centrifuge tubes (SS-34 rotor, Sorvall)	Beckmann Coulter, Brea, CA, USA
500 ml centrifuge tubes (874 rotor)	Heraeus Sepatech, Hanau, Germany
6-, 12-, 24-, 48-, 96 well plates (cell culture)	Costar, Corning, NY, USA
96-well plates, U-bottom	BD Falcon, Durham, USA
Bottle top filter	Costar, Corning, NY, USA
Cell culture flasks (25, 75, 175 cm2)	CellStar, Greiner, Frickenhausen, Germany
Cell scraper	Greiner Bio-One, Frickenhausen, Ger
Cryo vials, 2 ml	CellStar, Greiner, Frickenhausen, Ger
disposable bags PP	Brand, Wertheim, Germany
disposable hemocytometer C-Chip	DigitalBio, Nanoentek, Washington, USA
Disposable scalpel	Feather, Osaka, Japan
DNAzap	Ambion, Life Technologies, Carlsbad, USA
Electroporation cuvettes	Steinbrenner, Wiesenbach, Germany
Falcon tubes, 15 ml und 50 ml	Greiner, Frickenhausen, Germany
Gloves nitril	Sempermed,Wien, Austria
Kimtech Wipes	Kimberley-Clark, Irving, USA
LoBind reaction tubes 1.5 & 2 ml	Eppendorf, Hamburg, Germany
Needles	BD Microlance, Durham, USA
Parafilm PM-996	Pechiney, Paris, France
Pasteur pipettes	Costar, Corning, NY, USA
Pasteur pipettes	Sarstedt, Newton, USA
PCR reaction tubes	Eppendorf, Hamburg, Germany
Petri dishes	Greiner, Frickenhausen, Germany
Photographic film *Kodak Biomax light*	Sigma-Aldrich, St. Louis, USA
Pipette tips *Tip One*	Star Lab, Merenschwand, Switzerland
Pipette tips	Greiner, Frickenhausen, Germany
PVDF-Membrane *Hybond N+*	Amersham, Buckinghamshire, UK
Reaction tubes, 0,2 - 2 ml	Eppendorf, Hamburg, Germany
Reagent reservoirs 50 ml	Costar, Corning, NY, USA
Sterile filter tips *DeckWorks*	Corning, NY, USA

Sterile plastic inoculation loops	Neolab, Heidelberg, Germany
Syringe filters, 0.2 & 0.45 µm	Corning, NY, USA
Syringes	Beckton Dickinson, New Jersey, USA
Toothpicks (sterilized by autoclaving)	Papstar, Kall, Germany
Ultracentrifugation tubes 14 x 95 mm, PA	Beckmann, Palo Alto, CA, USA

5.8 Equipment

Agarose gel carriage	Tecnomara, Fernwald, Germany
Agarose gel running chamber *Sub Cell GT*	Bio-Rad, Munich, Germany
Analytical Balance *BP 210D*	Sartorius, Goettingen, Germany
Autoradiography cassettes	Siemens, Berlin, Germany
Balance *BP 310S*	Sartorius, Goettingen, Germany
CCD Camera	Proscan, Lagerlechfeld, Germany
Centrifuge *1K15*	Sigma, Osterode a.H., Germany
Centrifuge *5810 R*	Eppendorf, Hamburg, Germany
Centrifuge *Biofuge 13*	Heraeus, Hanau, Germany
Centrifuge *RC-5B* Refrigerated Superspeed	Sorvall, Thermo Fisher Scientific, MA, USA
Centrifuge *Varifuge 3.0R*	Heraeus, Hanau, Germany
Culture Shaker *Certomat R*	Sartorius, Goettingen, Germany
Culture Shaker *Multitron*	Infors, Basel, Switzerland
DNA-Sequencer *ABI 3100 Genetic Analyser*	Applied Biosystems, Foster City, USA
Electron Microscope *EM 912 Omega*	Zeiss, Jena, Germany
Elektrophoresis chamber *Mini Protean II*	Bio-Rad, Munich, Germany
French Press *EmulsiFlex-C5*	Avestin, Canada
Gel documentation *GelDoc 2000*	Bio-Rad, Munich, Germany
Incubation hood *Certomat H*	Sartorius, Goettingen, Germany
Incubator	Heraeus, Hanau, Germany
Laminar Flow Hood *Biowizard Silverline*	Kojair, Vilppula, Finland
Magnetic stirrer *MR 2002*	Heidolph, Schwabach, Germany
Microscope *CK 40*	Olympus, Tokio, Japan
Microwave oven	Siemens, Berlin, Germany
Mikrotiter plate reader *Multiskan EX*	Thermo Electron Corp., Karlsruhe, Ger
Peristaltic pump *Econo Pump*	Bio-Rad, Munich, Germany
pH-meter *PB-11*	Sartorius, Goettingen, Germany
Pipettes *Pipetman*	Gilson, Bad Camberg, Germany
Pipettor *Pipetboy 8-5010*	Neolab, Heidelberg, Germany

Potter-Elvehjem-Homogenizer	B. Braun, Melsungen, Germany
Power Supply *EV 231*	Consort, Turnhout, Belgium
Power Supply *Power Pac 300*	Bio-Rad, Munich, Germany
Roller mixer *RM5*	CAT, Staufen, Germany
rotor 874	Heraeus, Hanau, Germany
rotor SS-34	Sorvall, Thermo Fisher Scientific, MA, USA
rotor SW 32 Ti	Beckmann, Palo Alto, CA, USA
Shaker *Promax 2020*	Heidolph, Schwabach, Germany
Sonicator Sonopuls HD/UW 2070 MS72	Bandelin, Berlin, Germany
Speed Vac *DNA Speed Vac 110*	Savant, Holbrook, USA
Table top centrifuge *2K14*	Eppendorf, Hamburg, Germany
Thermocycler *Mastercyler Gradient*	Eppendorf, Hamburg, Germany
Thermomixer *5436*	Eppendorf, Hamburg, Germany
Ultracentrifuge Discovery 90 SE	Sorvall, Thermo Fisher Scientific, MA, USA
Vortex *MS1 Minishaker*	IKA, Staufen, Germany
Waterbath *SW 20*	Julabo, Seelbach, Germany

5.9 Software

Adobe Acrobat Reader 6	Adobe, San Jose, CA, USA
Adobe Photoshop Elements 4	Adobe, San Jose, CA, USA
AID ELISpot Software	AID, Strassberg, Germany
BLAST - Basic Local Alignment Search Tool	National Center for Biotechnology Information, Bethesda, MD, USA
ChromasLite 2.01	Technelysium, South Brisbane, Australia
Endnote X6	Thomson Reuters, New York, NY, USA
GIMP 2.8	GNU General Public License (GPL & LGPL)
SYFPEITHI software	Rammensee et al. [138]
GraphPad Prism 6.04	GraphPad Software, San Diego, CA, USA,
HP Precision Scan Pro 3.1	Hewlett-Packard, Palo Alto, CA, USA
ImageJ 1.4.7	NIH, Bethesda, MA, USA
Magellan Standard	Tecan Group Ltd., Männedorf, Switzerland
Microsoft Office Professional Plus 2010	Microsoft Corp., Redmond, WA, USA
Microsoft Windows 7	Microsoft Corp., Redmond, WA, USA
SnapGene 2.2.2	GSL Biotech LLC, Chicago, IL, USA
Unicorn 2.0	GE Healthcare, Uppsala, Sweden

6 Methods

6.1 Manipulation of DNA

6.1.1 *Purification of plasmid DNA (Mini and Maxi preparation) from E. coli*

Plasmid DNA was isolated with the Qiagen Plasmid Mini or Maxi Kit according to the manufacturer's instructions. For small scale preparations, 2 to 5 ml of an overnight grown bacteria culture were used; for large scale production of plasmid DNA, 200 ml culture volume was applied.

6.1.2 *Determination of DNA concentration and purity*

DNA concentrations and purity were determined spectrophotometrically by measuring the absorption at 260 and 280 nm. Thereto, the DNA was diluted in aqua bidest. and transferred to a UV cuvette. H_2O was also used to set the blank value of the photometer.

The DNA concentration was calculated according to the following equation:

A_{260nm} x 50 µg/µl x dilution factor = c [µg/µl]

The absorption at 280 nm was used to determine the purity of the preparation. A ratio of A260 / A280 of 1.8 to 2.0 was considered to be pure; ratios of less than 1.8 indicate protein contaminations.

6.1.3 *Enzymatic cleavage of DNA*

Restriction endonucleases were used for the digestion of DNA according to the manufacturer's instructions. If the optimal buffer differed for a double digest, a compromising buffer was used if possible. If the reaction buffers were not compatible to each other, the digest was performed sequential. After digestion with the first enzyme, purification of the DNA was performed with the Roche PCR Purification Kit (6.1.4). DNA was eluted in 30 µl water and introduced to the next digest.
Enzymatic cleavage reactions were usually carried out at 37 °C for at least 2 hours. Cleaved products were separated and identified with agarose gel electrophoresis. For preparative digests, DNA was purified from the agarose gel with the QIAQuick Gel Extraction Kit. Introduced DNA amounts depended on the intended use of the products; for analytical digestions only 0.5 to 1 µg DNA was used in contrast to preparative digestions were 10 to 20 µg were applied.

Reaction mix for digestion:	10 - 20	µg	DNA
	10 - 20	U	per enzyme
	2.5	µl	10 x reaction buffer
	ad 25	µl	H_2O

6.1.4 *Purification of DNA*

DNA was purified (i.e. after enzymatic cleavage to remove buffer compounds) with the Roche PCR Purification Kit according to the manufacturer's instructions. DNA was eluted in 30 to 50 µl DNAse free water whereby remaining traces of column material were strictly avoided to be co-transferred as this was found to inhibit further enzymatic reactions.

6.1.5 *Precipitation of DNA*

DNA had to be precipitated, e.g. before sequencing, to exchange the diluent or to reduce its volume. DNA fragments were supplemented with 3 M sodium acetate pH 4.6 (1/10 of the total volume). Subsequently, two volumes of 100% ethanol were added and thoroughly mixed. After incubation for 20 min at -20°C, the DNA was centrifuged for 15 min at 13,000 rpm. The pellet was then washed with 250 µl of 75% ethanol and centrifuged again (identical settings). The supernatant was carefully discarded and the pellet was left to dry for 10 minutes before 6 min Speed-Vac centrifugation was performed to remove remaining ethanol. Finally, the DNA was resuspended in H_2O or an appropriate buffer for subsequent procedures.

6.1.6 *Dephosphorylation of 5'ends of DNA*

DNA was treated with calf-intestinal alkaline phosphatase (CIP) after digestion with only one enzyme or after blunt end cutting. CIP removes phosphate residues of 5'ends and thereby avoids re-ligation of a DNA vector without insertion of the desired insert. After the digest, 2 µl of CIP enzyme were added directly to the vector DNA. The reaction was carried out for 15 min at 37°C and for 15 min at 56°C. Phosphatase was removed by DNA purification with the Roche PCR Purification Kit (6.1.4).

6.1.7 *Analytic and preparative agarose gel electrophoresis*

DNA molecules carry negatively charged phosphate residues which move towards the positively charged anode in an electrical field. The velocity of the DNA thereby depends on the fragment size. These characteristics are utilized for gel electrophoresis.

To prepare a 1 % agarose gel, 1 g of powdered agarose was dissolved in 100 ml 1 x TBE buffer by boiling in a microwave. After cooling to approx. 60 °C, ethidium bromide was added and the solution was poured in a gel casting tray containing a comb. The solidified gel was transferred into a 1 x TBE buffer containing chamber. Samples were mixed with 6 x loading dye and - depending on the expected product size - 100 bp or 1 kb ladder was used. After loading into the gel slots, electrophoresis was performed for 20 to 30 minutes at 110 - 140 V. Analytical gels were imaged under UV light (254 nm) to visualize DNA bands stained with fluorescent ethidium bromide. Preparative gels were only exposed to 366 nm UV light to avoid UV induced mutations. Size and concentration of DNA fragments were determined by comparison to the marker.

6.1.8 *Purification of DNA fragments from agarose gels*

For cloning, plasmid DNA or PCR products were digested in a preparative scale (6.1.3) and separated by preparative agarose gel electrophoresis (6.1.7). The desired fragments were visualized by UV light (366 nm) and excised using a scalpel. Subsequently, the DNA was purified from the agarose using the QiaQuick Gel Extraction Kit following the manufacturer's instructions.

6.1.9 *Ligation of DNA fragments*

After digestion and purification of vector and insert DNA, the ligation reaction was carried out. The linearised vector DNA was mixed with the insert DNA fragment in a ratio of 1:3. To insert the target DNA into the expression plasmid, the following mixture was used:

Ligation reaction mixture:	0.1 - 0.5	µg	linearised plasmid DNA (vector)
	0.5 – 1	µg	insert-DNA fragment
	1	µl	T4-DNA-ligase
	2	µl	10 x ligation buffer
	Ad 20	µl	H_2O

The ligation reaction was incubated over night at 12 °C in a water bath and was then used to transform bacteria (6.2.2).

6.1.10 *Polymerase chain reaction (PCR)*

The polymerase chain reaction (PCR) was used to amplify DNA fragments with specific primers to prepare DNA for cloning experiments, to check for a desired DNA sequence or to provide DNA for subsequent sequencing reactions. The $p16^{INK4a}$-coding DNA region for

cloning of the recombinant protein was amplified from Hela cDNA. The following mixture was used by default:

Standard and	50 ng	template DNA (for colony PCR: 0.3 µl inactivated culture)
Colony PCR:	0.5 µl	primer forward (10 pmol/µl)
	0.5 µl	primer reverse (10 pmol/µl)
	0.5 µl	dNTPs (10 mM)
	2.5 µl	10 x PCR buffer
	1.5 µl	$MgCl_2$
	0.3 µl	DMSO
	0.3 µl	DNA Taq-polymerase
	ad 25 µl	H_2O

After transformation of bacteria (6.2.2), colony PCR was performed to check selected clones for containing the correct plasmid. To obtain template DNA, a single colony was tipped with an autoclaved wooden toothpick and transferred to 25 µl aqua bidest. This mixture was inactivated for 10 minutes at 99 °C and further used as template for the colony PCR reaction.

DNA Sequencing

Cloning products were sequenced with the ABI 3100 device to confirm the correct DNA sequence. The method of choice is called dye terminator “Sanger” sequencing. The test sequence was first amplified by PCR in presence of the BigDye terminator reagent. The reagent contains four di-deoxynucleotide chain terminators which are labeled with fluorescent dyes, each of which with different wavelengths of fluorescence and emission. The growing chain is simultaneously terminated and labeled with the dye that corresponds to that base. During sequencing, all four colors are assessed within the same capillary and false stops go undetected because no dye is attached. These signals generated by capillary electrophoresis are then converted to an electronic DNA sequence trace chromatogram. For In-house DNA Sequencing a special Sequencing PCR had to be performed:

Sequencing PCR:	0.5 µg	template DNA (~ 1 µl of miniprep DNA sample)
	1.5 µl	primer forward (10 pmol/µl)
	4 µl	RR-Mix BigDye terminator reagent
	4 µl	Sequencing Buffer
	ad 20 µl	H_2O

The DNA was precipitated and the resulting pellet was re-suspended in 12 µl Hidi buffer, transferred to a 96 well sequencing plate and closed with the appropriate cap. Probes were stored at 4 °C or directly sequenced.

All PCR reactions were prepared on ice, mixed and put in the pre-heated PCR machine. The following PCR programs were used to amplify the DNA fragments:

Standard PCR		Colony PCR		DNA Sequencing	
94°C 4 min or 15 min (HotStart Taq)		95°C 4 min or 15 min (HotStart Taq)		96°C 10 min	
94°C 30 sec 55°C 45 sec 72°C 90 sec	x 35	95°C 40 sec 56°C 40 sec 72°C 90 sec	x 35	96°C 25 sec 56°C 35 sec 60°C 4 sec	x 25
		72°C 6 min			

The PCR products were analyzed by agarose gel electrophoresis (6.1.7) and purified using the Roche PCR purification kit following the manufacturer's instructions.

6.2 Microbiological methods

6.2.1 *Culture and storage of bacteria*

Bacteria were cultivated at 37°C either in liquid culture or on agar plates. For selection of bacteria with a resistance gene, the appropriate antibiotics were added. Liquid cultures were inoculated directly from glycerol stocks or from single colonies picked from agar plates and were subsequently incubated shaking with 200 rpm at 37°C overnight. Clones were obtained by streaking bacteria onto agar plates with the help of a glass pipette.
For long term storage, glycerol stocks were prepared by mixing 500 µl of an overnight bacteria culture with 500 µl sterile glycerin (86 %) in a cryo-conservation tube. The suspension was stored at -80°C.

6.2.2 *Transformation of bacteria by heat shock*

Free DNA, usually in plasmid form, can be transferred into competent E. coli strains by different methods, e.g. electroporation, chemical or heat shock transformation. During this thesis, bacteria were transformed using heat shock. For enhanced effectiveness, plasmids and respectively ligation reactions were first introduced into competent E. coli Top10 as this strain is suitable for highly efficient transformation and plasmid isolation. A 50 µl aliquot of

competent bacteria was thawed and incubated on ice with 2-5 µl of the ligation reaction (or 100 - 200 ng of isolated Plasmid DNA) for 30 minutes. The cells were then heat shocked in a 42°C water bath for exactly 30 seconds, thus allowing the DNA to enter the cells. After subsequent replacement on ice for 2 minutes, 250 µl of room temperature SOC medium was added and the mixture was shaken for 1 hour. To select transformed clones, 60-80 µl were spread onto an ampicillin-containing agar plate and incubated over night at 37°C. Colony PCR (6.1.10) was performed to check selected colonies for the appropriate insert and successfully transformed clones were used to isolate plasmid DNA from an overnight culture.

This plasmid DNA was then transformed into the expression strains E. coli BL21 and Rosetta. Thereto, a 20 µl aliquot of competent cells was transformed with 1 µl plasmid DNA as described above and 80 µl SOC medium were added before plating onto an LB-agar plate containing the appropriate antibiotics.

6.3 Cultivation and manipulation of eukaryotic cells

6.3.1 *Cryo-conservation and thawing of eukaryotic cells*

For long-term storage, cells were harvested (usually from T175 flasks) and pelleted by centrifugation. Between $5x10^6$/ml and $1x10^7$/ml cells were re-suspended in freezing medium (10% DMSO in FCS) and 0.5 or 1 ml of this cell suspension was transferred to cryo-vials. Cells were gradually cooled to -80°C in a cell freezing box overnight. Frozen cell vials were either stored at -80°C or transferred to liquid nitrogen tanks. For re-utilization, cell vials were topped up with pre-warmed medium and transferred to a centrifuge tube where 5 ml of the appropriate cultivation medium was added. After centrifugation for 7 min at 1,200 rpm, cells were resuspended in 5 to 10 ml medium (specific for cell type) and transferred to T25 or T75 culture flasks depending on frozen cell number and expected culture viability.

6.3.2 *Determination of cell number and vitality*

Cells were counted using Neubauer counting chambers (hemocytometer). Live and dead cells were discriminated by dilution in trypan blue; depending on the expected cell numbers different ratios of cells to trypan blue were used, usually 1:2 for cultured cells and 1:20 for mouse splenocytes.

$$\text{concentration} = \frac{\text{number of cells x } 10.000}{\text{number of squares counted}} \text{x dilution}$$

The mean number of cells in one square multiplied with the dilution factor and 10^4 represents the number of cells per ml in the original suspension.

6.3.3 *Transfection of mammalian cells*

For in vivo tumor protection and regression experiments, a $p16^{INK4a}$ -expressing mouse cell line is needed. To generate this cell line, different transfection methods were tested in a preliminary test with a pmaxGFP test plasmid to determine transfection efficacy and to choose the best method for further experiments. To this end, RMA-S cells were grown to ~70% confluency and transfected with

a. Nucleofection,
b. Effectene Transfection Reagent,
c. xtremeGENE 9 DNA Transfection Reagent,
d. PromoFectin Transfection Reagent or
e. FuGENE HD Transfection Reagent

according to the manufacturers' instructions. Brief protocols under specification of the applied cell numbers and DNA amounts are given below. For transfections b) - e), 7×10^4 RMA-S cells were seeded the day before transfection in 500 µl medium per well in a 48 well plate. For each transfection reagent b) - e) triplicates were prepared.
Transfection efficacy was monitored by fluorescence microscopy and the percentage of green fluorescent cells was evaluated in comparison to non-fluorescent cells 3, 20 and 48 hours post transfection.

a) Two days before transfection $5\text{-}7 \times 10^6$ cells were seeded into 10 cm cell culture dishes. For one nucleofection sample 2×10^6 cells were used, 2 µg maxGFP plasmid and 100 µl Nucleofector solution were added. Programs X001, A023, A024, A030, A20, T20, T30, X05, L29 and D23 were tested in duplicates. Negative controls were treated equally but without plasmid added.

b) The day before transfection, 7×10^4 cells per well in 500 µl medium were seeded in a 48 well plate. For one transfection, 0.15 µg test plasmid (maxGFP) was dissolved in DNA condensation buffer to a total volume of 50 µl and 1.2 µl enhancer was added. After room temperature incubation and spin down, 4 µl Effectene transfection reagent was added and mixed. Cells were washed with PBS during the 5 - 10 min incubation (RT) and 150 µl fresh growth medium was added to the cells. The transformation mixture was supplemented with 200 µl medium, mixed and added drop-wise to the cells.

c) 7×10^4 cells per well in 500 µl medium were seeded one day before transfection in a 48 well plate. 3 µl X-tremeGENE 9 DNA transfection reagent was diluted in 100 µl Opti-MEM (3:1 ratio). 1 µg pmaxGFP DNA was added and mixed gently. After 15 min room temperature incubation, 15 µl of the transfection reagent:DNA complex was added drop-wise to the cells and evenly distributed.

d) One day before transfection, 7 x 10^4 cells per well in 500 µl medium were seeded in a 48 well plate. For each well, 0.5 µg plasmid DNA (maxGFP) was diluted into 25 µl Opti-MEM and 1 µl PromoFectin / well was also diluted into 25 µl Opti-MEM. Both dilutions were mixed and incubated 15 - 30 minutes at room temperature. Then the 50 µl mixture was added drop-wise to the cells in serum containing RPMI medium.
e) Cells were plated 24 hours before transfection (7 x 10^4 cells / well in 500 µl medium in a 48 well plate). On the day of transfection, 2 µg pmaxGFP were diluted in 100 µl Opti-MEM and 6 µl FuGene was added. After 15 min RT incubation of the FuGene / DNA mixture, 12.5 µl were added per well.

6.3.4 *Production of Ripa-lysates for protein analysis*

Cells were cultured in 10 cm dishes till ~90% confluence. The medium was aspirated and the cells were gently washed with 3 ml PBS which was aspirated again. 1 ml PBS was added; cells were removed from the culture vessel with a cell scraper and transferred to a sterile tube. The cell suspension was centrifuged 10 min at 1200 rpm and PBS was discarded. The cell pellets were stored at -20°C or subsequently re-suspended in 200 µl RIPA buffer. This re-suspension and all of the following steps were performed at 4°C on ice. After addition of RIPA buffer, cells were sonicated for 30 seconds and put on a rotation incubator at 4 °C for one hour. The protein containing supernatant was then transferred to another reaction tube and frozen at -20°C for further use.

6.4 Purification and analysis of recombinant proteins

6.4.1 *Purification of HPV16 L1 capsomeres and chimeric fusion proteins combining HPV16 L1 and p16^{INK4a} from E. coli*

Protein expression

For the expression of GST-HPV16 L1 and the chimeric proteins containing GST, HPV16 L1 and p16^{INK4a}, E. coli Rosetta or BL21 bacteria were transformed with the pGex-4T-2 vector containing the respective genes (5.2.1). TB medium was inoculated in a ratio of 1:100 with an overnight culture (LB) of the plasmid containing bacteria and incubated while shaking at 200 rpm at 37°C. As soon as the cultures reached an optical density (OD600nm) of ~ 2.0 to 3.0 (respectively two following OD600 values indicated stationary phase entry), bacteria were cooled for 5 min on ice before adding IPTG to a final concentration of 0.1 mM to induce protein expression. After 16 to 18 h incubation at 200 rpm at 22 °C, bacteria were harvested by centrifugation for 20 min at 4,000 rpm at 4°C (874 rotor).

The HPV16 L1 expressed in E. coli was predominantly found to build intracellular inclusion bodies what also holds true for the chimeric capsomeres containing $p16^{INK4a}$ and L1. Although a small percentage of the protein was expressed in soluble form, sufficient amounts could not be purified with the available techniques. Therefore, we decided to establish an inclusion body purification protocol to overcome quantity issues. Shortly, the inclusion bodies were washed, cells were disrupted with a French press and the protein was extracted from the resulting pellet. Denatured protein was then refolded by dialysis and could be used for further studies.

Inclusion body preparation

HPV16 L1 capsomeres and chimeric capsomeres were purified using an adapted protocol described in the iFOLD® Protein Refolding System 1 User Protocol by Novagene [101]. Fresh or frozen cell pellets were re-suspended in IB Resuspension Buffer (5.4.2; 10 ml / 1 g cell paste) supplemented with protease inhibitor cocktail (1 tablet per 50 ml). 20 µl Lysonase were added per gram cell pellet and stirred for 15 minutes. Bacteria were lysed using a high-pressure homogenizer (French press). Subsequently ATP and $MgCl_2$ were added to the lysate to final concentrations of 2 and 5 mM, respectively. After 1 h incubation at room temperature, Triton X-100 was added to a final concentration of 1 % and incubated for 15 minutes on a roller mixer. Cell lysates were centrifuged at 8.000 x g (~10.000 rpm - SS-34 rotor, Sorvall) for 15 minutes and the supernatant was discarded. The resulting pellets were washed with IB Wash Buffer (10 ml buffer / 1 g cell pellet) whereby complete resuspension was achieved with the help of a Potter Elvehjem Homogenizer. The suspension was centrifuged again and the Triton X-100 washing was repeated one more time. After the second washing and centrifugation, remaining Triton X-100 was removed by washing the pellet twice in Resuspension Buffer, as described above. The purified inclusion body pellets were stored at -80°C until further use.

Denaturing of inclusion bodies and refolding of the protein

Per 0.5 g washed inclusion body pellet 10 ml Denaturing Buffer (5.4.2) was added and complete homogenization was achieved with a Potter Homogenizer. The solution was supplemented with 1.75 ml 30 % N-Lauroylsarcosine (5 % final conc.) and agitated on a roller mixer until it cleared after 30 min to 2 h. The solubilized, denatured protein was cleared by centrifugation at 25.000 x g (~18.000 rpm - SS-34 rotor, Sorvall) for 15 minutes at 4 °C. The supernatant was collected and dialyzed (MWCO 3.500 Da) against Dialysis Buffer (5.4.2) whereby a volume of 0.5 L was used per 10 ml denatured protein solution. After 4 hours of dialysis, the buffer was exchanged by freshly prepared buffer and dialyzed over night at 4°C. The refolded protein was then removed from the dialysis tube and further

analyzed by electron microscopy (6.4.9). Protein concentration was determined with the 2-D Quant Kit (GE Healthcare).

6.4.2 *Purification of p16^{INK4a} from E. coli*

Protein expression

For the expression of GST-p16^{INK4a}, bacteria were transformed with the pGex-4T-2 vector containing the full-length p16^{INK4a} gene (5.2.1.). TB medium was inoculated in a ratio of 1:100 with an overnight culture (LB) of the plasmid containing bacteria and incubated while shaking at 200 rpm at 37°C. As soon as the cultures reached an optical density (OD600nm) of 2 - 3, bacteria were cooled for 5 min on ice before adding IPTG to a final concentration of 0.1 mM to induce protein expression. After 16 to 18 h incubation at 200 rpm at 22 °C, bacteria were harvested by centrifugation for 20 min at 4,000 rpm at 4°C (874 rotor).

As p16^{INK4a} was found to be soluble expressed from E. coli cultures, the protein was purified by means of affinity chromatography. Endotoxin removal was achieved by triton X-114 treatment (6.4.11).

Preparation of cell lysates

The fusion protein was purified based on a protocol originally developed by Chen and co-workers [37]. We decided not to remove the GST tag from the p16^{INK4a} protein to ensure highest possible equality for immunological studies, as the GST tag was also not removed for the HPV16 L1 protein and the chimeric capsomeres purified from inclusion bodies (6.4.1). Fresh or frozen cell pellets were re-suspended in IB Resuspension Buffer (5.4.2; 10 ml / 1 g cell paste) supplemented with protease inhibitor cocktail (1 tablet per 50 ml). 20 µl Lysonase were added per gram cell pellet and stirred for 15 minutes. Bacteria were lysed using a high-pressure homogeniser (French press). Subsequently ATP and $MgCl_2$ were added to the lysate to final concentrations of 2 and 5 mM, respectively. After 1 h incubation at room temperature, cell lysates were centrifuged at 8.000 x g (~10.000 rpm - SS-34 rotor, Sorvall) for 15 minutes and the p16^{INK4a} containing supernatant was used for further purification.

Affinity Chromatography

The cell lysate containing the GST-p16^{INK4a} protein was slowly (0.1 ml/min) loaded onto a 5 ml GSTrap FF column (GE Healthcare) equilibrated in buffer L at 4°C. After washing the column with 10 to 20 bed volumes of buffer L (1.5 ml/min) the bound protein was eluted with 3 fractions of 3 ml Buffer L + 20 mM glutathione. The GSTrap columns were cleaned by washing with 2 CVs of 20 mM glutathione solution and 5 CVs of 6M GuHCl cleaning

solution. Afterwards columns were washed with 20-30 CVs of PBS and stored in 20% ethanol at 4°C.

6.4.3 *Explorative protein purification methods*

Denaturing of inclusion bodies

Inclusion bodies were denatured with 5 % N-Lauroylsarcosine, urea (4, 6 and 8 M) and 6 M guanidine hydrochloride. The protein lysate was incubated with the respective denaturing agent at RT on a roller mixer until the solution became clear.

Dialysis / Refolding screen

Dialysis conditions for denatured proteins were tested in small scale to determine optimal protein concentration and buffer receipts for refolding. Thereto, a 3,500 Da dialysis membrane was cut into 2 x 2 cm squares and equilibrated in aqua bidest. 1.5 ml Protein LoBind Eppendorf reaction tubes were cut at the 1.5 mark and the lid was filled with 100 µl of the denatured protein; diluted in denaturing buffer if required. Then, the dialysis membrane was clamped between the lid and the remaining reaction tube and put into the dialysis buffer of choice over night at 4°C. The next day, absorption at 340 nm was measured to quantify the amount of precipitated protein. The lower the value, the more soluble protein was present in the solution. This method allows testing of different buffer conditions and protein dilutions in an easy and economy way.

Other refolding methods

Refolding of denatured protein was attempted by rapidly diluting it into the buffer of choice. A fructose-based polymer, NV10 (NVoy) was also tested for refolding purposes.

Other purification attempts

The soluble expressed fractions of HPV16 L1 capsomeres and $p16^{INK4a}$ fusion proteins were also purified using affinity chromatography (GSTrap) followed by size exclusion chromatography: Bacteria cell lysates were cleared by centrifugation and then slowly (0.1 ml/min) loaded onto a GSTrap column (GE Healthcare) at 4°C. After washing the column with 10–20 bed volumes of buffer L, 40 U per ml bed volume of thrombin protease (GE Healthcare) in buffer L was added and the cleavage reaction was performed at RT for 18 h. Subsequently, the protein was eluted in buffer L. For further purification the GSTrap eluate was dialyzed against modified buffer L (L_{mod}) for 2 h at RT and subsequently run on the SEC column Superdex200 (GE Healthcare).

Also ProteinG and CnBr coupled anti-GST antibodies as well as size exclusion and ion exchange chromatography were applied to purify refolded proteins after IB purification (6.4.1).

6.4.4 *Denaturing SDS-polyacrylamide gel electrophoresis (SDS-PAGE)*

Analytical protein electrophoresis was performed using the Novex NuPAGE® SDS-PAGE gel system which is a polyacrylamide gel electrophoresis system that simulates the denaturing conditions of the traditional Laemmli system (Tris-Glycine SDS-PAGE gels) [139]. SDS-PAGE facilitates the separation of denatured proteins depending on their electrophoretic mobility which is a function of the molecular weight, charge and conformation of the molecule.
Samples were prepared according to the manufacturer's instructions as reduced samples and heated for 10 min at 70°C before loading onto the gel. The reaction tubes were spun down shortly to collect the liquid at the base of the tube. The appropriate volume and protein mass was then loaded and the gel was run for 35 minutes at 200 V.

6.4.5 *Coomassie-staining of protein gels*

Protein gels were Coomassie-stained after electrophoresis (6.4.4) using either the Coomassie G-250 SimplyBlue™ SafeStain reagent following the manufacturer's instructions or a self-made Coomassie Staining Solution (see 5.4.4 for details) over night. To reduce background staining of coomassie gels (e.g. after overnight staining), gels were waved for 10 to 60 minutes in 10 % ethanol and subsequently washed with aqua bidest.

6.4.6 *Silver-staining of protein gels*

Silver staining of protein gels was performed according to the manufacturer's instructions using the SilverQuest Silver Staining Kit (Invitrogen).

6.4.7 *Western blot analysis*

The western blot technique is a sensitive method to detect even small amounts of s special protein. The sample is separated by means of gel electrophoresis (6.4.4) and subsequently transferred to a nitrocellulose membrane where they can be stained with antibodies specifically binding to the target protein.
The western blot was performed according to the manufacturer's instructions (Invitrogen, "Using the XCell II Blot module"). Shortly, the transfer buffer was prepared while the gels were still in process. After ending of the run, the gels were carefully removed from the gel

cassette with the help of a special knife and placed in the pre-soaked nitrocellulose membrane filter paper sandwich. Trapped air bubbles were removed by gently rolling over the prepared sandwich using a glass pipette. Pre-soaked blotting pads were added as depicted in Figure 10; then, the blot module was inserted into the buffer chamber, filled with transfer buffer and run at 30 V for 1 hour.

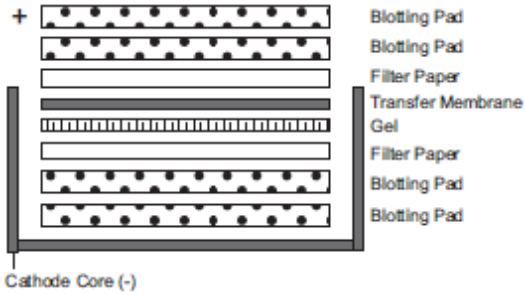

Figure 10: Western Blot - sandwich setup (adapeted from Invitrogen, XCell II™ Blot Module EI9051 [140])

Afterwards, the membrane was waved in aqua bidest. and immobilized, separated proteins were stained with Ponceau Red solution (Sigma-Aldrich) to ensure successful transfer. The membrane was transferred to a 50 ml falcon tube with the protein side oriented to the inside of the tube without overlaps. To avoid unspecific antibody binding, the membranes were blocked with blocking solution (5.4.4) for 1 h under gentle agitation. The antigen-specific antibody of interest (5.2.4) was diluted in blocking solution and incubated for 1 at room temperature or at 4 °C over night on a roller mixer. Unbound antibody was removed by washing the membrane 3 times with PBS-T for 15 minutes. Afterwards, the secondary HRP-labeled antibody (if needed) was applied same way as the first antibody and incubated 1 h. The membrane was then washed again and imaged. Thereto, luminol reagent (ECL) was applied to the membrane to start the chemiluminescence reaction. In a dark chamber, the membrane was exposed 5 sec to 5 min to x-ray films and developed subsequently.
Membranes could be re-used with another antibody after treatment with stripping buffer (5.4.4). Thereto, membranes were completely covered in this buffer and heated for 45 minutes at 50°C in a water bath. After washing with PBS-T, the above described procedure could be repeated starting with the blocking step.

6.4.8 *Determination of protein concentrations*

Protein concentrations were determined using the 2-D Quant Kit (GE Healthcare) following the manufacturer's instructions, by Bradford assay or densitometrically using the ImageJ software.

Bradford assay:

Protein samples were diluted if necessary and 5 µl were loaded into the wells of a 96well plate. BSA was used as calibration standard (5 µl/well) in a 1:2 serial dilution (500, 250, 125, 63, 32, 16 and 8 µg/ml). H_2O was used to determine the blank value with 5 µl per well. The Bradford reagent (Bio-Rad) was diluted 1:5 with H_2O and 195 µl per well were added to the samples. All samples were tested in duplicate. After 2-10 min the absorption was measured at 595 nm (reference wavelength 405 nm) using an ELISA reader. With the help of the Magellan Software, a BSA standard curve was generated and used for the calculation of the protein concentrations of the analysed samples.

Densitometry:

Samples were analyzed by SDS-PAGE (6.4.4) and subsequent Coomassie-staining (6.4.5) whereby BSA (5, 2.5, 1.25, 0.63 µg) was used as a calibration standard and run on the same gel. SDS-PAGE gels were scanned and with the help of ImageJ the intensity of each band was measured (peak area). The values for the different BSA amounts were used to generate a standard curve and the protein concentrations of the analyzed samples were calculated from the standard curve equation.

6.4.9 *Sedimentation analysis*

50 µg of purified chimeric fusion proteins (consisting of HPV16 L1 and $p16^{INK4a}$, 6.4.1) were loaded onto 5-50% (w/v; dissolved in dialysis buffer) linear sucrose gradients and centrifuged at 36,000 rpm for 3 h at 4°C using the SW41Ti rotor. Fractions of 600 µl (20 aliquots) were collected from the top of the tube and analyzed by western blotting (6.4.7). BSA (4S, Sigma) and HPV16 VLPs purified from insect cells were used for the calibration of the gradient.

6.4.10 *Transmission electron microscopy*

For evaluation of capsomere preparations by EM, suspensions of interest were prepared by 'negative staining' with uranyl acetate. Purified proteins were diluted in their appropriate buffer to about 0.1 mg/ml protein and 3 µl drops were applied to 400-mesh carbon-coated copper-grids, which were rendered hydrophilic by glow-dicharge (0.8 mbar/ 8 µA/ 10 sec). After passage through two drops of bi-distilled water, grids were wetted with 1% aqueous uranyl acetate, drained with filter paper (Whatman) and air-dried for direct observation in an electron microscope (Zeiss EM 912, operated at 120kV; CCD-Camera by Proscan, Germany).

6.4.11 *Determination of endotoxin concentrations and endotoxin removal*

Endotoxin amounts were determined using the LAL (limulus amoebocyte lysate) based colorimetric assay QCL-1000 (Lonza) following the manufacturer's instructions.
Treatment with Triton X-114 was used to remove endotoxin contaminations from protein preparations (6.4.2) purified with affinity and size exclusion chromatography. Inclusion body preparations were found to contain no residual endotoxin contaminations what is due to the Triton X-100 washing steps that were performed to purify the inclusion bodies. A suitable protocol for endotoxin removal was presented by Aida et al. [141] and was also used by Schädlich et al. [130] for the purification of HPV 16 L1 from E. coli. The Triton X-114 phase separation technique was therefore used in this project as it resulted in no significant protein loss or influence on the structural integrity of the particles. The protein preparations were mixed with 1 % Triton X-114 (Sigma), incubated first for 5 min on ice and then for 5 min at 37°C. To remove the Triton X-114 the samples were centrifuged for 5 min at 12,000 rpm and supernatants were collected. The procedure was repeated and endotoxin concentrations were measured in the supernatants.

6.4.12 *Antigen Capture ELISA*

96-well microtiter plates (Nunc) were coated overnight at 4°C with 50 µl of a polyclonal rabbit antiserum (#4543) raised against HPV-16 L1, diluted 1:500 in PBS-TM. The plates were washed with PBS-T and blocked for 1 h at 37°C with a blocking solution containing PBS, 5% skimmed milk and 0.1% Tween-20 (PBS-TM). Purified proteins were added to the wells and incubated for 1 h at 37°C. After four washing steps (200 µl PBS-T / well), 50 µl of a HPV-16 L1 conformation specific mouse monoclonal antibody (#1.3.5.15) were added to each well in a dilution of 1:1,000 and the plates were incubated for 1 h at 37°C. The plates were washed four times and 50 µl of a rabbit anti-mouse peroxidase conjugate was added (Thermo Scientific; 1:5,000 in PBS-TM). After 1 h incubation at 37°C the plates were washed thoroughly before 100 µl of TMB substrate was used to detect HRP activity. The reaction was stopped with 50 µl 1 M H_2SO_4 after 5 - 20 minutes and the plates were read at 450 nm in an ELISA reader (reference wavelength: 620nm).

6.5 Immunization of mice

6.5.1 *Immunization by subcutaneous injection*

Mice were immunized subcutaneously at the neck using a blue G23 needle. 5 to 50 µg of recombinant antigen was diluted in PBS and mixed; if necessary, with adjuvant. Mice were

usually immunized 3 times at biweekly intervals with an injection volume of 100 µl unless mentioned otherwise. Negative control mice were treated with PBS with purified irrelevant antigens.

6.5.2 *Immunization by topical application*

Mice were immunized by topical application with 50 µg recombinant protein formulated in 50% DMSO. Thereto, it was necessary to shave the back of the mice with an electric clipper. Mice were held at their tail and carefully shaved across the grain. Between the first shaving and the first antigen application, three days were paused to heal potential wounding of the skin.
Mice were creamed daily for about 1 minute till the mixture was absorbed through the skin. This procedure was carried out 2 x 5 days with 2 days rest in-between. Blood and spleens were sampled (6.5.3 and 6.5.4) 4 days after the last topical application and analyzed for humoral and cellular immune response (6.6).

6.5.3 *Blood sampling of immunized mice*

Before each immunization, blood samples were taken by puncture of the superficial temporal vein. Final blood samples were taken by cardiac puncture. The blood samples were incubated for 30 min to 3 h at room temperature, to allow for complete clotting, and then centrifuged for 9 min at 3,000 rpm at 4°C. Supernatants (sera) were transferred into clean microcentrifuge tubes and stored at -80°C.

6.5.4 *Splenectomy and preparation of spleen cell suspensions*

Mice were sacrificed using carbon dioxide and sterilized with 70% ethanol. All steps were carried out in a flow hood under sterile conditions. Spleens were dissected by cutting through the skin and peritoneum at the left abdomen below the lowest rib. The connective tissue was removed and the spleens were placed in 10 ml sterile PBS on ice until further use. To generate a single cell suspension, the spleen was pressed through a metal mesh (mesh size: 0.5 mm) into a Petri dish using the plunger of 5 ml-syringe. The cell suspension was then transferred into a 15 ml centrifuge tube and harvested by centrifugation (8 min, 1,200 rpm). The cell pellet was re-suspended in 3 ml pre-warmed ACT lysis buffer (5.5.2) and incubated for 5 min in a 37°C water bath in order to lyse erythrocytes. Cells were centrifuged again for 8 min at 1,200 rpm, re-suspended in 3 ml RPMI medium and were subsequently used in an IFNy ELISpot assay (6.6.3).

6.6 Analysis of humoral and cellular immune responses

6.6.1 *VLP-capture ELISA to determine L1-specific antibodies*

96well microtiter plates (Nunc) were coated with 50 µl/well of the purified polyclonal HPV16 L1-specific serum (#4543) in a 1:500 dilution in PBS at 4°C overnight. All incubation steps were performed 1 h at 37°C unless mentioned otherwise and plates were washed after each incubation step 4 times with PBS-T. After washing off unbound coating antibody, plates were blocked 1 h with 5 % milk in PBS-T. HPV16 VLPs were diluted 1:500 (0.3 µg/well in blocking solution) and 50 µl per well were added and incubated. Plates were washed and sera of immunized mice were applied in duplicates in a 1:10 dilution (100 µl/well). The positive control “1.3.5.15” (HPV16 L1) was also diluted 1:10. Incubation was followed by another washing step and a horseradish peroxidase conjugated anti-mouse IgG antibody (50 µl/ well; 1:5000) was applied. After 1 h, plates were washed and 50 µl TMB substrate were added to the wells and incubated at room temperature. The reaction was stopped after 5 to 10 minutes with 50 µl per well of 1 M H_2SO_4 and absorbance at 450 nm (reference wavelength: 620 nm) was measured in an ELISA reader. Sera were considered to be L1 antibody positive if the absorption value was above cut-off. The cut-off value is based on the distribution of absorbance values of control sera and was calculated as the mean value of negative controls plus three times standard deviation.

6.6.2 *$p16^{INK4a}$ - peptide pool ELISA to determine $p16^{INK4a}$ -specific antibodies*

$p16^{INK4a}$ specific antibodies were detected with overlapping peptides covering the complete sequence (5.2.3). To this end, 5 peptide pools consisting of 2 or 3 peptides were used by default. 96well microtiter plates (Nunc) were coated with a dilution of 40 µg per petide per ml in PBS. 50 µl per well were incubated at 4°C overnight. Plates were washed 4 times with PBS-T after each step and incubation was performed for 1 h at 37°C. After peptide coating, remaining binding sites were blocked with 0.5 % casein in PBS-T (coating for 1 h at room temperature. After washing, sera of immunized mice were applied in duplicates in a 1:10 dilution (50 µl/well) and incubated. Plates were washed again and a horseradish peroxidase conjugated anti-mouse IgG antibody (50 µl/ well; 1:5000) was applied and incubated. TMB substrate was used to detect HRP activity and the reaction was stopped after 30 minutes with 50 µl 1 M H_2SO_4. The yellow reaction product was read at 450 nm in an ELISA reader (reference wavelength: 620nm). Individual sera were scored as antibody-positive or negative using a cut-off value that was calculated as the mean value of negative controls plus three times standard deviation Sera were considered to be positive if at least one of the tested peptide pools showed a value above cut-off.

6.6.3 *Detection of antigen-specific cytotoxic T-lymphocytes by IFNγ-ELISpot*

An ex vivo IFNγ-ELISpot assay was performed 7 days after the last immunization and all steps on day one and two were carried out under sterile conditions in a flow hood. On day 1, 96well MultiScreen-HA plates (Millipore) were incubated for 5 minutes with 70 µl of 70% Ethanol, washed 4 times with 200 µl PBS /well and coated with 100 µl/well anti-mouse IFNγ capture antibody (0.6 µg per well, 5.2.4) diluted in PBS. The plates were wrapped in aluminium foil and incubated at 4°C over night or at 37°C for 1 - 2 hours. On day 2, plates were washed with PBS 4 times and then blocked with 200 µl RPMI culture medium supplemented with 10% FCS and Pen/Strep (5.3.2) for 1-2 hours at 37°C. Splenocytes of the sacrificed mice (6.5.4) and peptide working solutions (5.2.3) were further processed during this incubation time. The blocking medium was removed stepwise and 1.3 - 1.5 x 10^6 cells/well were seeded in a volume of 100 µl. Per mouse three wells were used for the assay positive control which were stimulated unspecifically with 2 µg ConA per well in 100 µl; three wells were toped up with 100 µl culture medium for the background negative control. Also the test peptides or the p16 peptide pool were each tested in triplicates with 10 ng/well antigenic peptide in 100 µl medium. A typical loading scheme is depicted in Figure 11, yet it was adapted corresponding to the number of mice and peptides tested. After incubation for 18 to 20 hours at 37°C cells were removed and plates were washed 4 times with PBS-0.01% Tween20 and once with PBS. 0.1 µg of a biotinylated rat anti-mouse IFNγ antibody diluted in PBS (100 µl) were added per well and incubated 1 - 2 h at room temperature. After removing the secondary antibody, plates were washed 6 times with PBS-T and once with PBS. Then, 100 µl per well streptavidin-alkaline phosphatase diluted 1:1,000 in PBS were added and incubated for 30 min at room temperature in the dark. Plates were subsequently washed 3 times with PBS-T and 3 times with PBS and 100 µl/well BCTP/NBT substrate (Sigma) were added and incubated in the dark. After 5 to 10 minutes, the staining reaction was stopped by rinsing the plates extensively with distilled water and plates were left to dry over night. Spots were then quantified with an ELISpot reader.

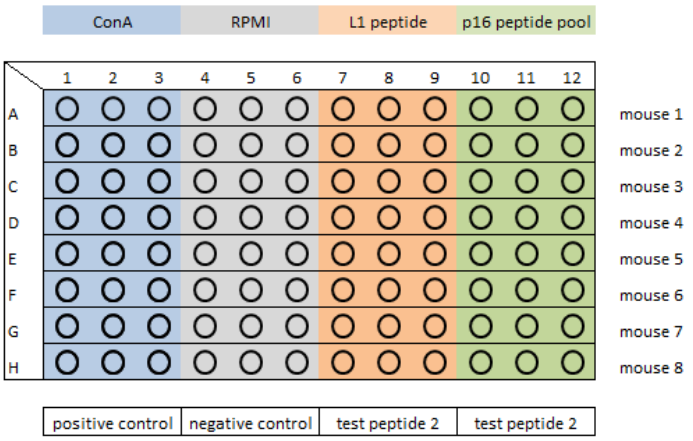

Figure 11: Exemplary loading scheme for IFNγ ELISpot. Negative control: RPMI medium; positive control: Concavalin A mitogen; test peptides: antigen-specific CTL epitope peptide L1 or $p16^{INK4a}$ overlapping peptides (pooled).

III. Results

In the field of prophylactic HPV vaccination much advancement was achieved in the recent years leading to reduced incidence of HPV-associated lesions [142]; although this only holds true for high-income countries. The need for effective therapeutics targeting neoplastic precursors and cancer is still high, especially in low-resource countries with inadequate screening coverage. Furthermore, women who are already infected with papillomaviruses do not benefit from the available prophylactic vaccines as these do not have any therapeutic effect [140, 143]. This led to various strategies in the development of therapeutic vaccines, with more or less effect considering clinical outcome.

In this thesis, three different constructs containing L1 and $p16^{INK4a}$ were cloned into the bacterial expression system. The GST-fusion proteins were expressed in E. coli and a suitable purification protocol was established. The purified proteins were then evaluated for their structural characteristics and immunological potential. These chimeric capsomeres produced in bacteria present a cost effective alternative to established VLP-based vaccines and could present a unique therapeutic approach by activating the immune system to target $p16^{INK4a}$ overexpressing cancer cells.

7 Generation and validation of the expression vectors

To evaluate the antigenic effect of different structural isoforms three constructs containing L1 and $p16^{INK4a}$ were generated by means of PCR cloning (7.1) and evaluated by restriction digestion and sequence analysis (7.2). Therefore, the complete $p16^{INK4a}$ encoding cDNA sequence was cloned a) upstream and b) downstream of a modified HPV16 L1 sequence [76] into the pGex-4T-2 expression vector. For the third construct c) the helix 4 region of L1 was replaced by $p16^{INK4a}$ [129]. The pGex-4T-2 vector was used to enable expression as GST-fusion proteins and purification by GSTrap affinity chromatography and was kindly provided by Dr. Lysann Schädlich and Prof. Lutz Gissmann (DKFZ Heidelberg, Germany). The vector construct used as a starting point for all further cloning attempts contained the modified HPV16 L1 sequence (L1ΔN10Δ408-431ΔC29) and the full length HPV16 E7 oncogene which was fused to the C-terminus of the L1 sequence.

7.1 Cloning of the expression plasmids

pGex-L1-p16^{INK4a}

The pGex-L1ΔN10Δh4ΔC29-p16^{INK4a} construct was cloned by means of PCR, whereby the p16^{INK4a} sequence was amplified from HeLa cDNA with primers containing the appropriate restriction sites NsiI and HindIII. The E7 sequence was cut out of the origin vector pGex-L1ΔN10Δh4ΔC29-E7 at the restriction sites and replaced with p16^{INK4a} DNA (see Figure 12).

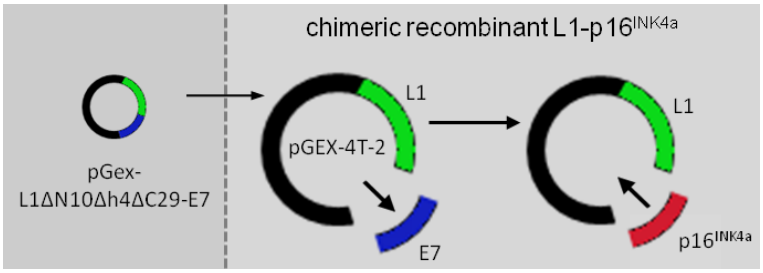

Figure 12: Cloning of pGex-L1-p16^{INK4a}.
L1-p16^{INK4a} was cloned into pGex-4T-2 (6.1) by cutting out the E7 insert from the original plasmid and replacing it with p16^{INK4a}. The plasmid was transformed into in the E. coli strains BL21 and Rosetta.

During digestion with the restriction enzymes, processing was kept under surveillance with agarose gel electrophoresis (Figure 13). Each step entails a loss of DNA which is especially due to purifications after each digestion. These purifications are necessary because the two restriction enzymes require different buffer conditions. The decreasing DNA amount is visualized by gel electrophoresis shown in Figure 13. The DNA amount of the p16^{INK4a} insert is initially lower as this is a purified PCR product.

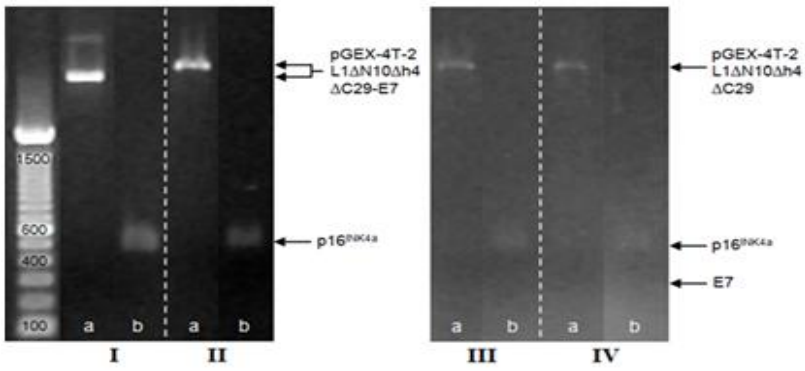

Figure 13: Single steps of the restriction digest were monitored by agarose gel electrophoresis. a: vector DNA, b: insert DNA. I) before digestion, II) after HindIII digest, III) after NsiI digest, IV) after final purification. Cut out E7 is present in III and IV a but hardly visible due to the very low DNA amount.

To avoid excessive re-insertion of the original E7 insert, the vector DNA was separated from the cut out insert and excised from an agarose gel before it was used for the ligation reaction with the p16^{INK4a} insert. E. coli Top10 cells were transformed with the ligation

mixture and colony PCR was applied to select clones with the desired insert. Figure 14 shows the PCR products that were obtained with plasmid DNA of a selected Top10 clone. This clone was (amongst others) picked from an agar plate after transformation and its DNA was isolated from a saturated over night culture. Column I shows a PCR product of 162 bp which was generated with primers binding within the p16 site. The size of the product in II was expected to be 216 bp as it is shown in Figure 14. This product was amplified from the overlapping region of L1 and $p16^{INK4a}$ with a forward primer binding at the end of the L1 sequence and a reverse primer that binds at the beginning of $p16^{INK4a}$. Column III shows a 568 bp product that was amplified with a forward primer binding at the end of the L1 region and a reverse primer binding within the p16 sequence. These results indicate the presence of the desired L1-$p16^{INK4a}$ insert due to successfully ligated and transformed plasmid DNA.

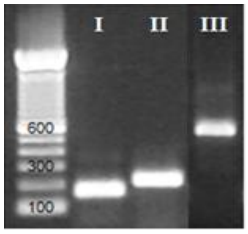

Figure 14: Colony PCR of a selected E. coli Top10 clone containing pGex-L1-p16 (template: isolated plasmid DNA). PCR product sizes: I) 162 bp, generated with primers $p16^{INK4a}$_forward and $p16^{INK4a}$_reverse, II) 216 bp, generated with L1-p16_ forward and L1-p16_reverse, III) 568 bp, generated with seq_L1-p16_forward and $p16^{INK4a}$_reverse.

To validate the presence of the correct sized insert after transfection into E. coli Rosetta and BL21, isolated plasmid DNA was digested with NsiI and HindIII. Figure 15 shows the cut out insert which is 471 bp heavy and therefore in line with the calculated size of the $p16^{INK4a}$ insert.

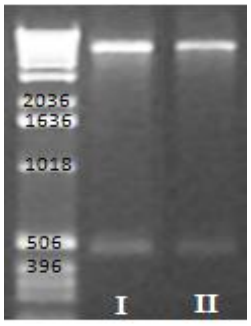

Figure 15: Control digest of pGex-L1ΔN10Δh4ΔC29-$p16^{INK4a}$ plasmid DNA with restriction endonucleases NsiI and HindIII. Isolated plasmid DNA from I) E. coli Rosetta and II) BL21. The expected insert size of 471 bp could be confirmed.

The generated pGex-L1-$p16^{INK4a}$ plasmid was used to express the GST-tagged L1ΔN10Δh4 ΔC29-$p16^{INK4a}$ protein.

pGex-$p16^{INK4a}$-L1

pGex-$p16^{INK4a}$-L1ΔN10Δh4ΔC29 was generated by overlap PCR (see Figure 17). Thereto, $p16^{INK4a}$ was amplified from HeLa cDNA with a reverse primer containing the beginning of

the L1 sequence (5.2.2). The L1 sequence was amplified from the origin vector pGex-L1ΔN10Δh4ΔC29-E7 using a forward primer containing the end of the p16^{INK4a} sequence. Both PCR products were then used as templates for a third PCR to amplify the complete p16^{INK4a}-L1 sequence which was then cloned into the expression vector as depicted in Figure 16.

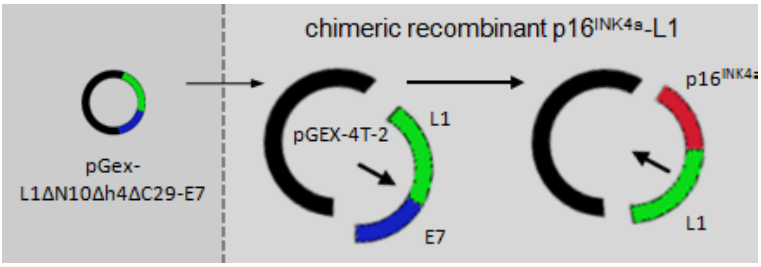

Figure 16: Cloning of p16^{INK4a}-L1.
p16^{INK4a} -L1 was cloned into pGex-4T-2 (6.1) by using an overlap PCR strategy (see below). The plasmid was transformed into in the E. coli strains BL21 and Rosetta.

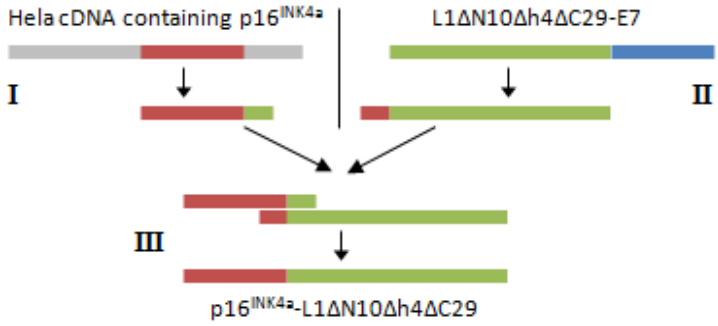

Figure 17: Schematic representation of the overlap PCR strategy used to generate the p16^{INK4a}-L1 insert from I) HeLa cDNA (for the amplification of the p16^{INK4a} sequence) and II) the origin vector L1ΔN10Δh4ΔC29-E7 (for the amplification of L1ΔN10Δh4ΔC29). The fragments I and II were amplified with primers including the overlap sequence and the appropriate restriction sites required for insertion to the vector. In an overlap PCR (III) products from I and II were used as templates to generate the p16^{INK4a}-L1 insert.

Results of the corresponding polymerase chain reactions (PCRs) are shown in Figure 18. All PCRs generated products of the expected size. The 1811 bp fragment (overlap PCR III) was digested with BamHI and HindIII to provide sticky ends for the ligation reaction with the likewise digested and purified pGex vector backbone.

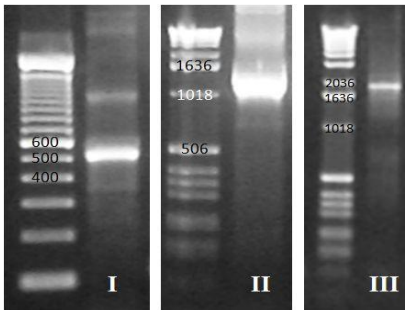

Figure 18: Cloning of the p16^{INK4a}-L1 insert. PCR I to amplify the p16^{INK4a} sequence with primers p16_BamHI_forward and p16L1_reverse (product size: 493 bp), PCR II to amplify the L1 sequence with primers p16L1_forward and L1_HindIII_reverse (product size: 1354 bp), PCR III (overlap PCR) was performed with primers p16_BamHI_forward and L1_HindIII_reverse (product size: 1811 bp). The product from PCR III was ligated into the pGex-4T-2 backbone and transformed into E. coli Rosetta and BL21.

After successful generation of the p16^{INK4a}-L1 insert, it was ligated into the expression vector pGex-4T-2 and transformed into E. coli Top10. Plasmid DNA was isolated and a control digest was performed to verify the correct insert size of 1797 bp (Figure 19). The plasmid DNA was then transformed into E. coli Rosetta and BL21 to express chimeric GST-p16^{INK4a}-L1ΔN10Δh4ΔC29 capsomeres.

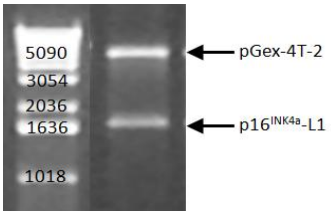

Figure 19: Control digest of pGex-p16^{INK4a}-L1ΔN10Δh4ΔC29 plasmid DNA with restriction endonucleases BamHI and HindIII. Isolated plasmid DNA from I) E. coli Top10. The expected insert size of 1797 bp could be confirmed.

pGex-L1-p16^{INK4a}-L1

The third insert, L1ΔN10Δh4-p16^{INK4a}-ΔC29 was designed on the basis of a study by Murata and colleagues [129] who showed that the helix 4 region of the HPV16 L1 capsomeres can function as an antigen display site for non-HPV encoded epitopes. The insert sequence was synthesized by Genscript and delivered in a pUC57 vector. After cutting the insert at the BamHI and HindIII sites, it was ligated into the pGex-4T-2 expression vector (Figure 20).

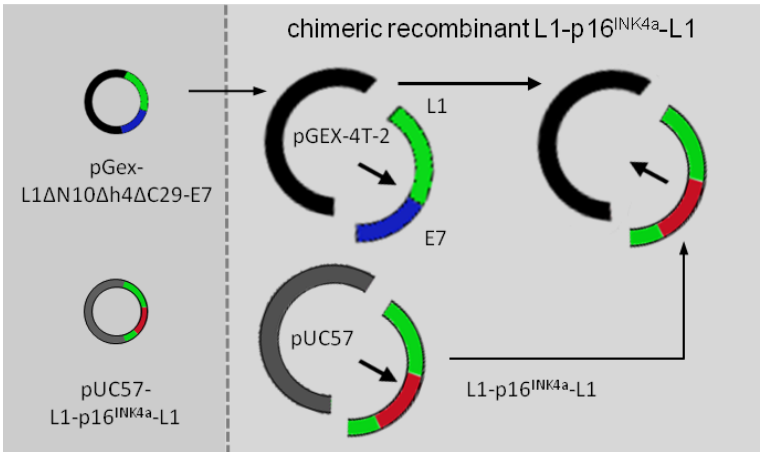

Figure 20: Cloning of L1-p16^{INK4a} -L1.
L1-p16^{INK4a} -L1 was cloned into pGEX-4T-2 (6.1) after cutting the insert from a pUC57 vector (Genescript). The plasmid was transformed into in the E. coli strains BL21 and Rosetta

After transformation into E. coli, colony PCR (6.1.10) with different primer pairs verified the presence of the insert (see Figure 21). pGex-L1-p16^{INK4a}-L1 was used to express the chimeric GST-L1ΔN10Δh4-p16^{INK4a}-ΔC29 protein.

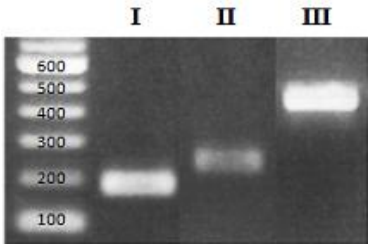

Figure 21: Colony PCR of the E. coli Rosetta clones, transformed with pGex-L1-p16^{INK4a}-L1. I: primers pGex-4T-2_seq + seq_p16L1_reverse (product size: 183 bp); II: primers L1d_forward + L1d_reverse (product size: 242 bp); III: primers p16INK4a_forward + pGex-4T-2_reverse (product size: 414 bp). With theses primer pairs, the presence of the correct sized insert was verified.

pGex- L1

The expression plasmid containing only the modified HPV16 L1 (pGex-L1ΔN10∆h4ΔC29) was generated by PCR whereby the reverse primer was used to add the HindIII restriction site. pGex-L1-E7 was used as template DNA for the reaction. This construct was used for the expression of GST-L1 for comparative purposes and to be used as an anitgen for the L1 control group in the in vivo experiments (see chapter 0).

pGex-p16^{INK4a}

The p16^{INK4a} sequence was amplified from HeLa cDNA with primers p16_BamHI_forward and p16_HindIII_reverse to add the appropriate restriction sites. Vector DNA pGex-4T-2 and the amplified p16^{INK4a} insert were digested with BamHI and HindIII and purified by Gelextraction (Quiagen Gelextraction Kit). Afterwards they were ligated and transformed into BL21 and Rosetta to express the GST-p16^{INK4a} fusion protein.

GST-p16^{INK4a} was produced for comparative purposes and as an anitgen for the p16-control group in the in vivo experiments (see chapter 0).

7.2 Sequence analysis of the generated plasmids

To finally validate the recombinant chimeric constructs on the DNA level, all pGex-4T-2 constructs were sequenced after transformation into the expression strains BL21 and Rosetta to finally ensure correct orientation of the insert and to exclude mutations and thereby resulting frame shifts or amino acid changes.
In the following, sequencing results are shown for plasmid DNA isolated from E. coli Rosetta as this strain was later used for large scale protein expression. BL21 bacteria were transformed in parallel with the exact same plasmid DNA that was extracted from E. coli Top10 beforehand. The selected BL21 clones were sequenced and analyzed likewise and were also found to contain the correct plasmids (data are not shown).

pGex-L1-p16^{INK4a}

To ensure the correct nucleotide sequence, pGex-L1-p16^{INK4a} transformed clones were sequenced with the ABI 3100 (6.1.10) and checked with the SnapGene software and the Basic Local Alignment Search Tool (NCBI BLAST).

Figure 22 shows the sequence alignment map generated with SnapGene. The sequences were obtained with the indicated primers (pink, pGex-4T-2_seq, L1p16_forward and p16^{INK4a}_forward) and alignments that match the subject sequence are depicted as red arrows. It is evident that the correct insert is present in the pGex-L1-p16^{INK4a} construct as the critical cutting sites, NsiI and HindIII, were the p16 sequence was introduced, are covered by the sequence alignment.

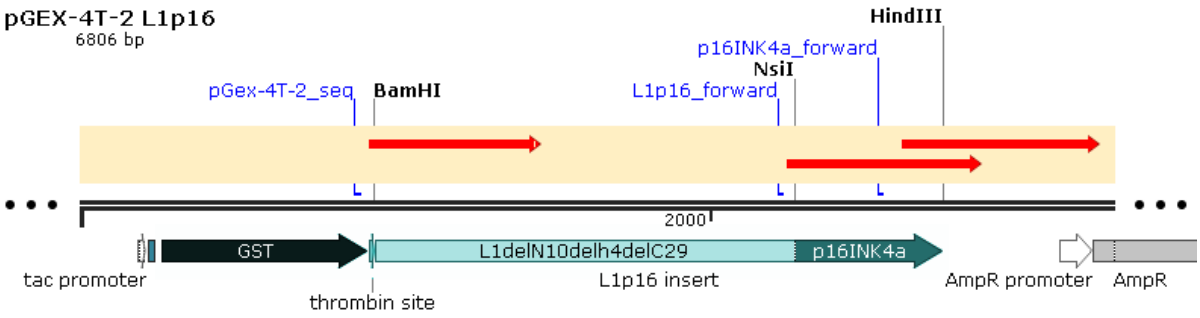

Figure 22: pGex-L1ΔN10Δh4ΔC29-p16^{INK4a} sequence alignment map (compiled with SnapGene). Aligned sequences are shown as red arrows; primers used for sequencing (ABI 3100, see 6.1.10) are depicted in blue. The complete plasmid map is provided in the supplementary material (VII, Figure 63)

pGex-p16^{INK4a}-L1

Plasmid DNA from pGex-p16^{INK4a}-L1_transformed bacteria was sequenced with primers binding in the GST tag (pGex-4T-2_seq), right before the p16-L1 overlap (p16L1_forward) and at the end of the L1 region (seq_L1-p16_forward) to validate the insert and the overlapping region. Sequence alignment was performed with the SnapGene software and the Basic Local Alignment Search Tool (NCBI BLAST).

Figure 23 shows the sequence alignment map generated with SnapGene. The sequences were obtained with the indicated primers (pink) and alignments that match the subject sequence are depicted as red arrows. It is evident that the correct insert is present in the pGex-p16^{INK4a}-L1 construct as the critical cutting sites, BamHI and HindIII, were the p16-L1 sequence was introduced, are covered by the sequence alignment.

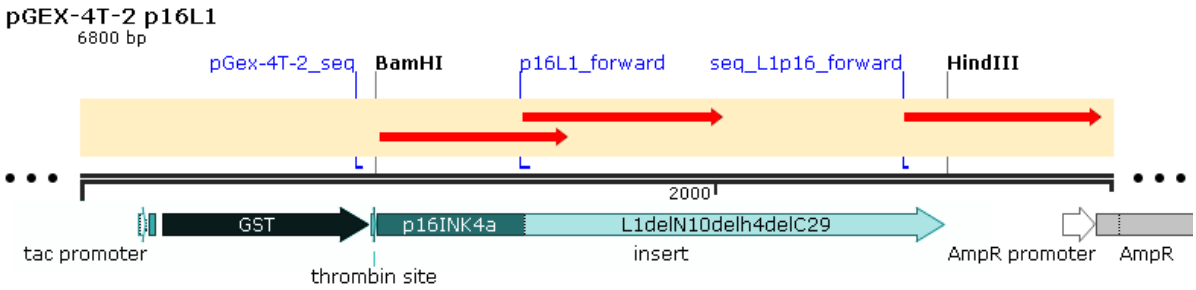

Figure 23: pGex-p16^{INK4a}-L1ΔN10Δh4ΔC29 sequence alignment map (compiled with SnapGene). Aligned sequences are shown as red arrows; primers used for sequencing (ABI 3100, see 6.1.10) are depicted in blue. The complete plasmid map is provided in the supplementary material (VII, Figure 64)

pGex-L1-p16^{INK4a}-L1

The pGex-L1-p16^{INK4a}-L1 plasmid isolated from transformed clones was sequenced (GATC) with primers pGex-4T-2_seq, L1d_forward, p16^{INK4a}_forward pGex-4T-2_reverse. The results were analysed with the SnapGene software and the Basic Local Alignment Search Tool (NCBI BLAST) to validate the correct nucleotide sequence.

Figure 24 shows the sequence alignment map generated with SnapGene. The sequences were obtained with the indicated primers (pink) and alignments that match the subject sequence are depicted as red arrows. It is evident that the correct insert is present in the pGex-L1-p16^{INK4a}-L1 construct as the critical cutting sites, BamHI and HindIII, were the L1-p16-L1 sequence was introduced, are covered by the sequence alignment.

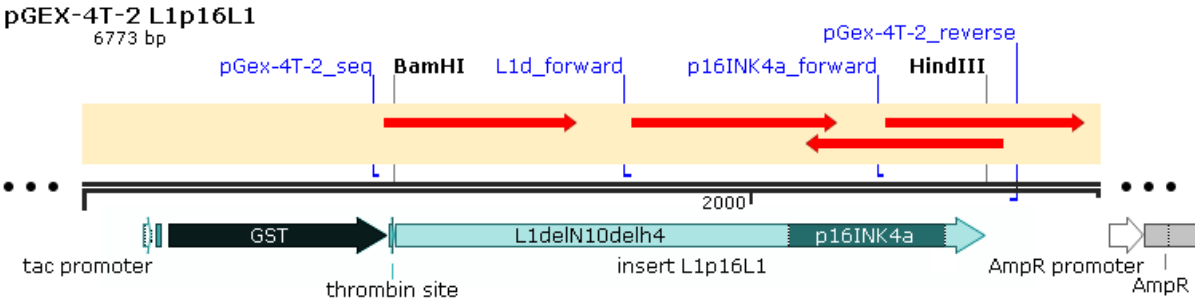

Figure 24: pGex- L1ΔN10Δh4-p16^{INK4a}-L1ΔC29 sequence alignment map (compiled with SnapGene). Aligned sequences are shown as red arrows; primers used for sequencing (GATC) are depicted in blue. The complete plasmid map is provided in the supplementary material (VII, Figure 65)

7.3 Conclusions

The desired pGex-4T-2 vector constructs (inserts shown in Figure 25) could be successfully cloned and transformed into the expression strains BL21 and Rosetta. The correct insert sequences were confirmed by digestion with the appropriate restriction enzymes and

sequencing with different primers. Several gaps and nucleotide mismatches could be manually excluded by means of the sequence chromatogram.

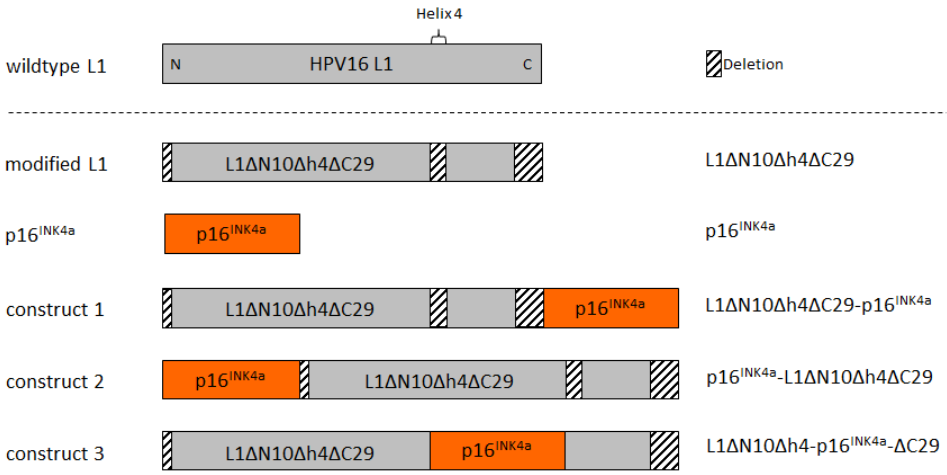

Figure 25: inserts used for protein expression in E. coli. The HPV16 L1 gene was previously modified to prevent capsid assembly [76]. The different constructs are depicted in cartoon format. For comparison, the wild-type HPV16 L1 gene is shown at the top. The modifications/features of each construct are shown as follows: grey bar - modified HPV16 L1, orange bar - $p16^{INK4a}$ sequence; hatched line - deleted region. To the right of each construct map is its complete name of the insert. All genes were cloned into the pGex-4T-2 vector to allow their expression and purification as GST-fusion proteins.

8 Protein Expression

After demonstrating successful cloning of the desired chimeric constructs on the DNA level, expression of the recombinant proteins in E. coli Rosetta and BL21 was evaluated and optimization attempts were made. Preliminary tests were accomplished with 100 ml small scale bacteria cultures to identify optimal growth and expression conditions, to check whether the protein of interest is expressed at all and to what extend it is present in soluble form. The small scale experiments revealed that all proteins that contain the modified L1 are particularly expressed as inclusion bodies and only a low percentage of the overall expressed protein could be harvested as soluble fraction. For this reason the large scale (5 L) production was used to express and accumulate as much protein as possible although it was present as insoluble inclusion bodies. These were purified according to an optimized protocol described in 6.4.1.

8.1 Small scale expression - evaluation and optimization

During exponential growth, optical densities of the bacteria cultures were monitored to induce protein expression at an appropriate time point. This would be the late exponential phase of growth. It was reported that the optimal OD600 for induction is 4.0 [144], however,

we found that the cultures can be grown to a maximum OD600 of 3.0 before entering the stationary phase. It was therefore decided to start induction at OD600 2.0 to 3.0, when two following OD600 values indicated stationary phase entry. The growth curves are shown in Figure 26 and indicate slower growth of the Rosetta cultures in comparison to BL21. Stationary phase entry is observable for BL21 L1p16 and Rosetta p16L1 at OD600 ~ 2.0.

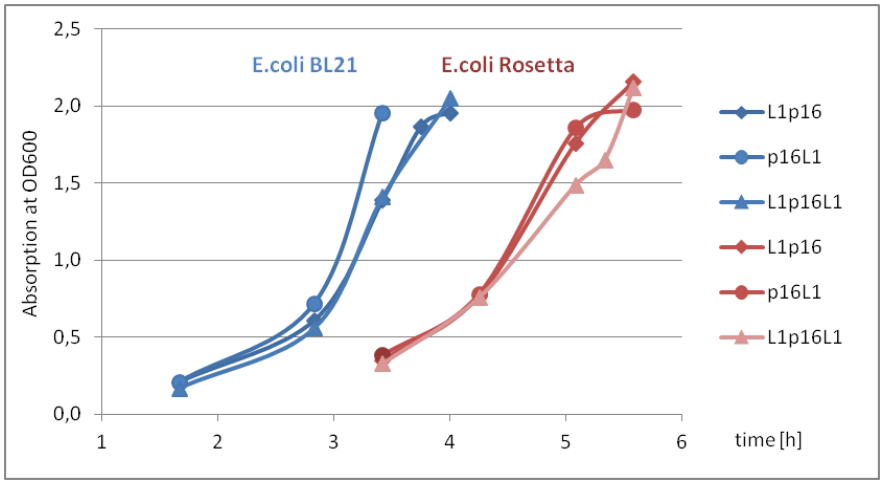

Figure 26: Growth characteristics of E. coli strains BL21 and Rosetta in Terrific Broth (TB) culture medium. Optical densities (OD 600 nm) were measured at different time points to monitor growth phase.

After expression of the protein, the cells were lysed by shear stress and decompression using a French press homogenizer. It was repeatedly observed that the bulk of the protein is of insoluble nature as it was found in the pelleted fractions after centrifugation as shown in Figure 27 and Figure 28. It is evident from Figure 27 that the solubility is equal for all the chimeric proteins (1: L1p16, 2: p16L1, 3: L1p16L1) independent of expression strain; also pGex-L1ΔN10Δh4ΔC29 transformed bacteria showed this specific solubility pattern (data not shown). pGex-p16^{INK4a} expression resulted in completely soluble protein (data not shown), indicating responsibility of the L1 proportion for inclusion body formation.

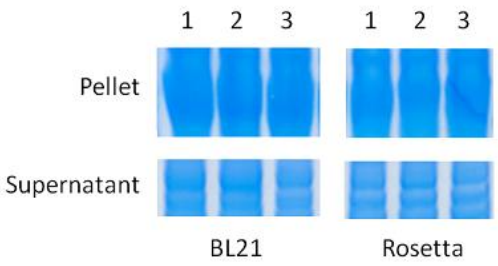

Figure 27: Protein amount after cell lysis (French press) in the pellet and in the supernatant of E. coli BL21 and Rosetta. 1: construct L1p16, 2: construct p16L1, 3: construct L1p16L1. After disruption of the bacteria, the majority of the protein is found in the pellet as insoluble fraction.

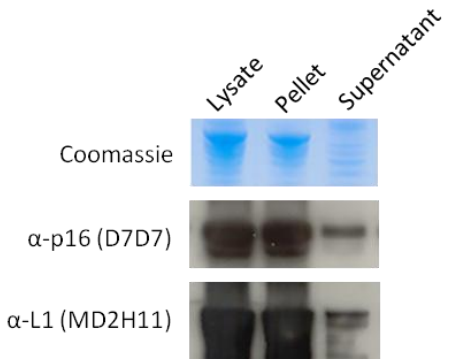

Figure 28: Analysis of protein solubility with Coomassie and antibody staining. BL21 expressing p16L1 are shown exemplary as the same pattern was observed for all L1 containing constructs. Bacteria were disrupted via French press and analyzed for their p16L1 fusion protein content. The bulk protein is present in the pelleted fraction; only small amounts that are rarely detectable by Coomassie staining are soluble.

Altogether it is evident that the proteins of interest are strongly overexpressed from the respective pGex vectors. As the supernatant samples miss this dominant band, it is obvious that solubility of the proteins is not optimal. The major proportion remains insoluble in the pellet fraction.

8.1.1 *Solubility screen*

To improve solubility of the target protein, a small scale solubility screen was performed with one of the constructs pGex-p16^{INK4a}-L1ΔN10Δh4ΔC29 as it was determined that the L1 containing proteins show similar properties regarding solubility. Therefore, the two transformed E. coli strains BL21 and Rosetta were induced with IPTG at optical densities 0.7 and 2.0 indicating early and late exponential growth phase. Furthermore, increasing IPTG concentrations were tested and samples were analyzed 3 and 17 hours post induction. After harvesting, the cells were disrupted by sonication and the supernatants were analyzed for soluble protein content. It is evident from Figure 29 that the different conditions resulted in varying amounts of soluble GST-tagged fusion protein that was expected to run at 92 kDa in the SDS-Page. However, with none of the tested conditions, a clearly improved soluble expression resulting in a dominant gel band was identified. Nevertheless it could be concluded that protein expression is more effective after a longer induction period and that the induction should be started at an OD600 of 2.0 to 3.0, respectively right before entry to the stationary growth phase. As the increasing IPTG concentrations tested did not result in increased soluble expression, 0.1 mM IPTG was decided to be a sufficient concentration for further trials.

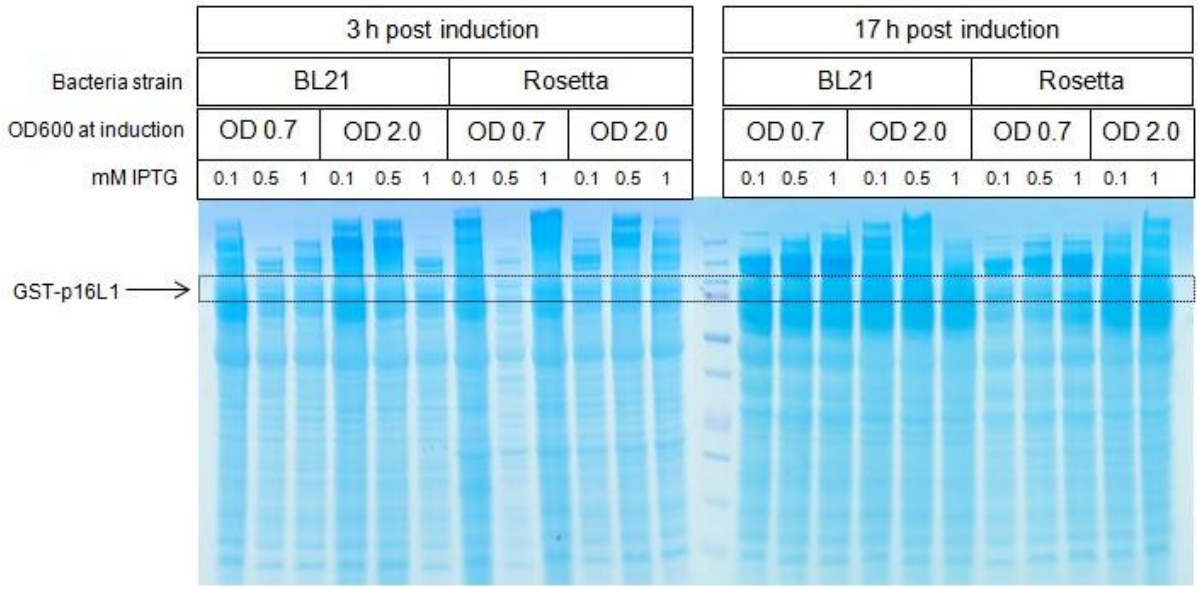

Figure 29: Small scale solubility screen (Coomassie gel, supernatants after cell lysis) using the p16-L1 construct to compare different induction conditions and expression strains. 25 ml TB-Medium containing the appropriate antibiotics were inoculated with BL21 or Rosetta transformed with pGex-p16^{INK4a}-L1ΔN10Δh4ΔC29. The cultures were grown to optical densities (OD 600nm) of 0.7 or 2.0 and then induced with IPTG in different molarities (0.1, 0.5 and 1 mM). The proportion of soluble fusion protein varies with the different conditions, however, no striking dominant band could be observed indicating independence of solubility from the induction conditions.

Besides testing different induction conditions, different induction temperatures (15, 22 and 37 °C) were compared (data not shown). However, also this did not lead to enhanced soluble expression of the L1 containing proteins.

8.1.2 *Osmosis screen*

To achieve soluble protein expression and, at best, avoid inclusion body formation, another small scale experiment was performed with application of heat shock and/or additives to increase the cellular concentration of osmolytes as osmotic and/or heat stress was reported to protect proteins from misfolding and aggregation [145].

Figure 30 shows the growth curves of bacteria under influence of the additives NaCl, sorbitol, betaine and glucose - added in mixture or alone and combined with heat shock as indicated in the legend. The optical density of 0.8 - 0.9 was chosen for protein induction as it resembles the end of the log phase for bacteria grown in LB medium. All the cultures show similar growth characteristics, whereby a delay can be observed with all additives in comparison to LB medium alone. The presence of 0.5 M sorbitol, 0.5 M NaCl and 1 mM betaine results in markedly slower growth of bacteria as the OD600 of 0.8 was reached after 6 h of growth in contrast to the other cultures where the required OD was reached after approximately 3 hours.

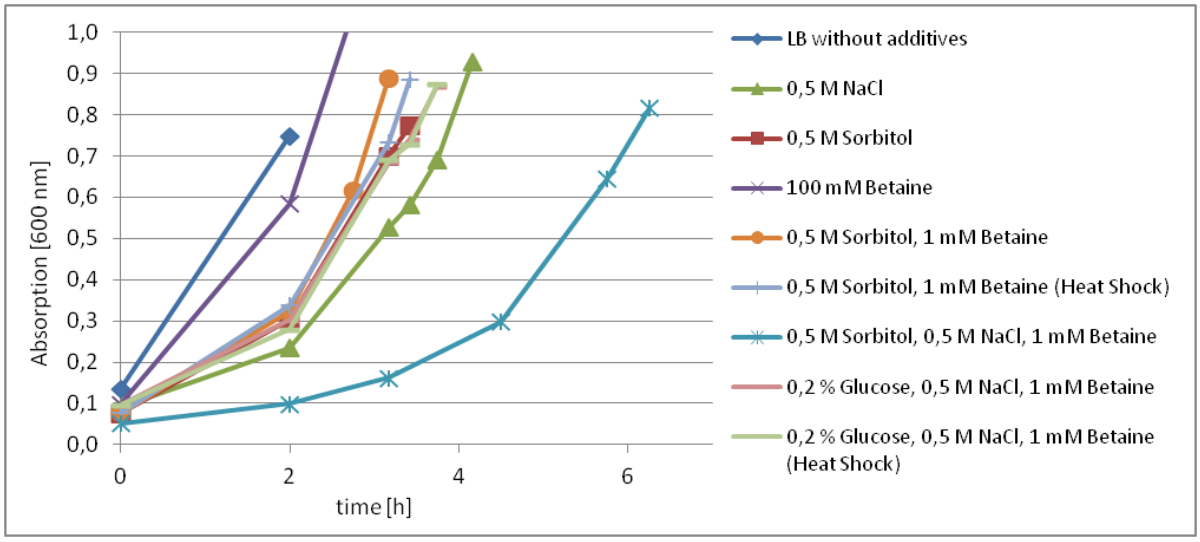

Figure 30: Growth curves Osmosis Screen. 10 ml LB medium with different additives was inoculated from an overnight culture of p16L1-expressing BL21 bacteria and grown to an optical density (OD600) of 0.8 - 0.9. Induction of protein expression was achieved by the addition of 100 µM IPTG.

After 17 hours of IPTG induced protein expression, cultures were harvested and lysed by sonication. The lysates were then cleared by centrifugation and supernatants and pellets were analyzed by Coomassie staining of a protein gel. Protein expression was increased under the influence of 0.5 M sorbitol as shown in Figure 31, lane 2 in comparison to LB medium without additives (lane 1). Presence of NaCl resulted in decreased expression (lanes 3 and 9) and betaine did not show any effect (lane 4), in fact it weakened the positive effect of sorbitol (lane 6). The heat shock was conducted right before IPTG induction and resulted in markedly decreased overall protein expression as visible in lanes 7 an 9. Comparison of supernatant samples with the pellets reveals no effect on soluble expression. The 92 kDa band of GST-p16L1 in the supernatant row is equal for all tested conditions, except in case a heat shock was applied where it is even weaker. The application of osmolytic and heat shock stress did therefore not improve the proportion of soluble expressed target protein.

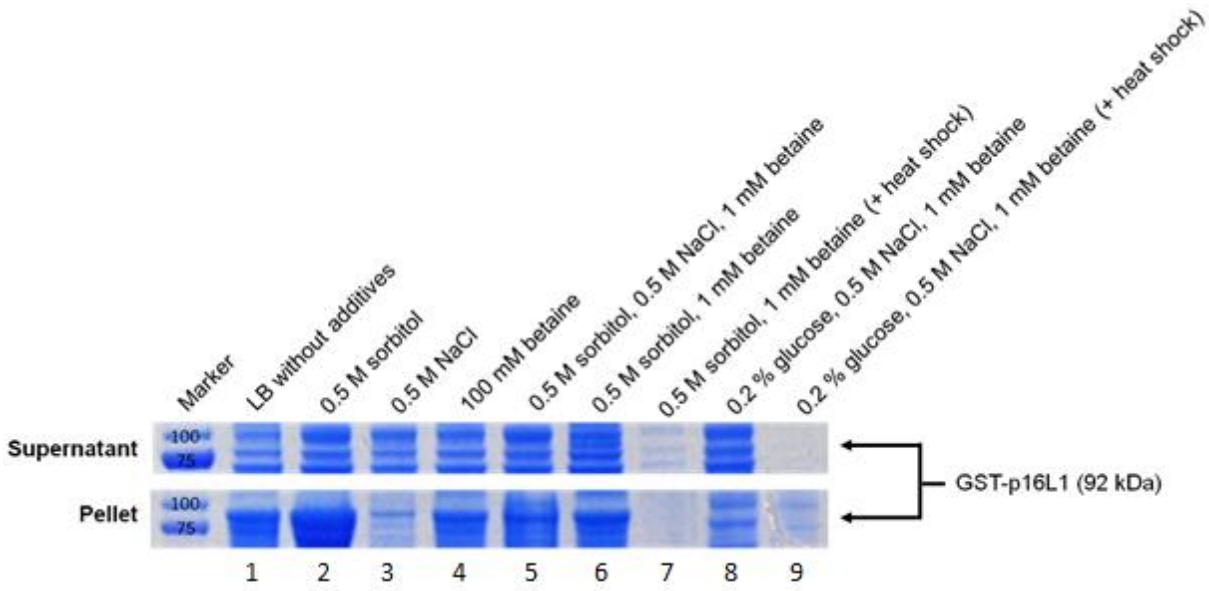

Figure 31: Coomassie gel of the osmosis screen. E. coli BL21 were cultured in LB with different additives and two cultures were treated with heat shock additionally. Cells were harvested and disrupted by sonication, centrifuged and equal amounts of supernatant and pellet were loaded for SDS-Page. A strong overexpression of GST-p16L1 could be observed for the sorbitol supplemented culture (in comparison to LB medium alone), whereby the addition of betaine did not improve expression. Addition of NaCl and application of heat shock resulted in an increased overall expression. From the supernatant samples it is evident that the application of osmolytic and heat shock stress did not improve the proportion of soluble target protein.

8.2 Large scale expression - protein production

As the small scale experiments did not reveal a suitable method for sufficient soluble protein expression, large scale cultivation of bacteria was performed in highly enriched TB-medium. Compared to LB-medium (data not shown), the expression in TB-medium led to higher overall protein yields.

It was constantly observed that all L1-containing protein lysates show several smaller fragments that were probably caused by degradation events or translation terminations, indicating problematic gene transcription or protein translation in E. coli. However, the target protein was found to represent the major proportion of the overall expressed proteins which was confirmed by Coomassie staining. Some of these truncated fragments could be removed during the purification process as described in chapter 9. Figure 32 shows the anti-L1 western blots of the capsomere preparations. The proteins were also analyzed with an anti-p16 antibody (D7D7, data not shown) which revealed truncated fragments likewise, except for the GST-p16^{INK4a} fusion protein that showed no signal as expected.

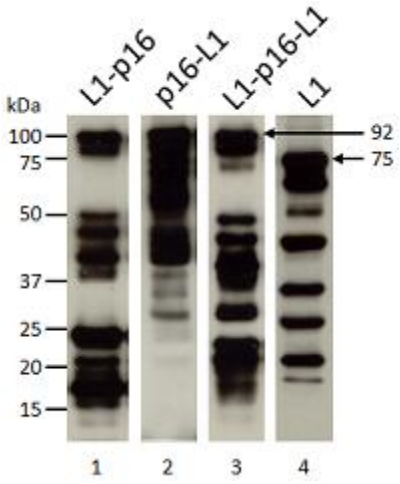

Figure 32: Large Scale Expression Rosetta - anti-L1 western blots (MD2H11) of GST-tagged L1-p16, p16L1, L1p16L1 and L1 supernatants. The three chimeric constructs have a size of 92 kDa each, L1 is 75 kDa (all including GST-tag). It was constantly observed that the expressed proteins show several smaller truncated fragments, probably translation terminations or degradation products.

The protein lysates were also analyzed for co-expression of bacterial chaperones, namely GroEL. Western blot analysis (see Figure 33) revealed that E. coli BL21 co-expresses large amounts of GroEL in contrast to Rosetta where only minimal GroEL traces could be detected. It further turned out that the tightly bound GroEL molecules are difficult to remove during protein purification. Also for this reason it was decided to use the Rosetta transformed clones for large scale purification attempts.

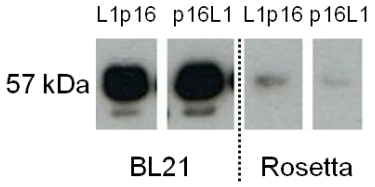

Figure 33: anti-GroEL Western Blot (A91/2) of cell lysates from E. coli BL21 and Rosetta expressing chimeric proteins L1p16 or p16L1. Equal protein amounts were loaded (2 µg per well). Strong expression of GroEL is visible in BL21 (detectable after 2 min exposure) in comparison to Rosetta where GroEL is only detectable with longer exposure time of the western blot (15 min).

8.3 Conclusions

The three chimeric constructs, L1-p16^{INK4a} p16^{INK4a}-L1 and L1-p16^{INK4a}-L1 as well as L1 and p16^{INK4a} could be successfully expressed in E. coli. Lysis of the bacteria revealed low solubility of the L1 containing proteins whereby p16^{INK4a} was found to be completely soluble. As the bulk protein remains in the pellet, this speaks for massive inclusion body production whereby inactive aggregates of protein accumulate and form insoluble structures.

To improve soluble protein expression, several attempts were made but did not result in markedly better solubility. The adaption of induction conditions and temperature as well as application of osmotic and/or heat stress did not lead to increased amounts of soluble expressed proteins. Therefore, the standard expression conditions (induction at OD600 2 - 3 with 0.1 mM IPTG for 17 h at 22°C) were used for the protein production. The comparison of the two tested E. coli strains, BL21 and Rosetta, did not reveal significant differences concerning protein yield. However, substantial co-expression of bacterial GroEL was

observed for the E. coli BL21 strain. As these chaperones were always found to be co-purified, it was decided to use E. coli Rosetta for further purification attempts.
The expressed fusion proteins contain several truncated fragments that could be identified by western blot analysis with anti-L1 and $p16^{INK4a}$ antibodies. This may be due to partial degradation, non-optimal gene transcription and/or ribosomal protein translation.

9 Protein Purification

Protein purification aims in the enrichment of a target protein from a complex biological mixture. This is often challenging as a great number of parameters has to be considered to maximize protein yield. Efficient protein purification is to select the most appropriate techniques to optimize performance while minimizing the number of required steps. It is often necessary to perform more than one purification step to reach the desired purity. Besides this, many proteins are problematic to purify, e.g. if they don't fold correctly or are expressed predominantly in insoluble form. [146]
This was also found to be the case for all constructs containing the modified L1ΔN10Δh4ΔC29 sequence. Although the proteins were expressed as GST fusions from a pGex vector, they were found to be hardly soluble independent of varying expression conditions as described in chapter 8. Therefore, a special inclusion body purification protocol (6.4.1) was developed to reach protein yields in mg range (9.1). In contrast to the L1 containing proteins, $p16^{INK4a}$ was perfectly soluble expressed and was therefore purified by affinity chromatography (9.2). In 9.3 results are shown for the GSTrap and SEC purification of L1 containing capsomere preparations, as this was also performed to test the achievable enrichment from the soluble fraction. As the inclusion body purification did not contain a step for the removal of the GST-tag, different attempts were made to separate the tag from the protein preparation. These are described in 9.4. Contaminating endotoxins were removed by Triton X-114 treatment (9.5) and in 9.6 the purified proteins were analyzed by electron microscopy, sedimentation analysis and epitope specific ELISA.

9.1 Inclusion body purification of HPV16 L1 and chimeric capsomeres

Insoluble L1-containing proteins were purified with a special protocol that included several washing and re-suspension steps. The purified inclusion bodies were denatured with 5 % N-Lauroylsarcosine and refolded by dialysis (for details see 6.4.1). Thereby, E. coli host cell proteins could be removed and high recovery of the target proteins was ensured. Figure 34 shows the GST-tagged proteins present in the bacterial lysat after French press

homogenization, the supernatants obtained after centrifugation which contained only small amounts of soluble protein as described in chapter 8 and the purified inclusion bodies. It is evident that the major proportion of the individual proteins could be transferred through the inclusion body purification process with minimal losses. This is one of the most striking advantages of using inclusion bodies for the preparation of E. coli proteins. As shown in Figure 34, the inclusion bodies could be effectively separated from the large proportion of bacterial proteins. Several smaller fragments were detected by coomassie staining which were identified to be truncated L1 and p16 containing proteins (see Figure 35).

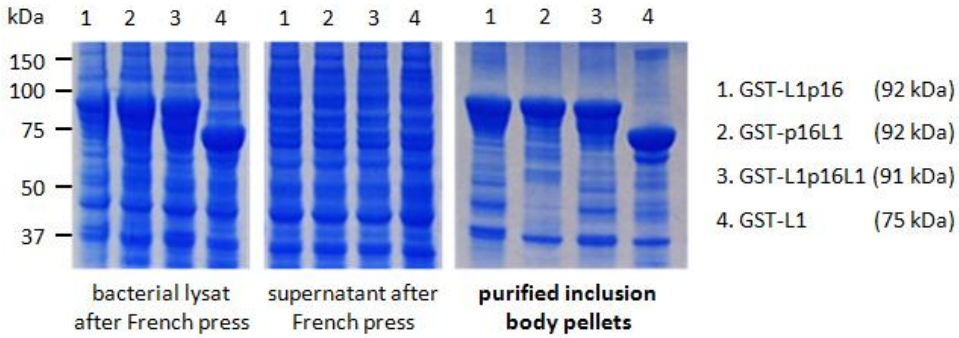

Figure 34: Coomassie stained protein gels before and after inclusion body purification. The bacterial lysates show strong overexpression of the target proteins; however the supernatants did not contain suitable amounts as shown before. After several washing and re-suspension steps, the purified inclusion body pellets still contain the majority of the GST-fusion protein. Several smaller bands were observed to co-purify and were identified as truncated target proteins.

After purification of the inclusion bodies, the aggregated and probably misfolded proteins had to be transformed into a soluble, at its best, native form. Therefore the proteins were first denatured and thereby solubilized with the anionic detergent N-Lauroylsarcosine. Subsequent refolding was achieved utilizing dialysis with decreasing concentrations of the detergent and salts (for details see 5.4.2 and 6.4.1).

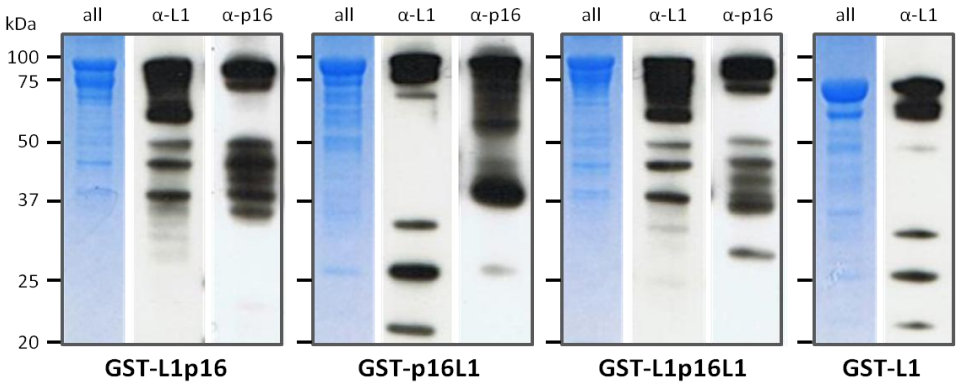

Figure 35: Analysis of protein preparations obtained from inclusion body purification after Lauroylsarcosine-denaturation and refolding of the target proteins. The whole protein content analyzed by coomassie staining, the anti-L1 (MD2H11) and the anti-p16 (D7D7) western blots are shown. In each case, the major proportion - respectively the dominant band in the coomassie gel - is made up of the target protein as analyzed by western blotting. Smaller fragments could also be identified to be predominantly of L1 or p16 origin speaking for truncated, co-purified proteins.

Figure 35 shows the results of the protein preparations obtained from inclusion bodies. For each of the L1 containing constructs, coomassie staining, anti-L1 and anti-p16 western blot are shown in comparison. The intense bands at ~92 kDa, respectively 75 kDa for GST-L1, indicate the GST-tagged fusion proteins. Below this upper dominant band, several smaller fragments could be identified in all the preparations. Western blot analysis revealed that these fragments must be of L1 or p16 origin, and thereby presenting truncated or degraded target proteins. Compared to Figure 32 that shows the anti-p16 western blot of the proteins right after expression, several smaller bands are missing or less intense after inclusion body purification, indicating successful enrichment of the target proteins.

To determine the protein concentration of the full length target protein, densitometry was applied (6.4.11) on a coomassie blue-stained sodium dodecyl sulfate-polyacrylamide gel (SDS-PAG). Therefore, different bovine serum albumin (BSA) standard solutions were compared to the fusion proteins by graphical analysis using ImageJ software. This method was chosen as it allows determination of the concentration of the 92 kDa (respectively 75 kDa for GST-L1) protein present in the sample. The overall protein concentration was determined with the 2D-Quant kit. For subsequent immunological trials, the densitometrically determined concentrations were applied to ensure correct dosage of the target proteins. From Table 3 follows that the full-length target proteins account approx. for one third of the whole protein content.

Table 3: Protein concentrations of the GST-fusion proteins purified from inclusion bodies determined by densitometry (ImageJ analysis; concentration of the full-length target protein, excluding truncated products), 2D-Quant analysis (total protein content) and calculated protein amount that was obtained from 100 ml culture volume.

Protein	Densitometry [mg/ml]	Total protein [mg/ml]	target protein / 100 ml culture volume [mg]
GST-L1p16	0.94	3.17	28.67
GST-p16L1	1.32	3.16	40.26
GST-L1p16L1	1.11	3.66	33.86
GST-L1	1.79	3.21	54.60

9.2 $p16^{INK4a}$ GSTrap purification

As GST-$p16^{INK4a}$ was expressed in soluble form, it had to be purified in a different way than the insoluble L1 capsomeres. All protein lysates were treated equally as far as possible, e.g. they were lysed in the same buffer. Figure 36 shows coomassie and western blot analysis of the bacterial lysate after French press, the supernatant containing the soluble protein and the purified GST-$p16^{INK4a}$ after GSTrap affinity chromatography. The intense band at 42 kDa

in the coomassie gel was confirmed to be p16^{INKa} with western blot analysis. After disruption of the bacterial cells, the supernatant was collected and loaded onto a 5 ml GSTrap FF column (GE Healthcare). The GST-p16^{INK4a} protein was eluted with 20 mM glutathione to sustain the GST-tag. It was also possible to cleave p16^{INK4a} from the GST tag with thrombin. However, to ensure best possible comparability for subsequent immunological in vivo experiments, p16^{INK4a} was purified along with its GST-tag, at least for the application as control group protein in the mouse trials.

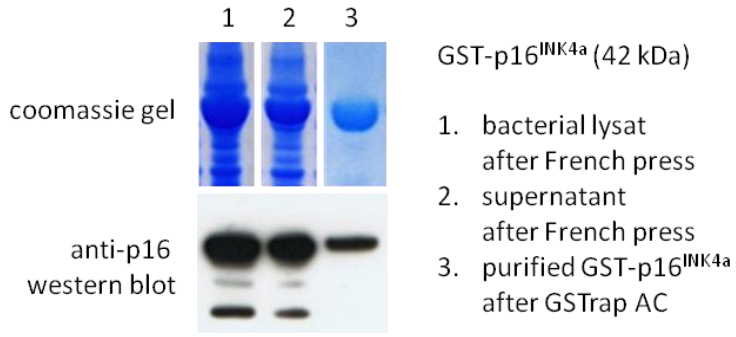

Figure 36: Coomassie staining and anti-p16 western blot of GST-p16^{INK4a} (soluble expressed protein of 42 kDa). Several contaminating proteins that are visible in lanes 1 and 2 of the coomassie gel could be removed during the purification process as shown in lane 3. The anti-p16 western blot (antibody D7D7) reveals presence of the correct sized GST-tagged protein.

With this purification, protein concentrations of up to 3 mg/ml were obtained in the first GSTrap elution fraction shown in lane 3, figure 35. The protein concentration was determined with the densitometry method (6.4.8) utilizing a BSA standard and graphical analysis of a coomassie gel.

The obtained protein was then analyzed for its LPS content and remaining endotoxins were removed by Triton X-114 treatment (see 6.4.11 for method and 9.5 for results).

9.3 GSTrap and SEC purification of soluble fusion proteins

Besides inclusion body purification, the cell lysates obtained from the chimeric L1 containing proteins were also purified using the originally planned strategy to evaluate its potential for the protein production for immunological studies. The originally planned purification procedure includes purification of the crude cell lysate by GSTrap affinity chromatography and subsequent SEC polishing as described in 6.4.3. GSTrap affinity chromatography was performed to give an impression of the achievable concentration of the target protein and SEC was applied to remove residual E. coli chaperones and for further purification.

In the following, data of the GST-p16L1 purification are shown exemplary as the other L1 containing constructs showed similar characteristics during the purification process.
The chromatograms for p16L1 GSTrap affinity chromatography are shown in Figure 37.

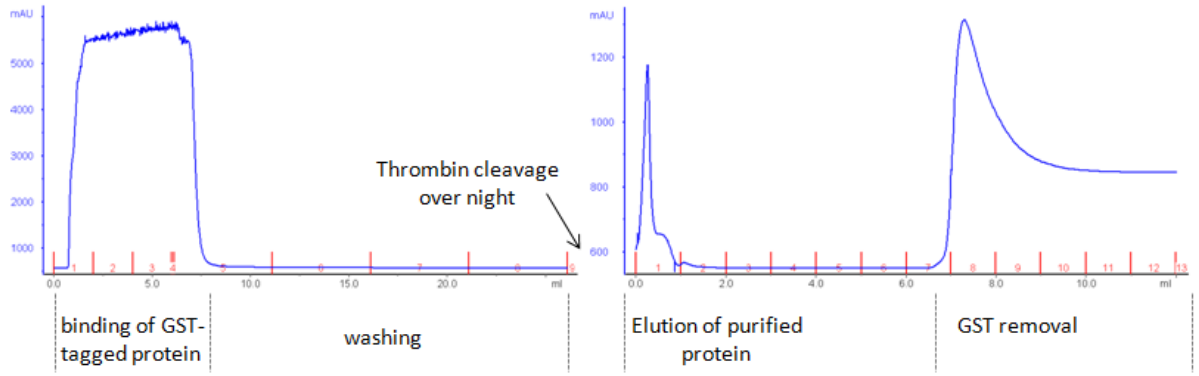

Figure 37: Chromatogram of the GSTrap FF (GE Healthcare) run, exemplary for GST-p16L1. Y-axis: absorbance at 280 nm; X-axis: transferred volume in ml. The GST-tagged protein binds to column matrix (glutathione sepharose) and contaminating proteins and substances are washed off the column. After thrombin cleavage over night, the fusion protein can be eluted. Residual bound GST is washed off with high molar glutathione.

The fractions obtained during the GSTrap run were analyzed by coomassie staining of a SDS-gel (see Figure 38) and western blot with anti-L1, anti-p16 and anti-GroEL antibodies. It was revealed that the protein can be purified with GSTrap, although the concentration in the eluted fractions is low. In contrast, high amounts of GST seem to be enriched, as demonstrated by the intense bands in the GST wash fractions and the comparable large peak area in Figure 37. This also explains a loss of target protein during GSTrap purification as free GST and GST-protein fragments occupy the available binding sites on the affinity column leading to reduced overall capacity. An anti-GroEL western blot (data not shown) showed that GroEL is co-eluted with the protein of interest.

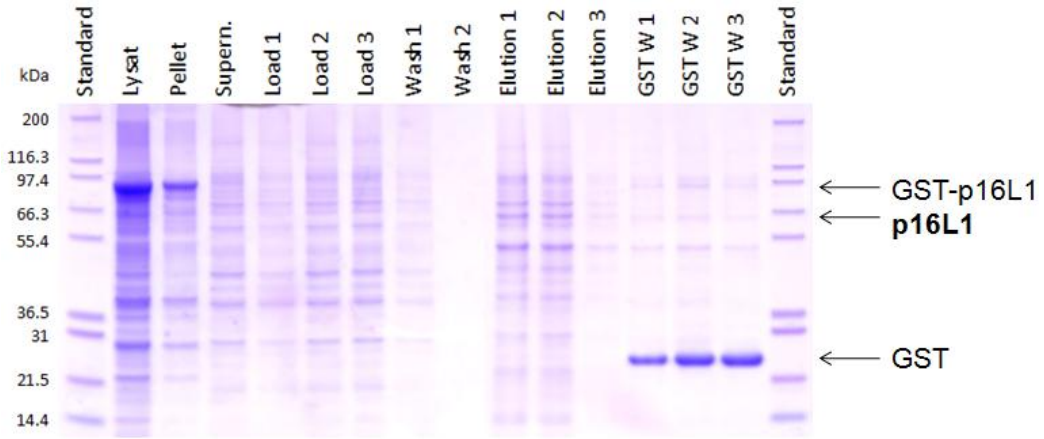

Figure 38: The GSTrap AC purification was analyzed by coomassie gel (SDS-PAG). Bacteria cell lysates were cleared by centrifugation and the supernatant containing the soluble fraction was loaded onto a GSTrap column. After washing the column, thrombin protease was added to cleavage the protein from the bound GST-tag. p16L1 was eluted and the column was washed with glutathione to remove residual GST. Elution fractions 1 and 2 show a slight enrichment of p16L1, however, the purified fractions show a considerable number of other bands. GST was bound to a high degree, although the fusion partner could not be retained in this concentration.

To remove E. coli chaperones gel filtration was performed. The corresponding chromatogram, exemplary for p16L1, is shown in Figure 39.

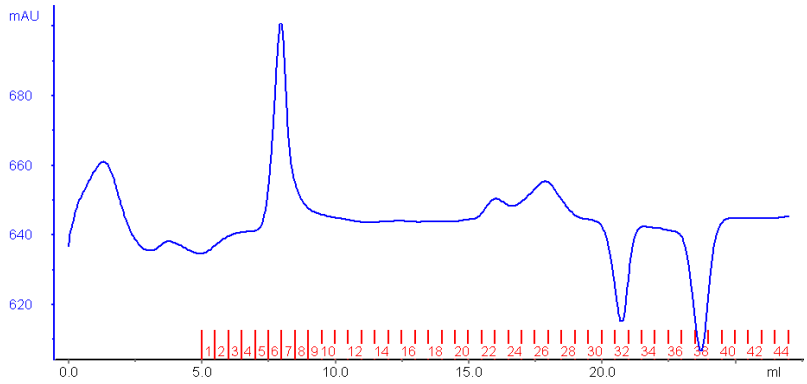

Figure 39: gel filtration chromatogram of p16L1 (Superdex200, GE Healthcare) exemplary for GST-p16L1. Y-axis: absorbance at 280 nm; X-axis: transferred volume in ml. The fusion protein is eluted right after the void volume at 7.42 ml indicating agglomerated capsomeres with a molecular weight >850 kDa.

The SEC fractions indicated in Figure 39 were analyzed by silver staining, anti-L1, anti-p16 and anti-GroEL western blotting. The overall retained protein amount was low, nevertheless, anti-p16 and anti-L1 western blots revealed presence of the desired fusion protein (Figure 40). Besides the p16L1 fusion protein, substantial amounts of free L1 and $p16^{INK4a}$ could be detected indicating breaking or degradation of the chimeric protein. Also uncut protein is present; consequently the GST-tag was not completely removed. GroEL was found to elute in the fractions 16 and 17 and was thereby separated from the target protein.

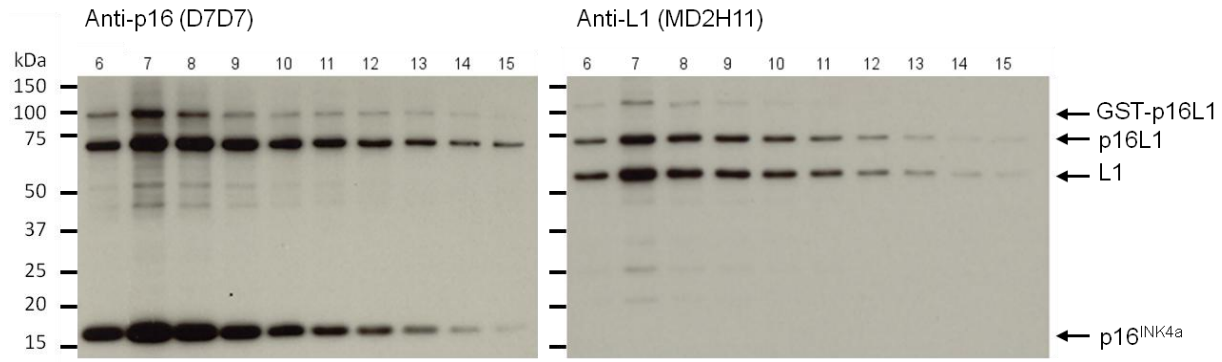

Figure 40: anti-p16 and anti-L1 western blots of the peak fractions of the p16L1 gel filtration run. Besides the protein of interest, p16L1, L1 and p16 are also present as truncated proteins indicating a predetermined breaking or degradation of the chimeric p16L1 fusion.

With the presented strategy utilizing GSTrap affinity chromatography and gel filtration it is possible to purify the proteins of interest, however sufficient protein amounts could not be obtained. This is probably due to the relatively low content of soluble target protein in the cell lysate after centrifugation as the bulk amount of protein remains in the pelleted fraction. An enrichment of the target protein is not possible with these methods. The GSTrap binding is potentially ineffective due to fact that free GST was found to occupy the available binding sites and thereby limiting capacity for the full length fusion protein.

9.4 Other purification attempts and separation of the GST-tag

The following schema gives a review of the attempts that were made to produce the L1 containing capsomeres in sufficient amounts and high purity. It shows selected experiments that were performed for this purpose, amongst others.

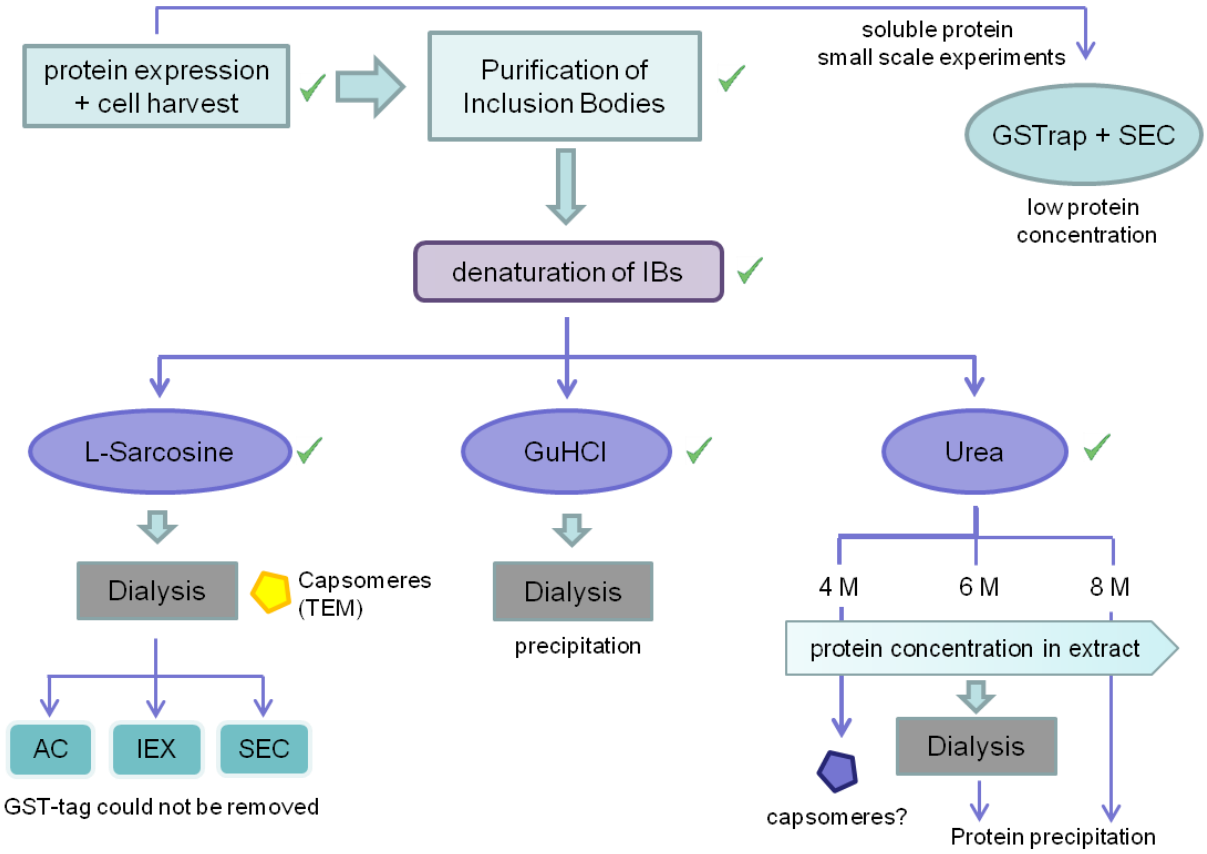

Figure 41: Flow chart displaying purification attempts that were made to remove the GST-tag from the refolded inclusion body preparations. Abbreviations: AC: affinity chromatography, GuHCl: guanidine hydrochloride, IBs: inclusion bodies, IEX: ion exchange chromatography, L-Sarcosine: N-Lauroylsarcosine, SEC: size exclusion chromatography, TEM: transmission electron microscopy.

After optimization and evaluation of the protein expression and cell harvesting, the purification of inclusion bodies from the insoluble fraction of the cell lysate was found to be the only possibility to produce sufficient protein amounts for further studies. As described in chapter 9.3, the purification of the soluble protein content did result in very low protein concentrations and was therefore postponed. Inclusion bodies were first denatured by N-Lauroylsarcosine as described in the iFOLD Protein Refolding System 1 User Protocol (Novagene, [101]). After refolding by dialysis, GSTrap affinity purification (AC) was performed to further purify the protein and cutting off the GST-tag. Thereby it was found that the refolded glutathione-S-transferase-tag is completely inactive and it was not possible to achieve enzyme mediated binding to glutathione. GSTrap affinity chromatography using glutathione sepharose was therefore excluded as not feasible for the separation of the tag.

It was further tried to remove the cut GST-tag utilizing anti-GST antibodies, as these bind GST independent of its enzymatic activity. Different anti-GST antibodies were coupled to ProteinG and/or CnBr sepharose and the protein solution was loaded onto the so prepared anti-GST resins. However, these methods did not result in a sufficient separation of the GST-tag, as the target protein was predominantly found to precipitate on the resins. Before performing ion exchange chromatography and alternatively size exclusion chromatography, the GST-tag was also cut with thrombin. For IEX, it was necessary to dialyze the sample to remove remaining N-Lauroylsarcosine. This anionic detergent forms micelles and thereby solubilizes the protein. As long as sarcosine is present in the sample it will bind to the anion exchange resin. Nevertheless, the GST tag was found to elute in exactly the same fractions as the target protein does. This speaks for a tight association of GST to the capsomeres and/or residual detergent in the sample. IEX was therefore considered to be inapplicable as a method to detach GST from the capsomeres. Also a complete separation by gelfiltration could not be achieved as the tag was always eluted in parallel to the capsomeres.
Guanidine hydrochloride denaturation resulted in protein precipitation during refolding independent of the molarity of denaturing agent and was therefore not further explored. Urea was also used to extract the protein from the purified inclusion bodies, and as expected, the protein concentration in the extract increases with the used urea molarity. However, during refolding, the proteins denatured with 6 and 8 M urea were found to precipitate as well. Only the 4 M urea extract could be successfully refolded, although the protein yield was not optimal. The preparations were analyzed by TEM and found to form pearl necklace like structures. The GST-tag could be cut by thrombin protease, but could not be separated, as described for N-Lauroylsarcosine before.
Further characterizations (results shown in 9.1) revealed that the L-sarcosine denatured and refolded proteins appear to be of high purity and even the absence of contaminating endotoxins could be confirmed (9.5). Therefore, these preparations were used for subsequent immunological studies (see chapter 10), although it should be mentioned that the GST-tag was not removed for this purpose.

9.5 Analysis and removal of endotoxin contaminations in HPV16 L1 protein preparations from E. coli

Endotoxins, or lipopolysaccharides (LPS) are major components of the cell wall of gram-negative bacteria and present an important source of contamination for protein preparations obtained from bacteria cultures [147]. They play an important role in inflammation processes and elicit strong immune responses even in minimal concentrations. To avoid uncontrolled activation of the immune systems, endotoxins must be removed from vaccine

preparations. During this thesis, triton X-114 phase separation was used for this purpose [141]. To analyze the LPS content before and after Triton X-114 treatment, the quantitative endpoint assay QCL-1000 LAL Assay (Lonza) was used (see also 5.4.3 and 6.4.11).

Table 4 summarizes the results obtained with the endotoxin detection kit. The samples are listed with their corresponding absorption at 405 nm and the calculated EU/ml values that were calculated from the standard curve. All L1 containing proteins were purified as inclusion bodies and as this protocol (6.4.1) includes several triton X-100 washing steps, the LPS amounts in these preparations were found to be negligible low. Concluding from these data, the endotoxin removal protocol does not need to be applied on proteins retained from inclusion bodies. Contrary, GST-p16^{INK4a} was purified by GSTrap affinity chromatography (6.4.2) and contained LPS in high concentration. By triton X-114 treatment, the contaminating endotoxins could be entirely removed. Western blot of samples before and after LPS removal revealed only minimal loss of p16 protein (data not shown).

Table 4: Quantitative endotoxin analysis of the GST-fusion proteins expressed in E. coli Rosetta, obtained with the QCL-1000 Endpoint Chromogenic LAL Assay (Lonza).

Sample		A405 nm	EU/ml calc.
Standards	1	1,864	0,97
EU/ml	0,5	1,092	0,56
	0,25	0,541	0,26
	0,1	0,192	0,07
Blank	0	0,054	0,00
pos. control	2 EU	2,3	1,21
before LPS removal	GST-L1	0,09	0,01
	GST-p16	**>3**	**>1,59**
	GST-L1p16	0,077	0,01
	GST-p16L1	0,069	0,00
	GST-L1p16L1	0,061	0,00
after LPS removal	GST-L1	0,072	0,00
	GST-p16	**0,06**	**0,00**
	GST-L1p16	0,056	0,00
	GST-p16L1	0,058	0,00
	GST-L1p16L1	0,071	0,00

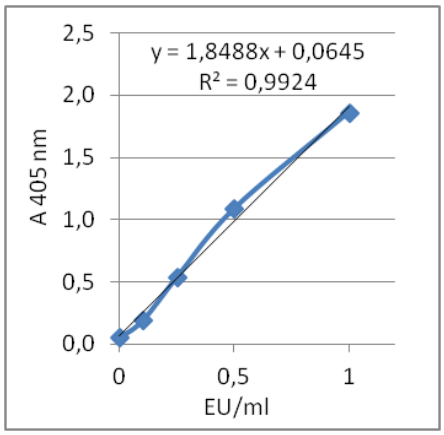

Figure 42: Calibration curve QCL-1000 Endpoint Chromogenic LAL Assay

9.6 Structural characterization of chimeric capsomeres

The purified capsomeres were analyzed for their structural integrity, sedimentation characteristics and the presence of conformation-specific epitopes by means of transmission electron microscopy, sedimentation analysis and conformation specific ELISA.

9.6.1 *Sedimentation analysis*

To verify the capsomere structures, purified protein extracts were subjected to sucrose gradient centrifugation. The collected fractions (20 in total, 600 µl each, fraction 1 from the top of the tube) were analyzed by western blotting (Figure 43). All expressed and purified fusion proteins contain the modified L1 sequence (5.2.1) with a deletion of the helix 4 region that prevents assembly into larger particles. Sedimentation analysis of the refolded proteins revealed the presence of capsomeres as demonstrated by western blot analysis with the L1-specific antibody MD2H11 (Figure 43). BSA (4S) was loaded as calibration marker and assembled VLPs were loaded as control. VLPs were found at the bottom of the centrifuge tube whereas the capsomeres accumulated at the top of the sucrose gradient (fractions 1 to 4) due to their low sedimentation coefficient. These sedimentation characteristics indicate the presence of small particles and are in line with previous studies [76, 137, 148].

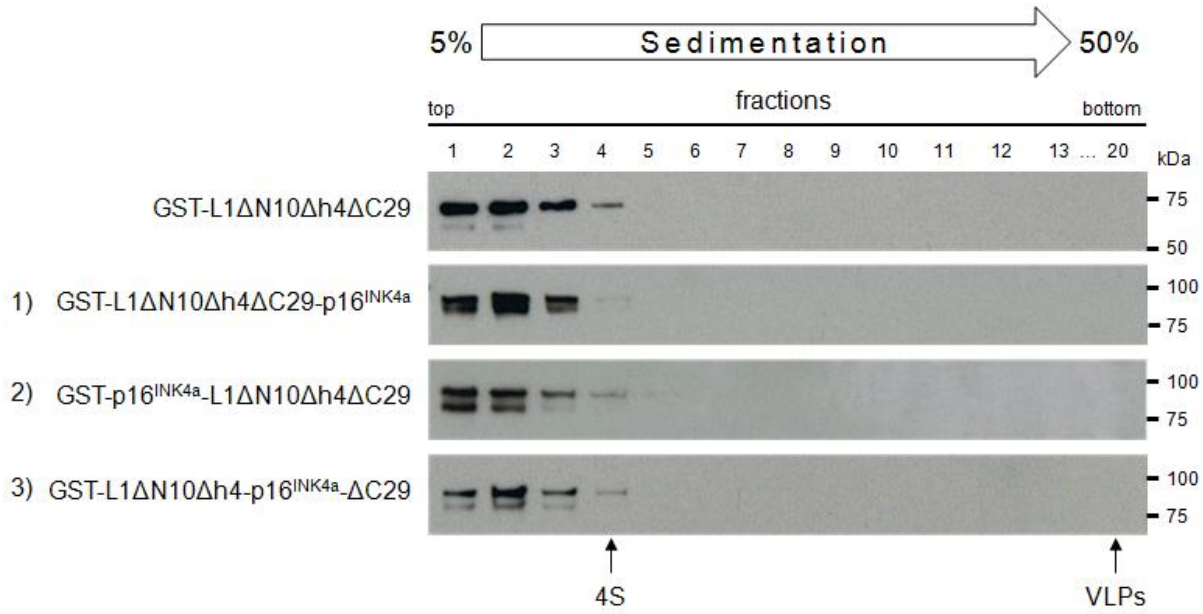

Figure 43: Sedimentation characteristics of the different L1 - p16^{INK4a} capsomeres. 50 µg of each protein were loaded onto linear sucrose gradients (5-50% in dialysis buffer) and centrifuged for 3h at 36,000 rpm in a SW41Ti rotor. The resulting gradients were divided into 20 fractions which were collected from the top of the tube and analyzed by immunoblotting with the MD2H11 antibody. The different L1- p16 proteins are all present as capsomeres in fractions 1 to 4 as the deletion of helix 4 prevents assembly into larger particles.

9.6.2 *Transmission electron microscopy*

The purified proteins were analyzed by transmission electron microscopy (TEM) and two representative replicas of each sample are shown in Figure 44. All preparations contained large amounts of 10 - 12 nm capsomeric structures which is in line with previous reports [76, 149, 150]. The characteristic donut-like appearance was also observed in some of the capsomeres but this was not a consistent finding. The black dot in the centre of the capsomeres originates from the staining of their cylindrical cavity [35]. As we used the C-terminally truncated L1 construct this dot was only sporadically visible as described before [144]. The capsomeres were found to be of variable size with a certain tendency to the formation of aggregates. Especially p16L1 and L1p16L1 showed higher grades of agglomeration compared to L1 and L1p16. In general, many non-assembled L1 monomers were observed as “background noise”. This often resulted in EM images with lower resolution as the uranyl acetate staining was challenging.

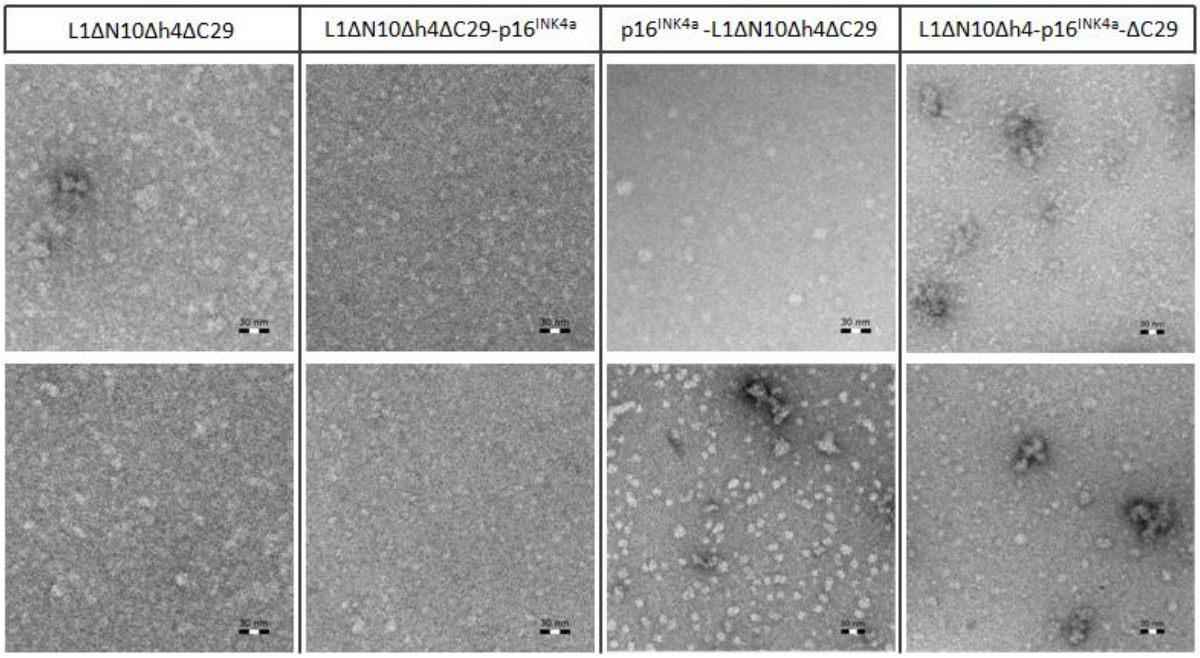

Figure 44: Structural analysis of the HPV16 L1 capsomeres. The structure of the purified proteins was analyzed by TEM employing negative staining as described in 6.4.10 (Transmission electron microscopy). All preparations formed 10 - 12 nm capsomeric structures with variable tendency to agglomeration. Two representative pictures per sample are shown; bars indicate 30 nm.

Altogether it is evident, that all proteins do refold into capsomeric structures after denaturing from inclusion bodies and dialysis. The intrinsic ability to assemble into capsomeres was not disrupted by the inclusion body purification procedure. Furthermore, these capsomeres were handled at room temperature and no negative influence on their stability could be observed.

9.6.3 *Conformation specific ELISA*

The different chimeric constructs were obtained from inclusion bodies including denaturation and refolding steps. Therefore it was not clear whether conformation-specific epitopes are present after the refolding procedure or not. An ELISA using the L1-directed monoclonal antibody #1.3.5.15 (Ritti01) was applied to elucidate this. VLPs from insect cells were used as a positive control to determine functionality of the test. The results of the conformation specific or 'antigen capture ELISA' (6.4.12) are summarized in Figure 45. As the absorption values are quite low even for the undiluted proteins, it can be supposed that conformation-specific epitopes are only present to low extend, if at all. These data indicate that L1 without the $p16^{INK4a}$ fusion presents, at least partly, the desired epitopes and that the p16L1 capsomeres are slightly more immunoreactive to the conformation specific antibody. The low overall reactivity of the capsomeres in this ELISA indicates the presence of rather missfolded L1 protein. At least the antibody-specific epitope seems to be masked although this does not exclude the presence of L1 in the form of higher order structures, such as capsomeres. However, for these proteins the value of that assay is limited.

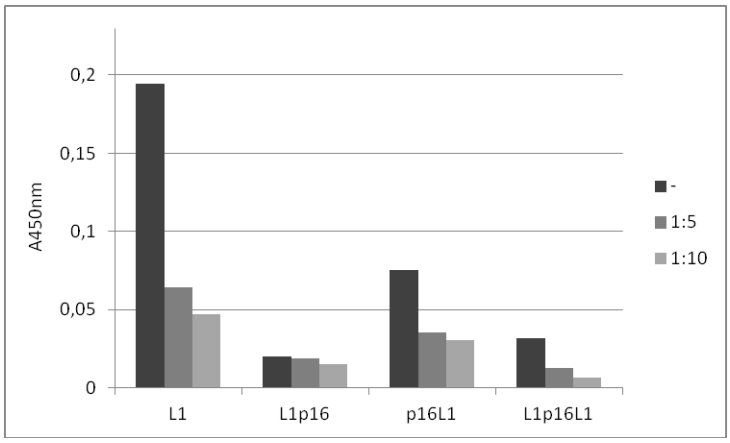

Figure 45: Antigen capture ELISA of protein preparations obtained from inclusion body purifications. Refolded proteins were applied undiluted (-), 1:5 and 1:10 diluted in dialysis buffer. VLPs (positive control) produced signals of 0.8, 0.7 and 0.5 AU for dilutions of 1:100, 1:500 and 1:1000 respectively, showing the general applicability of the test.

9.7 Conclusions

All the initially insoluble proteins could be successfully purified from E. coli inclusion bodies. Moreover it was possible to retain the proteins in very high amounts ranging from 29 to 55 mg per 100 ml bacterial culture. Also the soluble expressed protein, GST-$p16^{INK4a}$, was successfully purified via GSTrap affinity chromatography. We have evaluated different strategies to remove the co-expressed GST-tag from the protein preparations that were produced from inclusion bodies as the tag was not yet removed during inclusion body purification and refolding. It was found that the refolded GST-tag is completely enzymatically inactive and sufficient separation from the tag could not be achieved despite different attempts. Denaturation using the anionic detergent N-Lauroylsarcosine and

subsequent refolding via dialysis resulted in highest protein concentrations and appeared to be the mildest of the tested procedures, although the GST activity could not be restored with none of the applied strategies. However, structural analysis revealed the presence of capsomeres in the refolded samples with concurrent absence of contaminating bacterial endotoxins. Therefore, the use of N-Lauroylsarcosine in this context presents a suitable method for inclusion body denaturation and refolding.

10 In vivo immunogenicity of the vaccine candidates

The three purified p16-L1 fusion proteins as well as purified L1 and $p16^{INK4a}$ individually were used to immunize C57BL/6 mice. First of all, the $p16^{INK4a}$ (10.1) and the capsomere dose (10.2) for further experiments was determined using escalating doses of GST-$p16^{INK4a}$, respectively the GST-p16L1 construct. In 10.3, the results for the comparison of the three different structural isoforms are shown. Further, the immune response after a single immunization was tested (10.4). The last experiment in frame of this thesis was designed to test whether the co-administration of an adjuvant can further improve the immune response, especially concerning the p16 T cell response; the results are presented in 10.5.

L1-specific T cells were stimulated with the AGVDNRECI peptide (H2-Db-restricted CTL epitope of HPV16 L1 [137]) and detected by IFNy ELISpot; p16-specific T cells were detected with a pool of overlapping peptides covering the complete $p16^{INK4a}$ sequence. For the last experiment, Syfpeithi-predicted H2-Db-restricted nonameric peptides were used for the ELISpot analysis in addition. All spot numbers obtained from individual mice are presented as mean values from assay triplicates and were normalized by subtracting the mean spot numbers resulting from un-stimulated cells (assay negative control RPMI), unless mentioned otherwise. Mouse sera obtained at the day of ELISpot were checked for L1 antibody responses with a VLP-capture ELISA (6.6.1) and for $p16^{INK4a}$ -specific antibodies with 5 pools of overlapping peptides covering the complete $p16^{INK4a}$ sequence (for details see 5.2.3 and 6.6.2). The presented data are mean values calculated from assay duplicates and normalized by subtracting the mean absorption values of ELISA negative controls.

10.1 Determination of the $p16^{INK4a}$ dose for control groups

With the first in vivo experiment, the optimal dose of GST-$p16^{INK4a}$ that should be used in the following settings should be determined by vaccinating mice with different doses of this

protein**.** Figure 46 shows the number of IFNy spots counted for each mouse in the different dose groups (5, 25 and 50 µg $p16^{INK4a}$). The ELISspot numbers for L1 and $p16^{INK4a}$ are presented in one graph but were determined with the established L1 peptide AGVDNRECI for the L1 control group and with the p16 overlapping peptide pool for the p16-immunized mice respectively (for methods see 6.6). Based on these results, the middle p16 dose (25 µg) was chosen for the following experiments as it seemed to induce the best achievable T cell response and highest spot number. Although a dose response effect was expected it could not be demonstrated with the available data. However, the dosage was later increased to the maximal dose of 50 µg as the second experiment (10.2) did not show any p16 T cell reactivity at all.

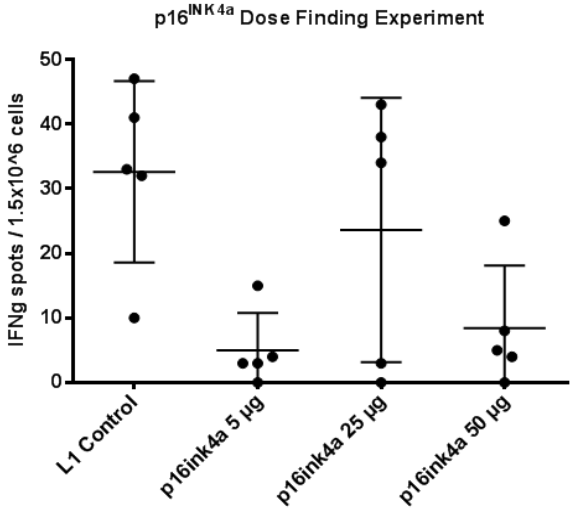

Figure 46: $p16^{INK4a}$ dose finding experiment - ELISpot results. C57BL/6 mice were immunized three times s.c. at biweekly intervals with 5 µg L1 (control group), 5 / 25 or 50 µg $p16^{INK4a}$ protein (test group). The horizontal bar represents the mean titer of each group, standard deviations for each groups are indicated by vertical bars.

10.2 Dose-response effect of p16L1 capsomere immunization

Cellular immune response determined by IFNy ELISpot

In this experiment the optimal dose of capsomeres should be determined with one of the constructs. The ELISpot results for different concentrations of GST-p16L1 (construct #2) are shown in Figure 47 (L1-specific T cells) and Figure 48 ($p16^{INK4a}$-specific T cells).

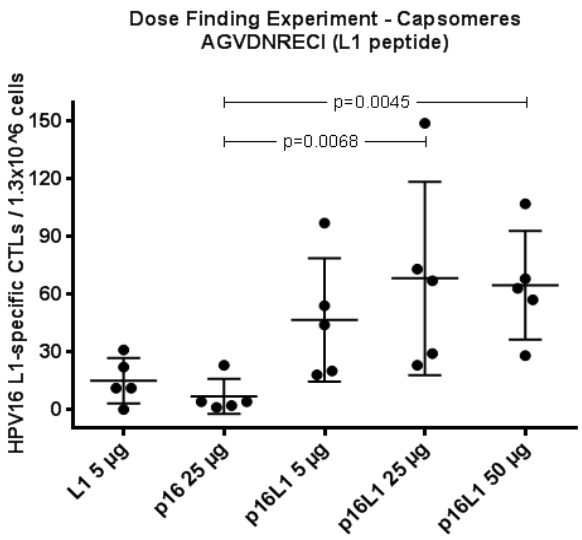

Figure 47: dose-finding experiment capsomeres - HPV16 L1-ELISpot using the AGVDNRECI peptide. C57BL/6 mice were immunized three times s.c. at biweekly intervals with 5 µg L1, 25 µg $p16^{INK4a}$ (negative control group) and 5 / 25 or 50 µg $p16^{INK4a}$-L1 protein (test group). Dots represent individual mice with mean and standard deviation indicated.

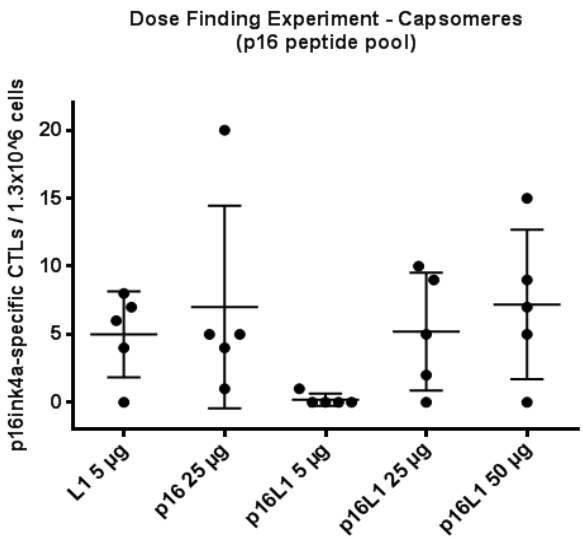

Figure 48: dose-finding experiment capsomeres - $p16^{INK4a}$-ELISpot using a pool of overlapping p16 peptides. C57BL/6 mice were immunized three times s.c. at biweekly intervals with 5 µg L1 (negative control group), 25 µg $p16^{INK4a}$ and 5 / 25 or 50 µg $p16^{INK4a}$-L1 protein (test group). Dots represent individual mice with mean and standard deviation indicated.

The L1 control group developed a number of 15 IFNy spots averaged when stimulated with the AGVDNRECI L1 peptide. The discrepancy to the L1 control group in the $p16^{INK4a}$ dose finding experiment (see Figure 46) could be explained by the applied cell number for ELISpot analysis which was decreased from 1.5 (p16 dose finding experiment) to 1.3 x 10^6 cells per well. This cell number was then applied for all further ELISpots. Based on these results, it was decided to increase the L1 dose for the control groups to 25 µg per mouse in the subsequent experiments.

Fisher's LSD test is a method for comparing treatment group means. The test was also applied for the data presented in Figure 47. A significant difference to the p16 25 µg negative control group was calculated for the p16L1 25 µg (p=0.0045) and 50 µg (p=0.0068) test groups. The results for the HPV16 L1 T cells do not show a clear dose response effect, however, in the 50 µg group only one mouse had a mean number (calculated from ELISpot triplicates) of 28 spots. In the 5 and 25 µg groups, 2 out of 5 mice had values lower than 30 spots.

For the p16 cellular immune response presented in Figure 48, no significant differences could be detected. In this context it is necessary to mention that the p16-specific t-cell numbers are very low and must therefore be critically reviewed.

Humoral immune response determined by ELISA

Considering the antibody responses, a definite dose-response effect is apparent for p16- as well as for L1-specific antibodies (see Figure 49 and Figure 50). Individual sera were scored as antibody-positive or negative using a cut-off value that is based on the distribution of absorbance values of control groups. With the VLP-capture Elisa (Figure 49), the dose-response trend was confirmed as with increasing capsomere dose, an increasing absorbance value at 450nm was detected whereby all tested sera were positive for VLP-capturing antibodies.

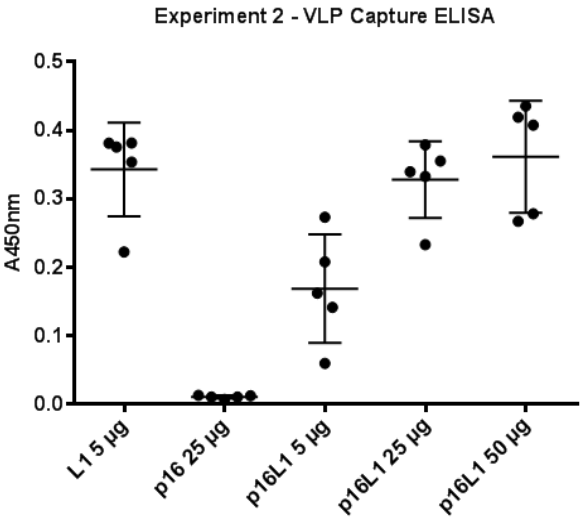

Figure 49: dose-finding experiment capsomeres - VLP-capture Elisa. C57BL/6 mice were immunized three times s.c. at biweekly intervals with 5 µg L1, 25 µg $p16^{INK4a}$ (negative control group) and 5 / 25 / 50 µg $p16^{INK4a}$-L1 protein (test group). Dots represent individual mice with mean and standard deviation indicated.

Mouse sera were also tested for p16 specific antibodies (Figure 50) using 5 peptide pools including all 13 overlapping peptides covering the complete p16 sequence (for peptide sequences see 5.2.3). The peptides were also tested separately (data not shown) but as different peptides showed reactivity in the ELISA, all were included to analyze the sera. Sera were considered to be positive if at least one of the tested peptide pools showed a value above cut-off which was calculated from the negative control group (L1 5 µg). With 5 µg p16L1, 2 out of 5 mice were defined to be positive for p16-specific antibodies (Figure 50), in the second group that received 25 µg of the fusion protein, 3 out of 5 mice and all mice that received 50 µg were tested positive for p16-specific antibodies. It is noticeable that the p16 control group did not develop any p16-specific antibodies and that the L1 negative control shows quite high p16 antibody titers. This observation was made for all mouse experiments (see also Figure 55 and Figure 57).

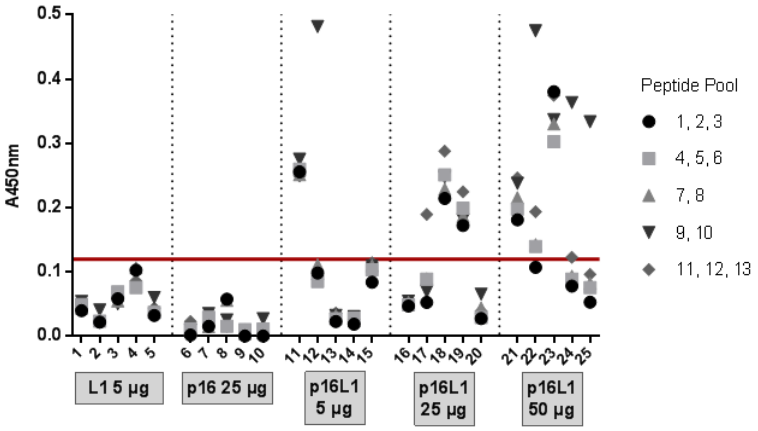

Figure 50: dose-finding experiment capsomeres - $p16^{INK4a}$ -petide Elisa. C57BL/6 mice were immunized three times s.c. at biweekly intervals with 5 µg L1 (negative control group), 25 µg $p16^{INK4a}$ and 5 / 25 / 50 µg $p16^{INK4a}$-L1 protein (test group). Numbers on x-axis indicate individual mouse sera that were tested with the different peptide pools. The horizontal line marks the calculated cut off based on the L1 negative control values.

The capsomere dose for the following experiments was defined to be 50 µg per mouse as a clear dose response effect could be observed, at least considering the humoral immune response. The L1 control (5 µg) induced only low T cell numbers as the p16 control did. Because of this we decided to increase the L1 dose to 25 µg and the $p16^{INK4a}$ dose to 50 µg per mouse for further experiments.

10.3 Comparison of the different HPV16 L1 - $p16^{INK4a}$ capsomere constructs

Cellular immune response determined by IFNγ ELISpot

Another experiment was performed to elucidate immunological differences between the three different capsomere constructs. Figure 51 depicts that all three fusion protein constructs induce high L1-specific T cell numbers in immunized mice whereby construct #3 (L1p16L1) shows the highest T cell response with a mean of 172 spots. Also the other constructs #1 (L1p16) and #2 (p16L1) with mean spot numbers of 82 and 67 gave higher L1 responses than the L1 control group with a mean of 27 spots. Fishers LSD test revealed significance for the comparison of the L1 control group to the test groups p16L1 ($p<0.0001$) and L1p16L1 ($p=0.0002$). The L1 protein was administered in lower dose for the control group, as it has to be considered that the 50 µg fusion protein dose does not contain 50 µg pure L1 but GST, $p16^{INK4a}$ *and* L1 and thereby presents a comparable L1 proportion altogether. The presence of $p16^{INK4a}$ seems to boost the L1 specific T cell response what could be due to the presentation of T helper epitopes in this formulation. Concerning the $p16^{INK4a}$ T cell response (shown in Figure 52) the same analysis problem occurred with this ELISpot as it was found previously. However, significantly higher T cell numbers could be detected for construct #2 (p16L1, $p<0.0001$) and #3 (L1p16L1, $p=0.0002$) compared to the

control group which only received L1 protein. It should be noted that the number of counted spots is very low and was therefore not normalized for RPMI control. As a number of up to 13 spots was found to be regular assay background (see Figure 53 and corresponding text), these spot numbers must be considered to be background response that would also have appeared without peptide stimulation. This shows that with using the pool of overlapping p16 peptides for the ELISpot test, only low numbers of p16-specific T cells can be detected.

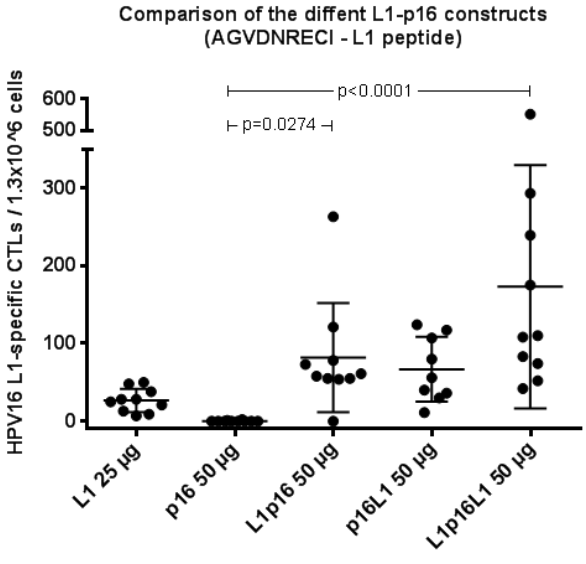

Figure 51: Comparison of the 3 different capsomere constructs - HPV16 L1-ELISpot using the AGVDNRECl peptide. C57BL/6 mice were immunized three times s.c. at biweekly intervals with 25 µg L1, 50 µg $p16^{INK4a}$ (negative control group) and 50 µg of either L1p16 (#1), p16L1 (#2) or L1p16L1 (#3) protein (test group). Dots represent individual mice with mean and standard deviation indicated.

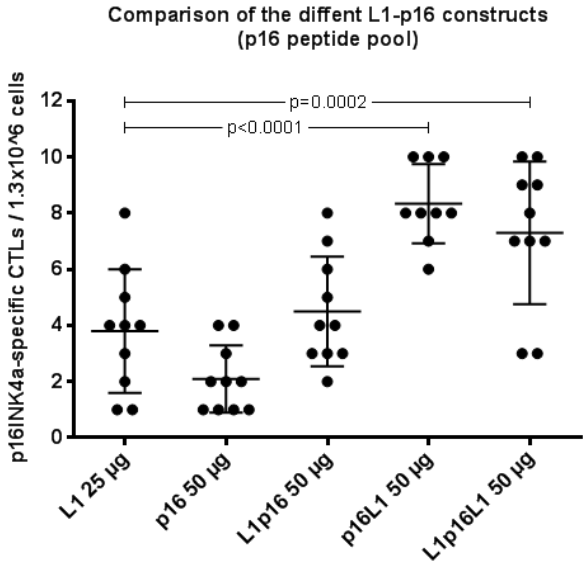

Figure 52: Comparison of the 3 different capsomere constructs - $p16^{INK4a}$-ELISpot using a pool of over-lapping p16 peptides. C57BL/6 mice were immunized three times s.c. at biweekly intervals with 25 µg L1 (negative control group), 50 µg $p16^{INK4a}$ and 50 µg of either L1p16 (#1), p16L1 (#2) or L1p16L1 (#3) protein (test group). Dots represent individual mice with mean and standard deviation indicated. Un-normalized data.

Figure 53 shows the HPV16 L1-ELISpot results split for each group, whereby L1 25 µg and $p16^{INK4a}$ 50 µg represent the control groups. Grey bars indicate assay negative control spot numbers that were counted from unstimulated (RPMI) cells, black bars indicate L1-specific T lymphocytes. Splenocytes from mice vaccinated with L1 or one of the L1 containing chimeric constructs produced significantly more IFNy spots when stimulated with the AGVDNRECI peptide compared to unstimulated cells. This is true for all test groups. The control group of 10 mice that only received $p16^{INK4a}$ protein, did not develop L1-reactive T cells, which demonstrates specificity of the ELISpot assay.

The graphic also displays a boxplot diagram after Tukey to visualize the distribution of RPMI spot numbers in a large cohort of animals (n=50), respectively the assay negative control, obtained in this experiment. From this we can conclude, that spot numbers up to 13 can

appear although no peptide specific stimulation preceded. Mice number 14 and 25 were thereby identified as outliers.

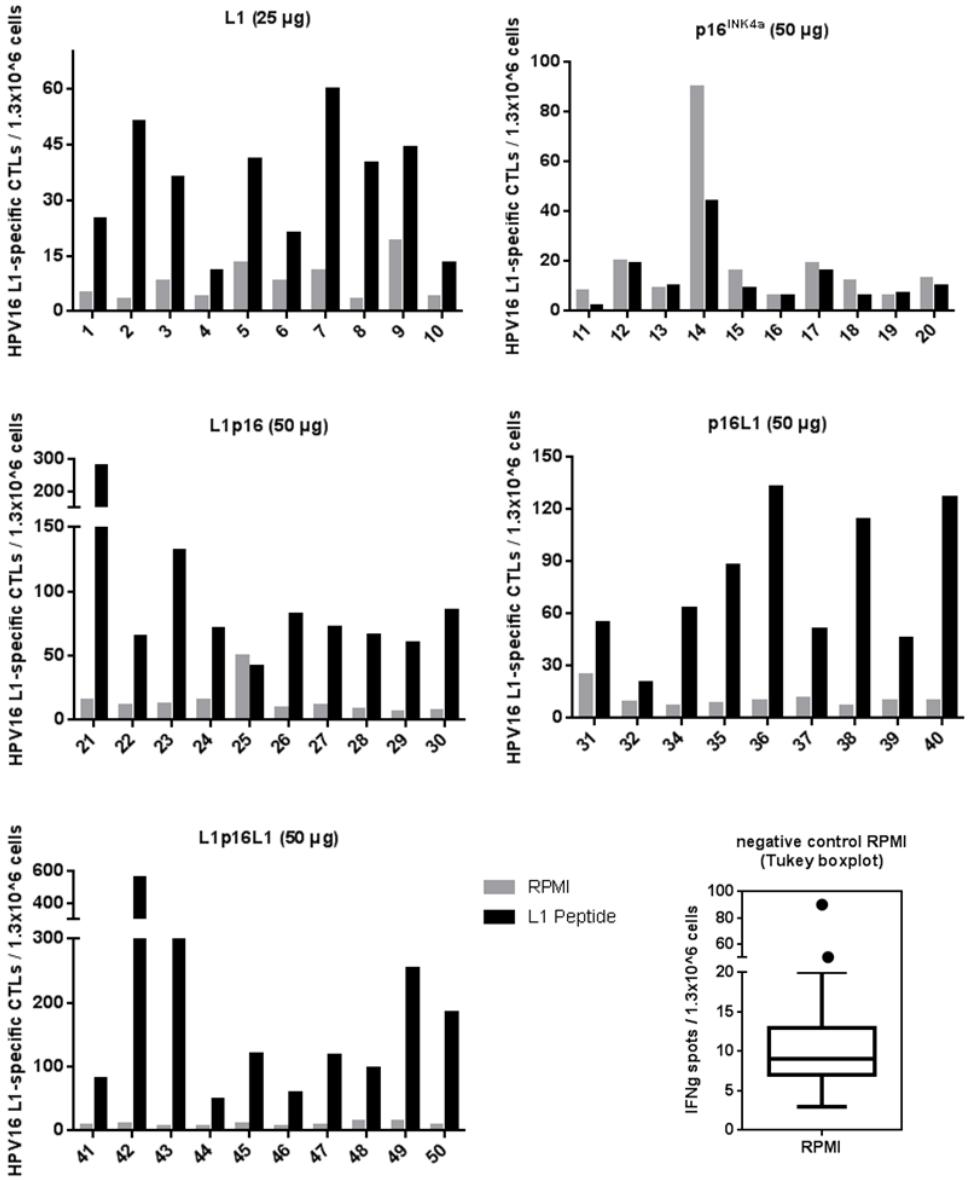

Figure 53: Comparison of the 3 different capsomere constructs - HPV16 L1-ELISpot using the AGVDNRECI peptide, uncorrected results for each group. Numbers on x-axis indicate individual mouse sera whereby IFNy spot numbers for assay negative control (RPMI) and the test peptide (L1) are shown in comparison. The boxplot diagram shows the distribution of the assay negative control values (unstimulated cells) for the 50 mice of this experiment (median= 9; 25% percentile=7; 75% percentile=13). Outliers were identified for mice #14 and 25.

Humoral immune response determined by ELISA

The VLP-capture ELISA of these sera is presented in Figure 54. All tested sera were found to be positive for VLP-capturing antibodies whereby construct #2 (p16L1) gave the highest response rates (mean A450nm = 0.660) which were even higher (p=0.0498) than the L1 control group (mean A450nm = 0.543).

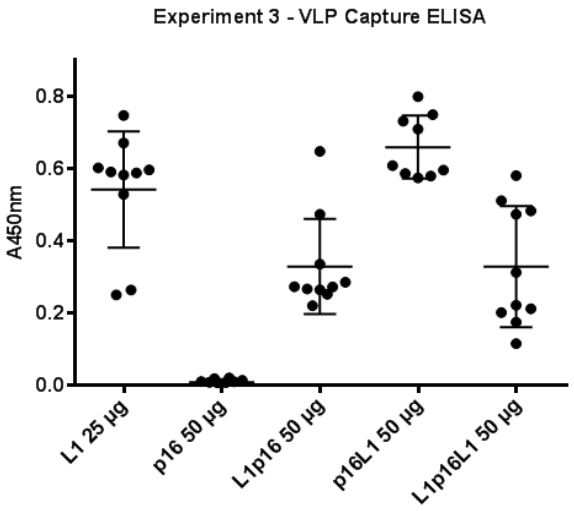

Figure 54: Comparison of the 3 different capsomere constructs - VLP-capture Elisa. C57BL/6 mice were immunized three times s.c. at biweekly intervals with 25 µg L1, 50 µg p16^{INK4a} (negative control group) and 50 µg of either L1p16 (#1), p16L1 (#2) or L1p16L1 (#3) protein (test group). Dots represent individual mice with mean and standard deviation indicated.

In Figure 55 the results of the p16^{INK4a}-peptide pool ELISA are shown. Surprisingly, the background p16^{INK4a} antibody response is quite high for the control group that only received 25 µg of L1 protein as it was observed for all mouse experiments. Contrary, the p16 control group shows basically no response at all. The threshold was calculated on the basis of the true negative control group which is the one that received HPV16 L1. Construct #1 resulted in eight positive out of ten mice and therefore depicts with 80% positivity the highest p16-specific antibody response that was achieved with this experiment. Also constructs #1 and #2 show signals in the ELISA but must be valued as background signal.

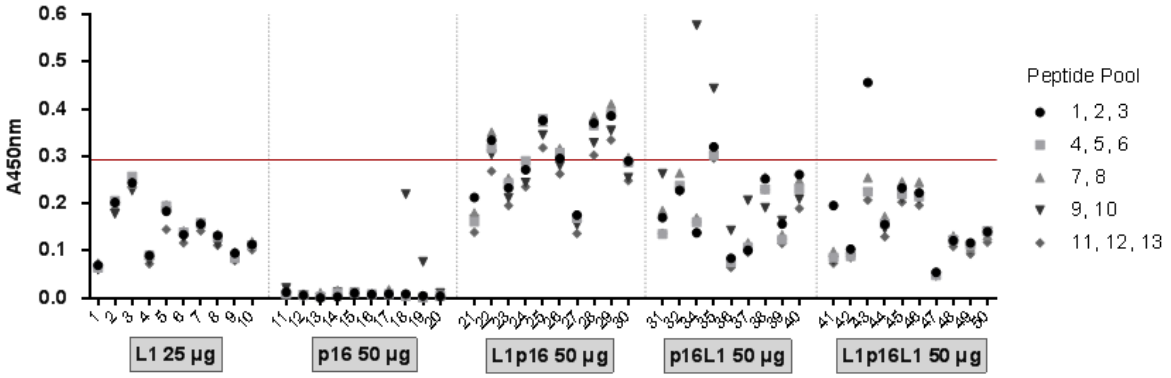

Figure 55: Comparison of the 3 different capsomere constructs - p16^{INK4a}-petide pool ELISA. C57BL/6 mice were immunized three times s.c. at biweekly intervals with 25 µg L1 (negative control group), 50 µg p16^{INK4a} and 50 µg of either L1p16 (#1), p16L1 (#2) or L1p16L1 (#3) protein (test group). Numbers on x-axis indicate individual mouse sera that were tested with the different peptide pools. The horizontal line marks the calculated cut off based on the L1 negative control values.

10.4 Immunogenicity of the HPV16 L1 - p16^{INK4a} capsomeres after single administration

With three mice that were immunized with 50 µg of p16L1 (construct #2), it was found that after single vaccination, all mice developed a HPV16 L1 specific T cell response which was

measured by ELISpot using the AGVDNRECI peptide. With spot numbers of 51, 110 and 121 (mean values, normalized for RPMI control) the cellular immune response against L1 is rapid and strong (data not shown) comparable to that achieved after repeated immunizations. However, a cellular p16 response could not be detected, even though three additional nonameric peptides were used to stimulate the cells (5.2.3).

Humoral immune responses were measured by means of ELISA and the results are shown in Figure 56 and Figure 57. The VLP-capture ELISA revealed that even after one immunization, a considerable induction of VLP-binding antibodies can be achieved in the majority of tested individuals and that the antibody titer induced with the capsomere constructs is higher than that induced with L1 protein alone. It should be noted, that the L1 protein used for the control group was applied at 50 µg per mouse for this experiment. This means, that the actual L1 proportion is even higher compared to the fusion proteins as the protein amount for immunizations was calculated with the total target protein and the chimeric capsomere preparations also contain $p16^{INK4a}$ protein. However, it must be considered that only 2, respectively 3 mice per group were used for this experiment.

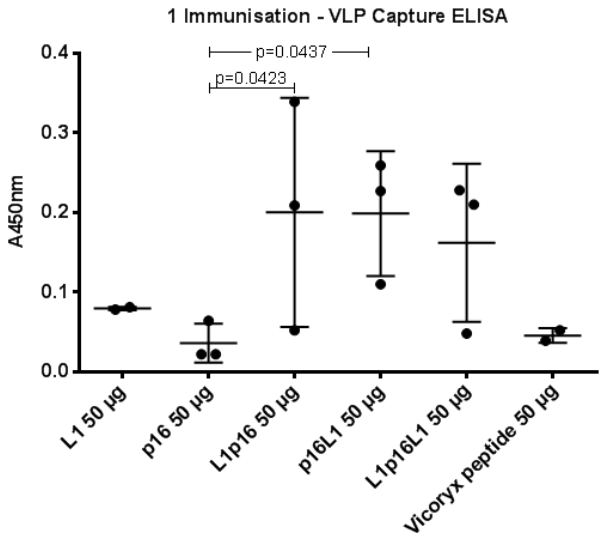

Figure 56: Humoral immune response after single immunization - VLP-capture ELISA. C57BL/6 mice were immunized once s.c. with 50 µg L1, 50 µg $p16^{INK4a}$ (negative control group) and 50 µg of either L1p16 (#1), p16L1 (#2) or L1p16L1 (#3) protein (test group). Dots represent individual mice with mean and standard deviation indicated. Significant differences are indicated with the respective p-values (uncorrected Fisher's LSD).

The results of the $p16^{INK4a}$-petide pool ELISA are depicted in Figure 57. A slightly increased $p16^{INK4a}$-specific antibody response is visible for all three fusion protein constructs. The relatively high L1 background response is present as it was found before, whereas p16 immunized mice did not develop antibodies at all.

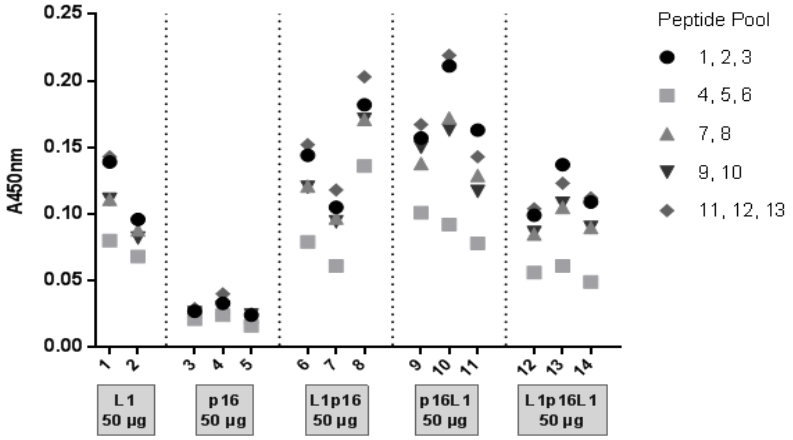

Figure 57: Humoral immune response after single immunization - $p16^{INK4a}$-petide pool ELISA. C57BL/6 mice were immunized once s.c. with 50 µg L1 (negative control group), 50 µg $p16^{INK4a}$ and 50 µg of either L1p16 (#1), p16L1 (#2) or L1p16L1 (#3) protein (test group). Numbers on x-axis indicate individual mouse sera that were tested with the different peptide pools.

Compared to the previously described results, it appears that boosting by repeated immunization is necessary for a stronger and therefore probably more effective immune response.

10.5 $p16^{INK4a}$-specific T cell reactivity verified with synthetic peptides

The presented experiment was originally conducted to ascertain the influence of an adjuvant (Montanide) on the overall immune response in comparison to a vaccine formulation in PBS (see also 10.6). Therefore, nine mice (3 per test group) were immunized s.c. three times at biweekly intervals with a) the L1p16 protein in PBS as it was applied in the previously described experiments, b) L1p16 in Montanide (1:1) or c) with the Vicoryx peptide (5.2.3) in Montanide (1:1) as it is used in this formulation in an ongoing clinical trial [125]. The ELISpot of splenocytes was performed according to the described protocol (6.6.3) and in addition to the L1 peptide and the p16 overlapping peptide pool, the three synthetic peptides P1 (TRGSNHARI), P2 (LPVDLAEEL) and P3 (GSARVAELL) were included. These peptides were predicted using the prediction algorithm SYFPEITHI [138] for H2-Db-restricted CTL epitopes of $p16^{INK4a}$. Figure 58 shows the detailed ELISpot results of this mouse experiment. The splenocytes were stimulated with the indicated peptides, respectively the p16 Pool and RPMI for the assay negative control. Each bar in the chart corresponds to a spot number mean value of assay triplicates and thereby shows the number of peptide-specific T lymphocytes that were detected. As it was observed before, a strong L1 cellular immune response (orange bars) is evident in all L1p16-immunized mice, whereby mouse number 9 shows the lowest spot number with averaged 29 spots. However, in comparison to the negative control (RPMI, black bars) this is a positive response as well.

The stimulation with the pool of overlapping p16^{INK4a} peptides (pink bars) did not result in spot numbers beyond the background signal as it was observed before. Because of the findings from previous ELISpots, three additional p16 peptides (green bars) were included. Mouse #1 and #7 show a markedly increased response to all of these peptides, and also to stimulation with the longer Vicoryx peptide (blue bars). This provides evidence for the induction of a robust, polyclonal T cell response as all tested single p16 peptides resulted in spot numbers from 28 (mouse #1, P3) to 59 (mouse #7, P1) which are clearly distinguishable from the background controls. The test group that received the Vicoryx peptide in Montanide was only tested with this peptide whereby one mouse was found to properly response with over 100 spots averaged. The Vicoryx group was included in this experiment to analyze the immune response that can be induced in mice to this peptide that is currently used in a clinical trial. Taken together, in each test group one out of three individuals was tested positive for p16 reactivity, whereby all of the mice that received L1p16 protein developed an anti-L1 cellular immune response. These results demonstrate the general possibility to induce a p16^{INK4a}-mediated T cell response with the chimeric capsomere vaccine.

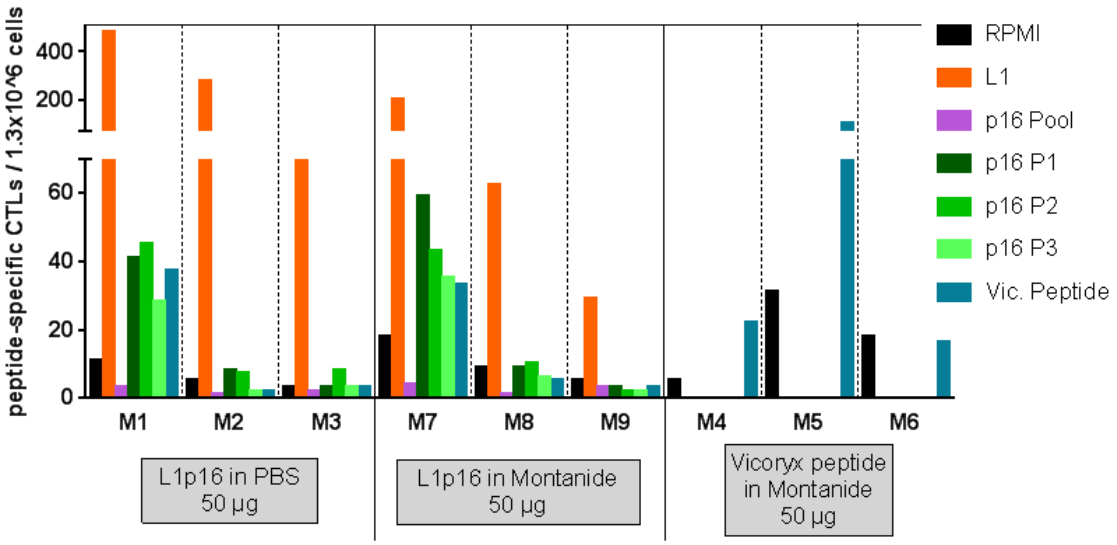

Figure 58: Montanide experiment - IFNy ELISpot, uncorrected results for each group. C57BL/6 mice were immunized three times s.c. at biweekly intervals with 50 µg of either L1p16 in PBS, L1p16 in Montanide or Vicoryx peptide in Montanide. Individual mouse sera are indicated on the x-axis. Spot numbers obtained after stimulation of splenocytes with RPMI, L1 peptide, the p16 peptide pool or different p16 peptides are shown in comparison. M# on x-axis indicates individual mouse sera that were tested with the different peptides.

10.6 Immunogenicity of the HPV16 L1 – p16^{INK4a} capsomeres with co-administration of Montanide adjuvant

In the previously described experiments p16 reactive T cells were generally hard to detect with the chosen peptides. With the co-administration of Montanide adjuvant, we intended to

generate stronger immune responses that can be quantified using the ELISpot assay. The results presented in 10.5 were therefore summarized and are graphically depicted in Figure 59 to illustrate the difference of IFNy spot numbers obtained with the L1p16 protein formulated in PBS vs. Montanide adjuvant. The grey bars represent mean values of spots that were counted for the 'L1p16 in PBS' immunized mice; black bars are mean values of the 'L1p16 in Montanide' group. A significant difference (p=0.0016) was found for the L1-stimulation whereby the PBS group developed a mean number of 273 spots and the adjuvant supplemented group of 97 Spots. Thereby a decreased immune response for the adjuvant group is shown, rather than the expected improvement. Considering the other tested peptides, no significant differences could be elucidated. Therefore it can be speculated that in this experimental setting the administration of L1p16 capsomeres in Montanide adjuvant does not improve the cellular immune response.

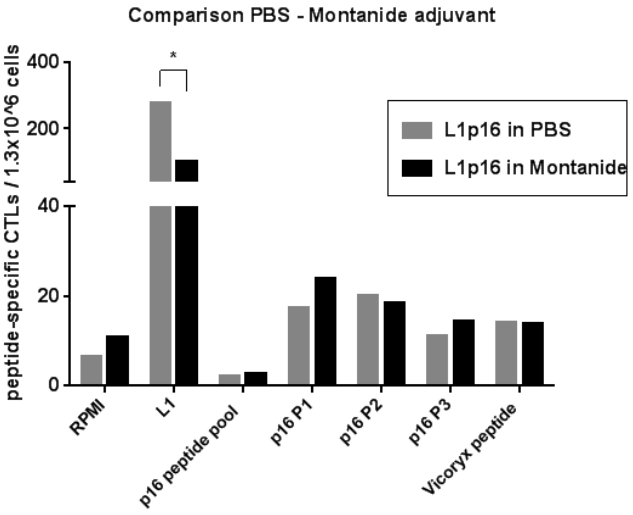

Figure 59: Efficacy of vaccine formulation in PBS vs. Montanide adjuvant. C57BL/6 mice were immunized three times s.c. at biweekly intervals with 50 µg of L1p16 in PBS or in Montanide adjuvant. The x-axis marks the peptides used for the stimulation of splenocytes.

The antibody responses of individual sera obtained with a VLP-capture ELISA are presented in Figure 60. As the Vicoryx-group did not receive the L1 protein, these sera were excluded for this test. The vaccine formulation in Montanide did not lead to an increased production of VLP-binding antibodies. The highest signal was even measured for the L1p16 in PBS group that did not receive the adjuvant. The mean value of the PBS group (n=3) is m=0.1901 AU, for the Montanide group (n=3) m=0.1239 AU; however a significant difference could not be detected (p=0.6803) probably because of the small number of mice tested.

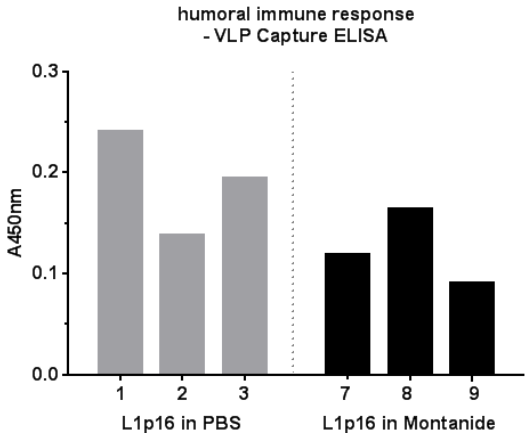

Figure 60: Vaccine formulation in PBS vs. Montanide adjuvant - humoral immune response measured by VLP-capture ELISA. C57BL/6 mice were immunized three times s.c. at biweekly intervals with 50 µg of L1p16 in PBS or in Montanide adjuvant. Bars represent individual sera. A significant difference of the two groups could not be detected (p=0.6803)

Figure 61 shows the p16^{INK4a} antibody response for the three different test groups that received 50 µg of either L1p16 in PBS, L1p16 in Montanide or the Vicoryx peptide in Montanide. It is evident that the vaccine formulation in Montanide did not improve the antibody response; as the highest p16 titers were measured for mouse #2 that did not receive the adjuvant. The antibodies titers induced by the Vicoryx peptide were found to be quite low.

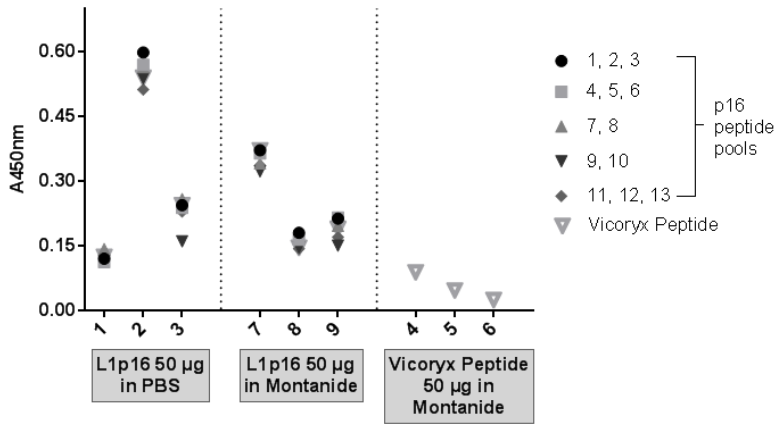

Figure 61: Vaccine formulation in PBS vs. Montanide adjuvant - humoral immune response measured by p16^{INK4a}-petide ELISA. C57BL/6 mice were immunized three times s.c. at biweekly intervals with 50 µg of L1p16 in PBS or in Montanide adjuvant. Numbers on x-axis indicate individual mouse sera.

10.7 Conclusions

Immunization with chimeric L1 - p16^{INK4a} capsomeres follows a dose response effect which was determined using the p16L1 construct. The dosage for further experiments was defined to be 50 µg chimeric protein per mouse, 50 µg p16 protein and 25 µg L1 for the control groups. Comparison of the three constructs revealed different immunogenicity. L1p16L1 induced highest L1-specific T cell numbers, p16L1 showed the best antibody response in the VLP-capture ELISA and L1p16 seemed to induce the best anti-p16 humoral immune response. With the last experiment performed during this thesis, finally a p16-specific cellular immune response could be detected in the ELISPot assay with four peptides (three

nonamers, one 26-mer: Vicoryx peptide) used to stimulate the splenocytes from Lp16 immunized mice. This speaks for a polyclonal, robust CD8+ T cell response as three different nonameres were recognized in the ELISpot assay. It may be speculated that $p16^{INK4a}$-reactive T cells have also been induced during the previous experiments, but to confirm this, further mouse studies need to be performed. The ubiquitous presence of p16-specific antibodies argues for the induction of B-cells that may have required $p16^{INK4a}$-specific T helper responses. The strong cellular immune response to L1 in the first experiments shows that at least the L1 proportion of all constructs is immunogen, that the immunization itself is capable of inducing an immune response and that the fusion proteins are processed and presented by MHC molecules.

Evaluation of a large cohort (n=50) revealed that spot numbers up to 13 can be considered as background response that appears even without any peptide specific stimulation in the applied ELISpot setting. By testing single immunizations, it turned out that boosting by repeated immunization is necessary for a strong, effective immune response. It was also found that the vaccine formulation in Montanide adjuvant did not improve the antibody response over the PBS formulation; although this should be confirmed using a larger cohort.

In summary, these in vivo results show that it is in principal possible to induce L1 and p16-specific T cells as well as antibodies targeting the human $p16^{INK4a}$ tumor suppressor protein. Furthermore, the inclusion body derived capsomere constructs are able to induce VLP-capturing antibodies indicating a probable HPV-neutralizing effect. Immunization with the purified capsomeres also resulted in high L1-specific T cell numbers. The p16 overlapping peptide pool was found to be unsuitable for the detection of $p16^{INK4a}$-specific T cells that were induced by immunization with the full length $p16^{INK4a}$ protein fused to HPV16 L1. However, these could be discovered with the synthetic peptides P1 (TRGSNHARI), P2 (LPVDLAEEL) and P3 (GSARVAELL) that were predicted for H2-Db-restricted CTL epitopes of full length human p16 protein.

IV. Discussion

In HPV-transformed precursor lesions and invasive carcinomas the cellular tumor suppressor $p16^{INK4a}$ is strongly overexpressed, whereas in normal tissues barely any $p16^{INK4a}$ expression is detectable. Therefore, $p16^{INK4a}$ is considered to be an interesting target for immunotherapy in patients with HPV-associated cancers. We designed chimeric particles consisting of 16^{INK4a} and HPV16 L1, the major capsid protein of HPV and antigen of the available prophylactic HPV vaccines, with the aim of using the adjuvant-like effects of L1 particles to improve $p16^{INK4a}$ immune responses and at the same time generating a vaccine candidate with combined prophylactic (L1) and therapeutic ($p16^{INK4a}$) properties.
For this purpose, three chimeric HPV16 L1 - $p16^{INK4a}$ capsomere constructs were cloned and expressed in bacterial systems. Due to their low solubility, an inclusion body purification protocol was developed to purify the proteins in high amounts. The produced particles were then evaluated for their structural properties and immunological potential. The in vivo immunogenicity of the capsomeres was tested in a C57BL/6 mouse model.

11 Generation of chimeric capsomeres consisting of HPV16 L1 and $p16^{INK4a}$

11.1 Production of HPV16 L1 - $p16^{INK4a}$ capsomeres in E. coli

Especially in developing countries where around 80% of cervical cancer deaths occur, the availability of prophylactic HPV vaccines is not optimal, respectively prophylactic vaccine coverage is poor and furthermore effective gynaecological screening programs are often absent. This explains an urgent need for an effective and save therapeutic vaccine that can be produced cost efficiently for the availability in these settings, as one of the greatest barriers towards introduction of a vaccine is its price. [21, 82, 83, 96, 151]
This led to various approaches to produce a cost-efficient vaccine that would, in the best case, not even require stable cold-chains for transport and storage. There are several therapeutic vaccines including DNA vaccination [77], live vector-based [152] and peptide or protein-based vaccines [98, 153] targeting the HPV E6 and/or E7 antigens; however with limited success so far. The production of a protein-based vaccine in bacteria provides several advantages over the production in eukaryotic expression systems as bacteria can be cultured rapidly, inexpensively and with easy scale-up possibilities; all while high biomass and high protein yields are achievable. For these reasons, several therapeutic proteins are already successfully produced in E. coli systems, e.g. human insulin (Humulin

R U-500, Eli Lilly, IN, USA) and bovine growth hormone (Posilac, Monsanto, Eli Lilly, IN, USA).

The recombinant production in bacteria was also the choice for the L1-based capsomeres generated during this thesis as L1 can be expressed and purified in high amounts from E. coli as demonstrated before [37, 154]. The production and effectiveness of capsomeres purified from bacteria was likewise explored in several studies [78, 79, 137, 149, 155].

Figure 62 gives an overview of the various steps that had to be carried into execution before immunological studies could be undertaken in vivo with the vaccine candidates. The most important findings that influenced further approaches are indicated as cursive text.

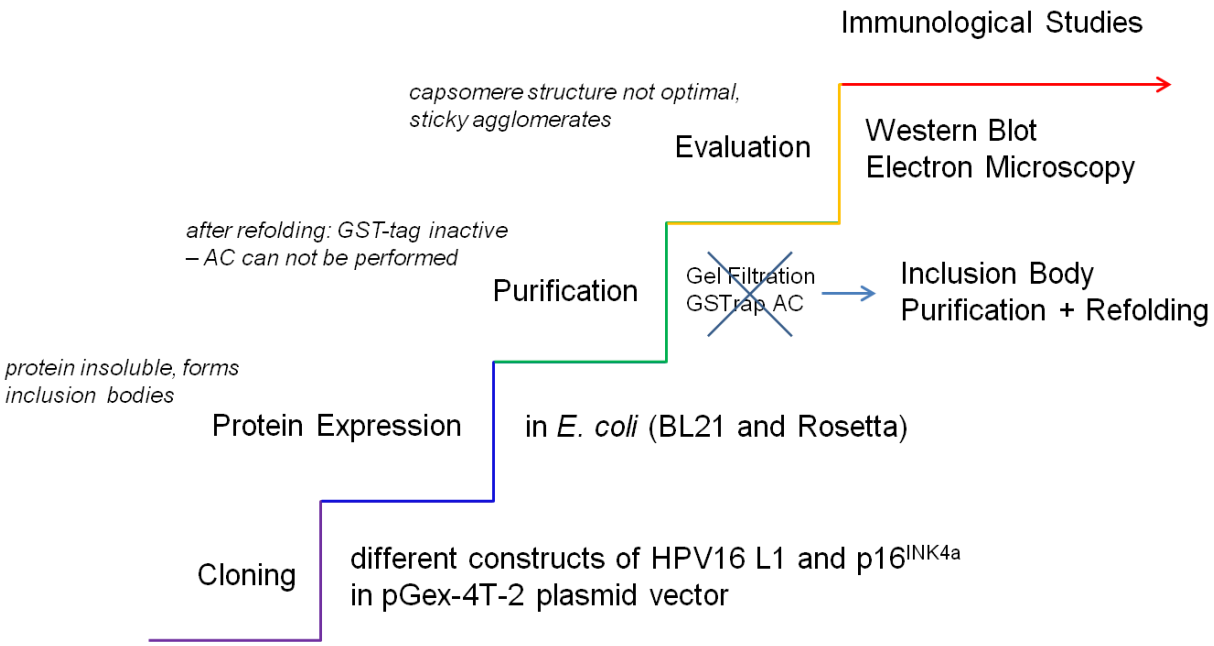

Figure 62: Course of the process - generation and evaluation of the L1 - $p16^{INK4a}$ vaccine constructs towards their application in immunological studies. The project started with cloning of the desired constructs into the expression vector pGex-4T-2. These plasmids were then transformed into the E. coli strains BL21 and Rosetta and expressed under various conditions. It was found that the L1-containing fusion proteins are highly insoluble. For this reason the originally planned GSTrap (followed by gel filtration) purification could not be performed and was replaced by a specifically developed inclusion body purification protocol. This purification process includes a denaturing and subsequent refolding step of the target proteins. After refolding, the GST-tag was found to be inactive and therefore further purification was challenging. However, the so produced capsomeres were found to be of high purity and solubility, even in concentrations in the mg range. Although electron microscopy revealed heterogeneous capsomere preparations with several truncated fragments identified by western blot analysis, the chimeric proteins were tested for their immunological potential in C57BL/6 mice as the major proportion was found to be full-length target protein.

First of all, the three different constructs were cloned into the pGex-4T-2 expression vector to enable IPTG-inducible expression using a tac promotor. The L1 sequence that was used as template sequence was provided by L. Schädlich / L. Gissmann (DKFZ Heidelberg) and contained several modifications including truncations of 10 N-terminal and 29 C-terminal amino acids and a deletion of the helix 4 region (aa 408-431). These modifications to the L1

protein still allow the formation of capsomeres (consisting of 5 L1 proteins, also referred to as pentameres) but prevent assembly of complete VLPs [37, 68]. It was reported that the yield and solubility of this modified L1 protein is 2- to 6-fold higher compared to assembly competent L1 as interactions between the chimeric fusion protein molecules can cause more aggregation [144]. Based on the work of L. Schädlich and L. Gissmann, two constructs, namely p16^{INK4a}-L1ΔN10Δ408-431ΔC29 and L1ΔN10Δ408-431ΔC29-p16^{INK4a} were cloned. The N-terminal fusion of E7 to this modified L1 sequence was found to elicit highest anti-tumor activity amongst several tested constructs. The induction of neutralizing antibodies was less efficient but could be overcome by repeated boosting immunizations. C-terminal fused E7 was found to induce strong antibody responses, with the possible drawback of thereby counteracting a strong anti-tumor response which in turn was speculated to be overcome by a suitable adjuvant [144]. A third construct, L1ΔN10Δ408-431-p16^{INK4a}-ΔC29, was generated based on the work of Murata and colleagues [129]. Here, the complete p16^{INK4a} encoding sequence was substituted for the deleted L1 helix 4 domain (aa 404-436) whereby 9 amino acids were deleted additionally as described in their report. They have shown that the helix 4 region can function as an alternative antigen display site within the L1 capsomeres thereby eliciting antibody responses against a non-HPV encoded protein (conserved neutralizing epitope of the human respiratory syncytial virus (RSV) fusion (F) protein). As the helix 4 projects outwards and laterally from capsomeres [36] it may be more susceptible for amino acid insertions compared to other regions of the protein [129]. The three desired pGex-4T-2 vector constructs could be successfully cloned and were transformed into the expression strains BL21 and Rosetta. The correct insert sequences were confirmed by digestion with the appropriate restriction enzymes and sequencing with different primers.

The three chimeric constructs, L1-p16^{INK4a} p16^{INK4a}-L1 and L1-p16^{INK4a}-L1 as well as the control proteins L1 and p16^{INK4a} were expressed in E. coli. The GST-p16^{INK4a} protein was expressed soluble, whereas the L1 containing proteins were all found to be highly insoluble with only smallest amounts that could be purified from the supernatants after cell lysis. As the bulk protein remains in the pellet, this speaks for massive inclusion body production as observed before [144, 154, 156, 157]. Inactive protein aggregates accumulate and form insoluble structures. Many recombinant proteins tend to undergo misfolding and accumulation as inclusion bodies when overexpressed in bacterial systems. However, the formation of inclusion bodies provides several advantages over soluble expression as the protein is present in a highly enriched form and can be easily separated from other host cell proteins. As long as proper refolding is ensured, the purification from inclusion bodies is one of the most effective protein production strategies. For these reasons several proteins are produced by solubilization and refolding from IBs, for example ovine growth hormone [158],

human growth hormone [159] or the recombinant bonnet monkey zona pellucida glycoprotein [160] (for review see [161]). Despite these successful examples, refolding of IB complexes can be extremely challenging. Therefore, soluble protein expression of the chimeric capsomeres was intended in the first instance. To improve soluble protein expression, several attempts were made but did not result in markedly better solubility. The adaption of induction conditions and temperature [162] as well as application of osmotic and/or heat stress [145] did not lead to increased amounts of soluble expressed proteins. Therefore, the standard expression conditions (induction at OD600 2 - 3 with 0.1 mM IPTG for 17 h at 22°C) were used for the protein production. This expression protocol was adapted from a modified protocol described in the thesis of L. Schädlich [144] and was reported to yield sufficient amounts of soluble protein. The delay in induction until relatively high cell densities (OD600nm > 4.0) was also reported to be beneficial for other proteins [163]. In our settings, with using highly enriched TB culture medium, OD600nm values of maximum 3.0 could be reached until entry into stationary phase. Therefore the cultures were induced when two following OD600 values indicated bacterial growth arrest. The comparison of the two tested E. coli strains, BL21 and Rosetta, did not reveal significant differences concerning protein yield; however, for the E. coli BL21 strain substantial co-expression of bacterial GroEL was observed. As these chaperones were always found to be co-purified, it was decided to use E. coli Rosetta for further expression and purification attempts. As solubility of the chimeric capsomeres could not be improved to a satisfying degree, we decided to proceed with the inclusion bodies.

11.2 Purification of chimeric capsomeres expressed as inclusion bodies

The insolubility observed for our L1-containing chimeric constructs was also found in previous studies with E6 and/or E7 fused to L1. Expression and purification of these chimeric fusion proteins in and from E. coli proved to be extremely challenging due to the high insolubility [144]. The modified L1 construct (L1ΔN10Δ408-431ΔC29) alone was reported to be more soluble when expressed in bacteria [76]; however this could not be confirmed or rather depends on the base of comparison. The N-terminal truncation and other modifications of L1 were introduced to improve solubility, but substantial protein loss and thereby inefficient purification due to insolubility was observed also with this protein [144]. In our case, the expression of L1 alone was very similar to that of the L1-$p16^{INK4a}$-fusion proteins. This indicates neither a supportive nor impairing effect of the $p16^{INK4a}$ fusion on the solubility of the proteins. The protein yield after purification was specified to be 0.75 mg per liter bacterial culture being the best achievable result in a paper published by L. Schädlich et al. [76]. This can be attributed to analytical overexpression. To enable efficient

production of a recombinant protein, including up-scaling possibilities and consideration of economical aspects, purification of the soluble fraction would not be suitable. With the inclusion body purification protocol developed during this thesis, including N-Lauroylsarcosin denaturation and refolding, target protein amounts of 29 mg (L1), 40 mg (L1p16), 34 mg (p16L1) and 55 mg (L1p16L1) could be obtained from 100 ml bacterial culture. This equates to a 727-fold increase just for the L1 protein purified from IBs compared to the results reported for the soluble fraction, whereby the exact same L1 vector construct (pGex-L1ΔN10Δ408-431ΔC29) was used. For the soluble fractions of the GST-tagged proteins, similar amounts were purified during this thesis, but as this is obviously a very inefficient purification strategy with low yields, it would require large culture volumes and many purification runs to produce sufficient amounts for further studies. This in turn increases material and employee costs and would therefore not be suitable to perform in low resource settings. For these reasons, the purification from inclusion bodies provides several advantages as high protein concentrations can be produced from smaller culture volumes. Even cost intensive chromatographic purification does not need to be applied, providing another beneficial feature of the described protocol.

The co-expressed GST-tag was initially contemplated to be used during purification as GST binds to glutathione with high affinity and the tagged protein can thereby be separated from other host cell proteins via affinity chromatography. We have evaluated various strategies to remove the tag from the protein preparations after inclusion body purification. Thereby it was found that the enzymatic activity of GST is substantially diminished, which is probably due to improper refolding after denaturation. Also antibody affinity, ion exchange (IEX) and size exclusion chromatography, which do not require GST activity, did not result in a sufficient separation of the tag. This indicates a strong association of GST with the target protein, possibly in aggregates. Another approach for further studies could be the removal of the tag before refolding of the protein, as this was not evaluated here. For example antibody affinity chromatography (Protein G or CnBr based) could be tested with the denatured proteins. Another alternative purification method could be the application of IEX with denatured proteins as it was described by Bian et al [157]. The GST-tag keeps otherwise insoluble proteins in solution [37, 164] and it was reported that its removal is a critical step with major protein losses caused by precipitation [144]. Therefore, the purification of chimeric proteins as full GST-fusions was suggested before [144] and even a clinical trial with a GST-E7 fusion protein was intended [165]. As this also bypasses the cost intensive thrombin mediated cleavage step, we continued with further evaluation of the GST-tagged chimeric L1 - $p16^{INK4a}$ proteins.

12 Evaluation of the purified chimeric capsomeres

12.1 Evaluation of the chimeric capsomeres purified from inclusion bodies

The capsomere preparations are stable at room temperature and after repeated freeze-thaw cycles. The proteins were handled at room temperature most of the time, including purification. This increased stability of capsomeres was reported to be advantageous over complete VLPs [150, 166, 167]. Besides good stability characteristics, the L1 - $p16^{INK4a}$ capsomeres were found to be of rather heterogeneous structure with many unassembled protein molecules as visualized by TEM. Assembled capsomeres had a diameter of about 10 nm which is consistent with previous reports [149, 167], however, a certain tendency to form aggregates was observed for all fusion proteins. Other groups also showed aggregation and poor yields for the L1ΔC34-E7 protein purified from baculovirus-infected insect cells [168] or for various chimeric capsomere constructs that were obtained from E. coli preparations [144]. Sedimentation analysis revealed the presence of small particles (1 - 4S) which is consistent with previous studies [76, 137, 148]. An antigen capture ELISA with the conformation-specific anti-L1 antibody 1.3.5.15 (Ritti01, [169]) exhibited few conformation-specific epitopes. This suggests that the L1 - p16 fusion proteins were at least partially misfolded which was also reported before for L1-E7 chimeras [144]. Nevertheless, the structural inconsistencies did not seem to influence immunogenicity of the chimeric capsomeres (see 12.2) as it was also shown for L1-RSV F pentamers [129].

The purified chimeric protein preparations also contained several truncated fragments that could be identified to be of L1 and $p16^{INK4a}$ origin. This phenomenon may be due to partial degradation, non-optimal gene transcription and/or ribosomal protein translation. Partial degradations and resulting truncated fragments were also observed previously [137]. Protein concentrations of the full length target proteins were therefore determined densitometrically to exclude those truncated fragments. With the presented inclusion body purification strategy it was possible to generate high concentrations of purified capsomeres (L1: 1.79 mg/ml; L1p16: 0.94 mg/ml; p16L1: 1.32 mg/ml; L1p16L1: 1.11 mg/ml) with markedly higher yields, ranging from 29 to 55 mg pure target protein obtained from 100 ml bacterial culture, than ever reported to date. Furthermore, the IB-derived capsomeres were found to be free of contaminating lipopolysaccharides (LPS), the major component of the outer membrane of Gram-negative bacteria like E. coli. LPS can cause severe side effects such as fever, tissue damage and septic shock when entering the blood stream [170-172]. To prevent the occurence of these LPS-caused reactions, the maximum amount for endotoxins allowed in i.v. injections in humans was set to be 5 endotoxin units (EU) per kg body weight per hour [147]. LPS contaminations can also impact the immunogenicity of e.g. a vaccine as demonstrated for HPV16 L1 capsomeres [130]. Therefore, different strategies

were developed to remove endotoxins from pharmaceutical products. Triton X-114 phase separation technique was found to be an effective method for removing bacterial endotoxins from protein preparations [130, 141] and was used during this project, too. To detect LPS contaminations in our purified proteins we used the Limulus Amebocyte Lysate (LAL) Test (Lonza) which is an “end-product endotoxin test for human and animal parenteral drugs, biological products, and medical devices” [173]. As the developed inclusion body purification includes several Triton X-100 wash steps, the L1-containing capsomere preparations were found to be free of endotoxins after refolding from IBs. Only the GST-p16 protein that was purified from the soluble fraction via GSTrap affinity chromatography contained considerable amounts of LPS. These were successfully removed by Triton X-114 phase separation while providing high protein recovery.

12.2 Immunogenicity of the capsomere constructs

The immunological potential of the purified chimeric capsomeres was evaluated in vivo in C57BL/6 mice. We could show that the immunization with chimeric $p16^{INK4a}$ -L1 capsomeres follows a dose response effect as it could be expected that the immune response increases with increasing antigen concentration. With the previously described H2-Db-restricted L1 peptide (AGVDNRECI), strong T cell responses could be measured. However, the detection of $p16^{INK4a}$-specific T cells by IFNγ ELISpot without known H2-Db-restricted epitopes was generally challenging. This was also previously observed for the E7 antigen fused to the modified L1 protein [144, 174]. A peptide pool comprising thirteen overlapping long peptides covering the complete $p16^{INK4a}$ sequence was found to be unsuitable for the detection of $p16^{INK4a}$-specific T cells. In a last experiment that was conducted during this thesis, three software-predicted synthetic peptides P1 (TRGSNHARI), P2 (LPVDLAEEL) and P3 (GSARVAELL) were used for the stimulation of splenocytes and L1p16 capsomeres were found to induce a polyclonal, robust cytotoxic T lymphocyte (CTL) response to these three different H2-Db-restricted $p16^{INK4a}$ peptides as determined by ELISpot assay. Furthermore, it appeared that the cellular response to the $p16^{INK4a}$ proportion was weaker than that to L1. This could be due to the fact that the chimeric capsomeres contain less $p16^{INK4a}$ protein than L1 as $p16^{INK4a}$ compromises a relative molecular weight proportion of only 18 percent of the fusion protein (GST: 28%; L1: 54%). This means that L1 is present in a 3-fold excess compared to $p16^{INK4a}$. CTL responses to these two antigens might also not be balanced because of immunodomination of the L1 protein whereby the cellular immunity focuses towards one antigenic determinant [175]. Another possibility is the presence of another dominant antigenic epitope, which was not predicted and therefore not covered by the ELISpot assay. The three different fusion proteins showed similarly high levels of L1-

specific T cells generated in response to the immunization with chimeric capsomeres. Therefore, the generation of p16-specific T cells seems plausible also in the other experiments where the predicted peptides were not yet used for the ELISpot, but the long overlapping peptide pool. However, p16-specific antibodies could be detected in most of the immunized mice. The strong cellular immune response to L1 shows that at least the L1 proportion is immunogenic in these previous experiments. This suggests that the fusion proteins are accessible to the antigen presentation machinery, can be presented by MHC I molecules and thereby stimulate cytotoxic T cells. Splenocytes consist of different cell populations such as T and B lymphocytes, dendritic cells and macrophages but it can be assumed that we detected a cytotoxic immune response as 9-mer peptides are capable of stimulating CD8+ T cells. The type of cellular immune response is important for cancer vaccines. CD8+ T cells are considered to be necessary targets for effective strategies and in many cancers, the presence of tumor infiltrating CD8+ T lymphocytes positively correlates with a good prognosis [176].

By testing single immunizations, it turned out that boosting by repeated immunization is necessary for a strong, effective immune response. Further it was found that the vaccine formulation in Montanide ISA 51 adjuvant did not improve the immune response over the PBS formulation in our setting - although this should be confirmed using a larger cohort. It should also be tested if the formulation in Montanide provides an advantage over PBS when a single immunization is applied. This is likely the case as a rapid antibody response was reported and it was claimed that booster injections may not be needed [177]. Montanide is based on metabolizable squalene oil, emulsified with mannide mono-oleate. It encapsulates antigens (antigen delivery vehicle) in a water-in-oil (W/O) emulsion which induces strong and long term immune responses and in particular CD8+ T cells [178, 179]. This adjuvant was used for the respective experiment as the peptide which is currently used in a clinical trial (Vicoryx, [125]) is also formulated in Montanide. W/O emulsions are standard vehicles for therapeutic vaccines against cancer and other diseases and various clinical trials in which thousands of individuals received Montanide with different antigens approved its efficacy and safety [178, 180].

The purified L1 - $p16^{INK4a}$ capsomeres were tested for contaminating endotoxins and were found to be free of those. Therefore, it can be assumed that the high immunogenicity of the particles can be attributed to L1 and not to an adjuvant effect of contaminating LPS. It should be considered that the GST-tag was also part of the immunized capsomeres. However, GST itself has also been shown to be highly immunogenic and was tested in clinical trials for use as a vaccine against schistosomiasis [181-184]. It was speculated that GST may interfere with the induction of a L1 (and therefore probably also with a $p16^{INK4a}$)

immune response [144]. This can be moderated by the finding that GST-COPV (canine oral papillomavirus) L1 pentamers provide protection against provoked infections of dogs' oral mucosa [149]. Also a GST-E7 protein was immunogenic and could protect mice from E7 transfected tumor cells [165].

The comparison of the three different constructs revealed different characteristics with regard to their immunogenicity. L1p16L1 induced highest L1-specific T cell numbers, p16L1 showed the best antibody response in the VLP-capture ELISA and L1p16 seemed to induce the best anti-p16 humoral immune response. Other studies by L. Schädlich et al. [144] showed that the E7-L1ΔN10Δ408-431ΔC29, the analogue to our p16L1 protein, had a high anti-tumor activity but required booster immunizations to induce efficient antibody responses. The C-terminal fusion L1ΔN10Δ408-431ΔC29-E7, analogue to our L1p16, elicited strong antibody responses. However, it is possible that a strong antibody response counteracts the development of a strong anti-tumor response [144], most likely because of the presence of pre-existing antibodies that neutralize subsequent antigen doses [185, 186]. Considering this, the finding that L1-VLPs induce much higher humoral immune responses than capsomeres [37, 68, 155], can be relativized as we mainly focus on the induction of an effective cellular immune response. Capsomeres are basically L1 pentameres in which the helix 4 region is deleted to prevent particle assembly into full VLPs. It has been speculated that the helix 4 itself contains an epitope that is essential for a strong antibody response [144] or that the assembly into larger structures than capsomeres is beneficial for high immunogenicity [76]. This is also supported by the finding that chimeric fusion proteins lacking the helix 4 region were most efficient at inducing neutralizing antibodies [144] what might be explained by the aggregation theory, too, as the chimeric particles showed a certain tendency to build agglomerates. In addition, our L1 - p16 capsomeres were mainly present in aggregated form with heterogeneous particles and sticky agglomerates. This appearance could possibly have a beneficial effect on the development of a potent anti-tumor immune response. Further mouse experiments will be conducted to elucidate this possibility and to compare the different structural isoforms.

13 Chimeric HPV16 L1 - p16^{INK4a} capsomeres as a potential vaccine

13.1 p16^{INK4a} as an antigen for therapeutic HPV vaccines

p16^{INK4a}, also known as the cyclin-dependent kinase inhibitor 2A (CDKN2A), regulates cell cycle progression and promotes cellular senescence. The HPV oncogenes E6 and E7

degrade the key regulator proteins p53 and retinoblastoma protein (pRb) respectively and thereby release $p16^{INK4a}$ from its negative feedback loop. This in turn leads to an increased expression of $p16^{INK4a}$ protein in cervical dysplastic lesions and carcinomas. [107, 117, 118, 122]

The role of $p16^{INK4a}$ as a tumor suppressor protein is somehow controversial in HPV16 E7 expressing cells as its biological activity is similar to that of an oncogene in these conditions as demonstrated by McLaughlin-Drubin and colleagues [121]. They showed that E7 expression causes an addiction of cervical cancer cell lines to the H3K27 targeting histone lysine demethylase (KDM6B). E7 triggers oncogene induced stress (OIS), a cell-intrinsic tumor-suppressive mechanism, and thereby induces $p16^{INK4a}$ expression. On the other hand E7 simultaneously targets pRb for proteosomal degradation as pRb is a key mediator of OIS and $p16^{INK4a}$ induced senescence. This way, the E7-caused epigenetic de-repression is mediated by $p16^{INK4a}$ which is an important KDM6B downstream target and inhibitor of CDK4/CDK6. In cervical cancer cells, where pRb is inactivated, $p16^{INK4a}$ is therefore necessary for the survival of transformed cells. [53, 121] The increased $p16^{INK4a}$ expression in HPV-associated tumors can thus be interpreted as an attempt to stop uncontrolled proliferation but as $p16^{INK4a}$ is released from its negative feedback control by pRb inactivation and KDM6B overexpression, elevated levels of this protein do not lead to cell cycle arrest in tumor cells. An alternative hypothesis states that the pRb degradation should rather abrogate the $p16^{INK4a}$-mediated response to oncogenic stress and thereby inhibit senescence [53].

The phenomenon of $p16^{INK4a}$ overexpression is utilized as a surrogate marker of transforming HPV-infected epithelia [22, 111, 117, 120] and should now also be exploited for the development of a therapeutic vaccine which specifically targets $p16^{INK4a}$ overexpressing cancer cells. $p16^{INK4a}$ is designated as a “tumor-associated antigen”. In contrast to “tumor-specific antigens” like E6 and E7, a certain level of expression in normal tissues often exists. For our chimeric L1 - p16 vaccine candidates this could be problematic in terms of tolerance to this antigen [176]. However, if it is possible to generate an immune response to this auto-antigen, not only patients with HPV-associated cancers would benefit from such a vaccine as many other cancers, including renal, prostate, breast, ovarian and a subset of lung cancers, express high levels of $p16^{INK4a}$ [187-192]. Furthermore, several precancerous neoplasias demonstrate increased $p16^{INK4a}$ expression [193, 194] and a $p16^{INK4a}$-directed vaccine might thus even prevent development of invasive cancer. The induction of an auto-immune response has high potential for anti-cancer therapies [195, 196]. Breaking of immune tolerance to "self-antigens" is therefore an attractive approach for tumor immunotherapy that was subject of different studies before. For example basic fibroblast growth factor (bFGF) was shown to activate normal dermal fibroblasts and makes

them have analogous properties with cancer-associated fibroblast. Mice that were immunized with bFGF-activated fibroblasts had an apparent protection from tumor onset and growth [197]. Also protein/peptide-based vaccines that are combined with adjuvants to induce regulatory T cells (Tregs) are being investigated for their potential in therapeutic vaccination against chronic inflammatory conditions [198] as the activation of Tregs would inhibit auto-reactive T effector cells and thereby have an anti-inflammatory effect [199]. Self-tolerance is also considered to be responsible for the limited capacity of the human immune system to control and prevent tumor outgrowth [195].

The p53 tumor suppressor protein shows several parallels to $p16^{INK4a}$ as it likewise prevents expansion of abnormal cells and its function is impaired in about 50% of human cancers [195]. Some of the differences and similar functions important in this context are listed in Table 5. In cervical carcinoma, p53 is degraded by the HPV E6 oncoprotein. Contrary to p16, p53 was intensively studied as a tumor antigen before and is considered to be an attractive target for immunological approaches [195, 200-202].

Table 5: Comparison of $p16^{INK4a}$ and p53 tumor suppressor proteins

	$p16^{INK4a}$	**p53**
encoding gene	CDKN2A	TP53
location	chromosome 9 (9p21.3)	chromosome 17 (17p13.1)
MW (kDa)	15.8	43.7
function	tumor suppressor and cell cycle regulator prevent expansion of abnormal, tumorigenic cells	
cell cycle	arrest at the G1/S phase	
role in cancer	frequently mutated or deleted in various tumors; often overexpressed in cancer cells	
targeting HPV oncogene	E7	E6

p53 is used as a well-studied example here as it also is an auto-antigen analogous to $p16^{INK4a}$ is. CD4+ as well as CD8+ T cell responses to the p53 protein could be induced by immunizations as demonstrated by different studies [200, 202]. Anti-self p53 responses were generally weak and not capable to eradicate tumor cells but the p53 tolerance can be overcome in vivo [201]. Further studies on p53 determinants revealed the presence of more tolerance-inducing T cells (Th2) than of those which could promote rejection (Th1) of p53 overexpressing cancer cells [195]. As $p16^{INK4a}$ was not subject of intense vaccination studies so far, the distribution of potential antigenic determinants for this protein remains elusive. If it would be the other way around for the $p16^{INK4a}$ protein, so that the rejection-

inducing determinants overweight the tolerance-inducing ones, the $p16^{INK4a}$ vaccination strategy would be additionally supported.

Altogether, it is conceivable that an intrinsic response to $p16^{INK4a}$, as it was observed in some patients before [123], can be provoked and enhanced by vaccination. This hypothesis is supported by studies with other auto-antigens like p53 and first insights with a synthetic long peptide p16-vaccine, Vicoryx [125]. Moreover, in this thesis, encouraging results are presented which demonstrate the induction of $p16^{INK4a}$-specific antibodies and also cytotoxic T lymphocytes by immunization with chimeric capsomeres comprising $p16^{INK4a}$. It should be considered that the human $p16^{INK4a}$ protein used during these studies could also elicit its T cell-inducing function via a xenogenic effect as the antigenic epitopes were mainly predicted within non-conserved sequences of human and murine $p16^{INK4a}$. However, with a vaccine containing the full-length $p16^{INK4a}$ protein we provide all antigenic epitopes possible to increase the chance for an effective immune response towards this auto-antigen. This would be an essential step in the area of therapeutic vaccines with the potential of inducing regression of $p16^{INK4a}$-positive tumors.

13.2 HPV16 L1 capsomere conjugation to full length $p16^{INK4a}$

The potential of chimeric virus-like particles (CVLPs) as self-adjuvanting immunogen delivery systems for the therapy of HPV-associated lesions and cervical cancer was demonstrated in different studies before [70, 174, 203, 204]. Also chimeric VLPs derived from bovine papillomavirus (BPV) [71, 168, 205], cotton-tail rabbit papillomavirus (CRPV) [206] and canine oral papillomaviruses (COPV) [81] were evaluated for their immunologic potential. Papillomavirus VLPs are able to induce strong immune responses and allow antigen presentation within a highly organized context as part of the regular array of assembled capsomeres [73, 74]. The oncogenes E6 and E7 were often the fusion partners of choice to specifically target HPV transformed cells. As VLPs were shown to be potent antigen carriers, other, non-HPV related antigens were also evaluated as fusion partners. For example the conjugation of mouse self-peptide TNF-α to papilloma VLPs leads to efficient induction of protective auto-antibodies [74]. The conjugation of influenza type A M2 protein to HPV VLPs was also found to be highly immunogenic and conferred good protection against lethal challenge of influenza virus in mice [72]. In another study, hepatitis B virus core antigen (HBcAg)-VLPs were successfully used for the display of a surface epitope of the tumor-associated marker claudin-18 [207].

However, assembly into complete VLPs was found to be no pre-requisite for the induction of an immune response [137, 166] and that antigenic domains are contained in capsomeres

[78]. HPV major capsid protein L1 capsomeres were also demonstrated to be efficient antigen carriers for the development of conjugate vaccines. Because of the structure of capsomeres, they exhibit an intrinsic adjuvant-like function as it was found for assembled VLPs, too. Chimeric L1-E7 capsomeres were early demonstrated to enable effective MHC class I-restricted antigen presentation and to induce an E7-specific CTL response in mice in absence of an adjuvant [174]. Also non-HPV related antigens, like the respiratory syncytial virus fusion protein [129], were successfully presented in the context of capsomeres to provide a therapeutic element. The capsomere production in E. coli was another step towards an efficient and economic therapeutic vaccine [37, 76, 157, 208].

Because of these encouraging results from other groups, we generated chimeric HPV16 L1 capsomeres fused to the full length $p16^{INK4a}$ protein with the aim of developing a combined prophylactic and therapeutic vaccine, although the main focus of this project was the therapeutic approach. The conjugation of an antigen to VLPs was shown to abrogate the ability of the humoral immune system to distinguish between self and foreign [74]. This is interesting as $p16^{INK4a}$ is also a weakly immunogenic, self-derived antigen and it can be assumed that this holds also true for capsomeres. We decided to use the full-length $p16^{INK4a}$ protein (156 aa) to provide the possibility of CTL and T helper cell induction against several epitopes and thereby preventing tumor cell escape by mutation of one relevant epitope. This strategy was previously proven to be effective with L1-$E7_{1–60}$ CVLPs [174] and also peptide immunization studies suggest the use of at least peptides longer than 9-mers as they show greater efficacy [180, 202, 209].

13.3 Evaluation of the prophylactic and therapeutic potential of the chimeric proteins

Women who are already infected do not benefit from the currently available prophylactic vaccines which are based on L1 VLPs and predominantly induce a strong humoral immune response against the major capsid protein of the virus [93, 94]. These antibodies then neutralize incoming virus particles and thereby prevent a new HPV infection. However, in high grade dysplasia and cervical carcinoma, no HPV capsid proteins are detectable due to the transformed phenotype which is released from its tightly controlled “normal” viral life cycle [95]. Contrary to the prophylactic vaccines, therapeutic vaccination aims in the induction of a strong, long lasting CD8+ cytotoxic T cell response to selectively target and eliminate tumor cells. Cell-based cancer immunotherapy is a promising method to treat cancer whereby the patients’ own immune system is harnessed to induce an anti-tumor response [197]. Various therapeutic attempts target the early proteins, mainly E6 and E7, with varying success so far [94, 97, 166, 174]. For example ProCervix (Genticel [210]),

which is based on an adenylate cyclase vector from Bordetella pertussis, was shown to induce E7-specific T cell responses in the majority of vaccinated patients. This vaccine will probably enter the market soon, but an important drawback is its intended application for HPV16/18 positive women, prior to the appearance of high grade cervical lesions. As most of those lesions resolve spontaneously, the actual use of ProCervix is questionable. Other candidate vaccines that were presented in the last years are e.g. ZYC101a, a DNA vaccine based on E6 and E7 fragments (HPV16 & 18) [77]; a live-attenuated Listeria monocytogenes vaccine Lovaxin-C [152]; MVA E2 (Modified Vaccinia Ankara virus) [211] and several E6 and E7 long peptide vaccines [98, 153].

In the context of these and other studies, the problem of only type-specific immunity induced by E6/E7 immunization is usually not discussed. To overcome those issues, we developed a capsomere-based vaccine comprising the tumor suppressor protein $p16^{INK4a}$ which is strongly expressed in cervical cancer and precursor lesions independent of the infectious genotype as demonstrated by various studies [22, 106-108, 110, 121, 126]. Table 6 lists some of the respective advantages and disadvantages of $p16^{INK4a}$ as a therapeutic element in comparison to the conventional E6/E7 targeting strategies.

Table 6: Comparison of advantages and disadvantages of therapeutic vaccination strategies using $p16^{INK4a}$ vs. E6/E7.

vaccine target	**$p16^{INK4a}$**	**E6/E7**
characteristics	• tumor suppressor protein • tumor-associated antigen	• viral oncoproteins • tumor-specific antigens
advantages **+**	• strong overexpression in HPV-associated cancer • universal cellular protein - type unspecific • potential use in other p16-expressing cancer types	• overexpression in HPV-associated cancer • no expression in uninfected/untransformed cells • immunogenic, viral antigens
disadvantages **-**	• weak expression in normal, senescent cells • self-antigen	• type specific oncoproteins • no cross-reactivity • despite excessive research - no therapeutic vaccine on the market yet

We generated HPV16 L1 capsomeres fused to the full length $p16^{INK4a}$ protein. Capsomeres are considered to be more stable than complete VLPs what could be confirmed during this thesis. The circumvention of cold-chains and inexpensive production in bacterial systems makes them ideal vaccine candidates, especially for developing countries [148, 166].

Traditional purification strategies often include a gel filtration step [37, 76, 137, 167]. This is difficult to scale-up and translation into a production process would be challenging. The purification from inclusion bodies, by avoiding such a step, therefore provides obvious advantages for a cost effective production of the vaccine. Furthermore, the inclusion bodies can be easily purified to high purity, and even absence of endotoxins can be ensured with such a protocol.

It was also demonstrated that the inclusion body derived proteins are able to induce antibody responses against VLPs and p16 peptides which could probably be further increased with a suitable adjuvant formulation. An effective humoral immune response is crucial for a prophylactic effect, and to prevent HPV infections. This underlines the potential of capsomere-based vaccines also as alternative prophylactic vaccine candidates that could be provided in low-resource settings. Moreover, the fusion proteins were able to induce a strong L1-specific T cell response and also $p16^{INK4a}$ -reactive T lymphocytes could be detected, even in the absence of an adjuvant. This provides the basis for CTL-mediated tumor cell killing and therefore a likely therapeutic effect. However, the full immunological potential of the chimeric L1 - $p16^{INK4a}$ capsomeres needs to be further evaluated in vivo with tumor challenging experiments.

Altogether, vaccination with chimeric HPV16 L1 capsomeres fused to the $p16^{INK4a}$ protein presents an alternative strategy to control and treat existing HPV infections and associated malignancies and justifies further evaluation.

13.4 Future prospects

Combined prophylactic and therapeutic vaccination against HPV induced neoplasias and cervical cancer would have high benefits for already infected women and a stable, cost efficient vaccine could also be implemented in low resource settings. This work is a milestone on the development of a vaccine targeting the cellular tumor suppressor protein $p16^{INK4a}$ which is de-regulated and highly overexpressed in HPV transformed cells. Because of the encouraging results presented in this thesis, the project will be continued in the near future.

We intend to address an alternative expression of the chimeric capsomeres without the GST-tag as its presence would most likely complicate regulatory approval of the vaccine candidates. Detailed investigations have led to the conclusion that either a pSE380 (Invitrogen, LifeTechnologies) or a pTrc99A (former Pharmacia, GE Healthcare) plasmid vector could be used for the expression of the chimeric capsomeres without any tag. It is likely that the L1-containing proteins will form inclusion bodies upon their expression in E.

coli as low solubility of L1 was shown in different studies before [144, 148, 154, 157]. In this case, the established purification protocol could be used to obtain high amounts of LPS-free fusion protein as it was demonstrated in this dissertation.

With the purified capsomeres, further in vivo studies are planned to evaluate their full immunological potential. Therefore we will compare the three constructs L1p16, p16L1 and L1p16L1 in another experiment, especially with respect to the inducible $p16^{INK4a}$ T cell response. Moreover, tumor protection and regression experiments are planned. However, beforehand a murine cell line needs to be generated which expresses the human $p16^{INK4a}$ protein. Preliminary experiments (data not shown) suggest that transfection using Nucleofection (Amaxa) will be suitable to introduce a $p16^{INK4a}$ encoding plasmid into RMA-S. These cells do not express murine $p16^{INK4a}$ as demonstrated by western blot of whole cell lysates (see Figure 67, VII Appendix), and could therefore be used as a negative control for the tumor challenge experiments, too. 2F11 cells could be an alternative for these attempts as they also do not show intrinsic $p16^{INK4a}$ expression. If it is not possible to generate a stable human- $p16^{INK4a}$ expressing murine cell line with RMA-S or 2F11 cells, C3 or TC-1 cells could be used to establish $p16^{INK4a}$-expressing tumors in mice as both cell lines do express murine $p16^{INK4a}$. This model would either require a xenogenic effect of mice vaccinated with human $p16^{INK4a}$ or would require the design of murine $p16^{INK4a}$ vaccine constructs in addition.

V. References

1. Parkin DM: **The global health burden of infection-associated cancers in the year 2002.** *IntJCancer* 2006, **118:**3030-3044.
2. Doorbar J: **The papillomavirus life cycle.** *JClinVirol* 2005, **32 Suppl 1:**S7-15.
3. Grm HS, Bergant M, Banks L: **Human papillomavirus infection, cancer & therapy.** *Indian JMedRes* 2009, **130:**277-285.
4. Dunne EF, Unger ER, Sternberg M, McQuillan G, Swan DC, Patel SS, Markowitz LE: **Prevalence of HPV infection among females in the United States.** *JAMA* 2007, **297:**813-819.
5. Richardson H, Kelsall G, Tellier P, Voyer H, Abrahamowicz M, Ferenczy A, Coutlee F, Franco EL: **The natural history of type-specific human papillomavirus infections in female university students.** *Cancer EpidemiolBiomarkers Prev* 2003, **12:**485-490.
6. Cuschieri KS, Cubie HA, Whitley MW, Seagar AL, Arends MJ, Moore C, Gilkisson G, McGoogan E: **Multiple high risk HPV infections are common in cervical neoplasia and young women in a cervical screening population.** *JClinPathol* 2004, **57:**68-72.
7. Doorbar J: **Molecular biology of human papillomavirus infection and cervical cancer.** *ClinSci(Lond)* 2006, **110:**525-541.
8. Stanley M: **Immunobiology of HPV and HPV vaccines.** *GynecolOncol* 2008, **109:**S15-S21.
9. **Cervical Cancer** [http://www.cancer.gov/cancertopics/types/cervical]
10. **Zervixkarzinom.** In *032 - 033* ((DKG) DK ed. Frankfurt: Arbeitsgemeinschaft der Wissenschaftlichen Medizinischen Fachgesellschaften e.V. (AWMF); 2012.
11. Beckmann MW, Mehlhorn G, Thiel F, Breuel C, Fasching PA, Ackermann S: **Therapiefortschritte beim primären Zervixkarzinom.** *Dtsch Arztebl International* 2005, **102:**979-.
12. Bernard HU: **The clinical importance of the nomenclature, evolution and taxonomy of human papillomaviruses.** *JClinVirol* 2005, **32 Suppl 1:**S1-S6.
13. Doorbar J, Quint W, Banks L, Bravo IG, Stoler M, Broker TR, Stanley MA: **The biology and life-cycle of human papillomaviruses.** *Vaccine* 2012, **30 Suppl 5:**F55-70.
14. Chow LT, Broker TR, Steinberg BM: **The natural history of human papillomavirus infections of the mucosal epithelia.** *APMIS* 2010, **118:**422-449.
15. Pim D, Banks L: **Interaction of viral oncoproteins with cellular target molecules: infection with high-risk vs low-risk human papillomaviruses.** *APMIS* 2010, **118:**471-493.
16. Lajer CB, von BC: **The role of human papillomavirus in head and neck cancer.** *APMIS* 2010, **118:**510-519.
17. Riechelmann H: **[Human papilloma virus in head and neck cancer].** *Laryngorhinootologie* 2010, **89:**43-48, quiz.
18. Harwood CA, Surentheran T, Sasieni P, Proby CM, Bordea C, Leigh IM, Wojnarowska F, Breuer J, McGregor JM: **Increased risk of skin cancer associated with the presence of epidermodysplasia verruciformis human papillomavirus types in normal skin.** *BrJDermatol* 2004, **150:**949-957.
19. Lazarczyk M, Pons C, Mendoza JA, Cassonnet P, Jacob Y, Favre M: **Regulation of cellular zinc balance as a potential mechanism of EVER-mediated protection against pathogenesis by cutaneous oncogenic human papillomaviruses.** *JExpMed* 2008, **205:**35-42.
20. Bosch FX, Manos MM, Munoz N, Sherman M, Jansen AM, Peto J, Schiffman MH, Moreno V, Kurman R, Shah KV: **Prevalence of human papillomavirus in cervical**

cancer: a worldwide perspective. International biological study on cervical cancer (IBSCC) Study Group. *JNatlCancer Inst* 1995, **87:**796-802.

21. Agosti JM, Goldie SJ: **Introducing HPV vaccine in developing countries--key challenges and issues.** *N Engl J Med* 2007, **356:**1908-1910.
22. von Knebel Doeberitz M, Reuschenbach M, Schmidt D, Bergeron C: **Biomarkers for cervical cancer screening: the role of p16(INK4a) to highlight transforming HPV infections.** *Expert Rev Proteomics* 2012, **9:**149-163.
23. **A Snapshot of Cervical Cancer** [http://www.cancer.gov/aboutnci/servingpeople/snapshots/cervical.pdf]
24. Modis Y, Trus BL, Harrison SC: **Atomic model of the papillomavirus capsid.** *EMBO J* 2002, **21:**4754-4762.
25. Hagensee ME, Yaegashi N, Galloway DA: **Self-assembly of human papillomavirus type 1 capsids by expression of the L1 protein alone or by coexpression of the L1 and L2 capsid proteins.** *JVirol* 1993, **67:**315-322.
26. von Knebel DM: **New markers for cervical dysplasia to visualise the genomic chaos created by aberrant oncogenic papillomavirus infections.** *EurJCancer* 2002, **38:**2229-2242.
27. Zheng ZM, Baker CC: **Papillomavirus genome structure, expression, and post-transcriptional regulation.** *Front Biosci* 2006, **11:**2286-2302.
28. Amador-Molina A, Gonzalez-Montoya JL, Garcia-Carranca A, Mohar A, Lizano M: **Intratypic changes of the E1 gene and the long control region affect ori function of human papillomavirus type 18 variants.** *J Gen Virol* 2013, **94:**393-402.
29. Johansson C, Somberg M, Li X, Backstrom Winquist E, Fay J, Ryan F, Pim D, Banks L, Schwartz S: **HPV-16 E2 contributes to induction of HPV-16 late gene expression by inhibiting early polyadenylation.** *EMBO J* 2012, **31:**3212-3227.
30. Ganguly N: **Human papillomavirus-16 E5 protein: oncogenic role and therapeutic value.** *Cell Oncol (Dordr)* 2012, **35:**67-76.
31. Pillai MR, Lakshmi S, Sreekala S, Devi TG, Jayaprakash PG, Rajalakshmi TN, Devi CG, Nair MK, Nair MB: **High-risk human papillomavirus infection and E6 protein expression in lesions of the uterine cervix.** *Pathobiology* 1998, **66:**240-246.
32. Buck CB, Cheng N, Thompson CD, Lowy DR, Steven AC, Schiller JT, Trus BL: **Arrangement of L2 within the papillomavirus capsid.** *J Virol* 2008, **82:**5190-5197.
33. Stauffer Y, Raj K, Masternak K, Beard P: **Infectious human papillomavirus type 18 pseudovirions.** *JMolBiol* 1998, **283:**529-536.
34. Fahey LM, Raff AB, Da Silva DM, Kast WM: **A major role for the minor capsid protein of human papillomavirus type 16 in immune escape.** *J Immunol* 2009, **183:**6151-6156.
35. Baker TS, Newcomb WW, Olson NH, Cowsert LM, Olson C, Brown JC: **Structures of bovine and human papillomaviruses. Analysis by cryoelectron microscopy and three-dimensional image reconstruction.** *Biophys J* 1991, **60:**1445-1456.
36. Chen XS, Garcea RL, Goldberg I, Casini G, Harrison SC: **Structure of small virus-like particles assembled from the L1 protein of human papillomavirus 16.** *MolCell* 2000, **5:**557-567.
37. Chen XS, Casini G, Harrison SC, Garcea RL: **Papillomavirus capsid protein expression in Escherichia coli: purification and assembly of HPV11 and HPV16 L1.** *JMolBiol* 2001, **307:**173-182.
38. Schiffman M, Castle PE, Jeronimo J, Rodriguez AC, Wacholder S: **Human papillomavirus and cervical cancer.** *Lancet* 2007, **370:**890-907.
39. Ruschoff J, Aust A, Middel P, Heinmoller E: **[Anal cancer: diagnostic and differential diagnostic issues].** *Pathologe* 2011, **32:**336-344.
40. Perry ME: **The specialised structure of crypt epithelium in the human palatine tonsil and its functional significance.** *J Anat* 1994, **185 (Pt 1):**111-127.

41. Boscolo-Rizzo P, Del Mistro A, Bussu F, Lupato V, Baboci L, Almadori G, MC DAM, Paludetti G: **New insights into human papillomavirus-associated head and neck squamous cell carcinoma.** *Acta Otorhinolaryngol Ital* 2013, **33:**77-87.
42. Johnson KM, Kines RC, Roberts JN, Lowy DR, Schiller JT, Day PM: **Role of heparan sulfate in attachment to and infection of the murine female genital tract by human papillomavirus.** *J Virol* 2009, **83:**2067-2074.
43. Abban CY, Meneses PI: **Usage of heparan sulfate, integrins, and FAK in HPV16 infection.** *Virology* 2010, **403:**1-16.
44. Kines RC, Thompson CD, Lowy DR, Schiller JT, Day PM: **The initial steps leading to papillomavirus infection occur on the basement membrane prior to cell surface binding.** *Proc Natl Acad Sci U S A* 2009, **106:**20458-20463.
45. Schiller JT, Day PM, Kines RC: **Current understanding of the mechanism of HPV infection.** *Gynecol Oncol* 2010, **118:**S12-17.
46. Ledwaba T, Dlamini Z, Naicker S, Bhoola K: **Molecular genetics of human cervical cancer: role of papillomavirus and the apoptotic cascade.** *Biol Chem* 2004, **385:**671-682.
47. Pyeon D, Pearce SM, Lank SM, Ahlquist P, Lambert PF: **Establishment of human papillomavirus infection requires cell cycle progression.** *PLoS Pathog* 2009, **5:**e1000318.
48. Raff AB, Woodham AW, Raff LM, Skeate JG, Yan L, Da Silva DM, Schelhaas M, Kast WM: **The evolving field of human papillomavirus receptor research: a review of binding and entry.** *J Virol* 2013, **87:**6062-6072.
49. Bergant Marusic M, Ozbun MA, Campos SK, Myers MP, Banks L: **Human papillomavirus L2 facilitates viral escape from late endosomes via sorting nexin 17.** *Traffic* 2012, **13:**455-467.
50. Schelhaas M, Shah B, Holzer M, Blattmann P, Kuhling L, Day PM, Schiller JT, Helenius A: **Entry of human papillomavirus type 16 by actin-dependent, clathrin- and lipid raft-independent endocytosis.** *PLoS Pathog* 2012, **8:**e1002657.
51. Brehm A, Nielsen SJ, Miska EA, McCance DJ, Reid JL, Bannister AJ, Kouzarides T: **The E7 oncoprotein associates with Mi2 and histone deacetylase activity to promote cell growth.** *EMBO J* 1999, **18:**2449-2458.
52. Antinore MJ, Birrer MJ, Patel D, Nader L, McCance DJ: **The human papillomavirus type 16 E7 gene product interacts with and trans-activates the AP1 family of transcription factors.** *EMBO J* 1996, **15:**1950-1960.
53. McLaughlin-Drubin ME, Crum CP, Munger K: **Human papillomavirus E7 oncoprotein induces KDM6A and KDM6B histone demethylase expression and causes epigenetic reprogramming.** *Proc Natl Acad Sci U S A* 2011, **108:**2130-2135.
54. Serrano M, Lin AW, McCurrach ME, Beach D, Lowe SW: **Oncogenic ras provokes premature cell senescence associated with accumulation of p53 and p16INK4a.** *Cell* 1997, **88:**593-602.
55. Busch C, Geisler J, Knappskog S, Lillehaug JR, Lonning PE: **Alterations in the p53 pathway and p16INK4a expression predict overall survival in metastatic melanoma patients treated with dacarbazine.** *JInvest Dermatol* 2010, **130:**2514-2516.
56. Piette J, Neel H, Marechal V: **Mdm2: keeping p53 under control.** *Oncogene* 1997, **15:**1001-1010.
57. Roden RB, Day PM, Bronzo BK, Yutzy WH, Yang Y, Lowy DR, Schiller JT: **Positively charged termini of the L2 minor capsid protein are necessary for papillomavirus infection.** *JVirol* 2001, **75:**10493-10497.
58. Chitadze G, Bhat J, Lettau M, Janssen O, Kabelitz D: **Generation of soluble NKG2D ligands: proteolytic cleavage, exosome secretion and functional implications.** *Scand J Immunol* 2013, **78:**120-129.
59. Patel S, Chiplunkar S: **Host immune responses to cervical cancer.** *CurrOpinObstetGynecol* 2009, **21:**54-59.

60. Stanley M: **Immune responses to human papillomavirus.** *Vaccine* 2006, **24 Suppl 1:**S16-S22.
61. Kanodia S, Fahey LM, Kast WM: **Mechanisms used by human papillomaviruses to escape the host immune response.** *CurrCancer Drug Targets* 2007, **7:**79-89.
62. Zhang B, Li P, Wang E, Brahmi Z, Dunn KW, Blum JS, Roman A: **The E5 protein of human papillomavirus type 16 perturbs MHC class II antigen maturation in human foreskin keratinocytes treated with interferon-gamma.** *Virology* 2003, **310:**100-108.
63. Fausch SC, Da Silva DM, Rudolf MP, Kast WM: **Human papillomavirus virus-like particles do not activate Langerhans cells: a possible immune escape mechanism used by human papillomaviruses.** *JImmunol* 2002, **169:**3242-3249.
64. Drijkoningen M, De Wolf-Peeters C, Degreef H, Desmet V: **Epidermal Langerhans cells, dermal dendritic cells, and keratinocytes in viral lesions of skin and mucous membranes: an immunohistochemical study.** *Arch Dermatol Res* 1988, **280:**220-227.
65. Da Silva DM, Velders MP, Nieland JD, Schiller JT, Nickoloff BJ, Kast WM: **Physical interaction of human papillomavirus virus-like particles with immune cells.** *IntImmunol* 2001, **13:**633-641.
66. zur Hausen H: **Papillomaviruses and cancer: from basic studies to clinical application.** *NatRevCancer* 2002, **2:**342-350.
67. Kirnbauer R, Booy F, Cheng N, Lowy DR, Schiller JT: **Papillomavirus L1 major capsid protein self-assembles into virus-like particles that are highly immunogenic.** *ProcNatlAcadSciUSA* 1992, **89:**12180-12184.
68. Bishop B, Dasgupta J, Chen XS: **Structure-based engineering of papillomavirus major capsid l1: controlling particle assembly.** *VirolJ* 2007, **4:**3.
69. Caspar DL, Klug A: **Physical principles in the construction of regular viruses.** *Cold Spring HarbSympQuantBiol* 1962, **27:**1-24.
70. Rudolf MP, Fausch SC, Da Silva DM, Kast WM: **Human dendritic cells are activated by chimeric human papillomavirus type-16 virus-like particles and induce epitope-specific human T cell responses in vitro.** *JImmunol* 2001, **166:**5917-5924.
71. Liu WJ, Liu XS, Zhao KN, Leggatt GR, Frazer IH: **Papillomavirus virus-like particles for the delivery of multiple cytotoxic T cell epitopes.** *Virology* 2000, **273:**374-382.
72. Ionescu RM, Przysiecki CT, Liang X, Garsky VM, Fan J, Wang B, Troutman R, Rippeon Y, Flanagan E, Shiver J, Shi L: **Pharmaceutical and immunological evaluation of human papillomavirus viruslike particle as an antigen carrier.** *JPharmSci* 2006, **95:**70-79.
73. Chackerian B, Lowy DR, Schiller JT: **Induction of autoantibodies to mouse CCR5 with recombinant papillomavirus particles.** *ProcNatlAcadSciUSA* 1999, **96:**2373-2378.
74. Chackerian B, Lowy DR, Schiller JT: **Conjugation of a self-antigen to papillomavirus-like particles allows for efficient induction of protective autoantibodies.** *JClinInvest* 2001, **108:**415-423.
75. Thones N, Herreiner A, Schadlich L, Piuko K, Muller M: **A direct comparison of human papillomavirus type 16 L1 particles reveals a lower immunogenicity of capsomeres than viruslike particles with respect to the induced antibody response.** *JVirol* 2008, **82:**5472-5485.
76. Schadlich L, Senger T, Gerlach B, Mucke N, Klein C, Bravo IG, Muller M, Gissmann L: **Analysis of modified human papillomavirus type 16 L1 capsomeres: the ability to assemble into larger particles correlates with higher immunogenicity.** *JVirol* 2009, **83:**7690-7705.
77. Garcia F, Petry KU, Muderspach L, Gold MA, Braly P, Crum CP, Magill M, Silverman M, Urban RG, Hedley ML, Beach KJ: **ZYC101a for treatment of high-grade cervical intraepithelial neoplasia: a randomized controlled trial.** *Obstet Gynecol* 2004, **103:**317-326.

78. Rose RC, White WI, Li M, Suzich JA, Lane C, Garcea RL: **Human papillomavirus type 11 recombinant L1 capsomeres induce virus-neutralizing antibodies.** *JVirol* 1998, **72:**6151-6154.
79. Fligge C, Giroglou T, Streeck RE, Sapp M: **Induction of type-specific neutralizing antibodies by capsomeres of human papillomavirus type 33.** *Virology* 2001, **283:**353-357.
80. Kreider JW, Bartlett GL: **The Shope papilloma-carcinoma complex of rabbits: a model system of neoplastic progression and spontaneous regression.** *AdvCancer Res* 1981, **35:**81-110.
81. Suzich JA, Ghim SJ, Palmer-Hill FJ, White WI, Tamura JK, Bell JA, Newsome JA, Jenson AB, Schlegel R: **Systemic immunization with papillomavirus L1 protein completely prevents the development of viral mucosal papillomas.** *ProcNatlAcadSciUSA* 1995, **92:**11553-11557.
82. Stanley MA: **Human papillomavirus vaccines.** *RevMedVirol* 2006, **16:**139-149.
83. Kawana K, Yasugi T, Taketani Y: **Human papillomavirus vaccines: current issues & future.** *Indian JMedRes* 2009, **130:**341-347.
84. Keam SJ, Harper DM: **Human papillomavirus types 16 and 18 vaccine (recombinant, AS04 adjuvanted, adsorbed) [Cervarix].** *Drugs* 2008, **68:**359-372.
85. Frederick PJ, Huh WK: **Evaluation of the interim analysis from the PATRICIA study group: efficacy of a vaccine against HPV 16 and 18.** *ExpertRevAnticancer Ther* 2008, **8:**701-705.
86. Harper DM, Franco EL, Wheeler C, Ferris DG, Jenkins D, Schuind A, Zahaf T, Innis B, Naud P, De Carvalho NS, et al: **Efficacy of a bivalent L1 virus-like particle vaccine in prevention of infection with human papillomavirus types 16 and 18 in young women: a randomised controlled trial.** *Lancet* 2004, **364:**1757-1765.
87. Villa LL, Costa RL, Petta CA, Andrade RP, Ault KA, Giuliano AR, Wheeler CM, Koutsky LA, Malm C, Lehtinen M, et al: **Prophylactic quadrivalent human papillomavirus (types 6, 11, 16, and 18) L1 virus-like particle vaccine in young women: a randomised double-blind placebo-controlled multicentre phase II efficacy trial.** *Lancet Oncol* 2005, **6:**271-278.
88. Lenz P, Thompson CD, Day PM, Bacot SM, Lowy DR, Schiller JT: **Interaction of papillomavirus virus-like particles with human myeloid antigen-presenting cells.** *ClinImmunol* 2003, **106:**231-237.
89. Fausch SC, Da Silva DM, Kast WM: **Differential uptake and cross-presentation of human papillomavirus virus-like particles by dendritic cells and Langerhans cells.** *Cancer Res* 2003, **63:**3478-3482.
90. Da Silva DM, Fausch SC, Verbeek JS, Kast WM: **Uptake of human papillomavirus virus-like particles by dendritic cells is mediated by Fcgamma receptors and contributes to acquisition of T cell immunity.** *JImmunol* 2007, **178:**7587-7597.
91. Wang Z, Christensen N, Schiller JT, Dillner J: **A monoclonal antibody against intact human papillomavirus type 16 capsids blocks the serological reactivity of most human sera.** *JGenVirol* 1997, **78 (Pt 9):**2209-2215.
92. Frazer IH: **Measuring serum antibody to human papillomavirus following infection or vaccination.** *GynecolOncol* 2010, **118:**S8-11.
93. Hung CF, Monie A, Alvarez RD, Wu TC: **DNA vaccines for cervical cancer: from bench to bedside.** *ExpMolMed* 2007, **39:**679-689.
94. Kanodia S, Da Silva DM, Kast WM: **Recent advances in strategies for immunotherapy of human papillomavirus-induced lesions.** *IntJCancer* 2008, **122:**247-259.
95. Greenstone HL, Nieland JD, de Visser KE, De Bruijn ML, Kirnbauer R, Roden RB, Lowy DR, Kast WM, Schiller JT: **Chimeric papillomavirus virus-like particles elicit antitumor immunity against the E7 oncoprotein in an HPV16 tumor model.** *ProcNatlAcadSciUSA* 1998, **95:**1800-1805.
96. Su JH, Wu A, Scotney E, Ma B, Monie A, Hung CF, Wu TC: **Immunotherapy for cervical cancer: Research status and clinical potential.** *BioDrugs* 2010, **24:**109-129.

97. Albers AE, Kaufmann AM: **Therapeutic human papillomavirus vaccination.** *Public Health Genomics* 2009, **12:**331-342.
98. Kenter GG, Welters MJ, Valentijn AR, Lowik MJ, Berends-van der Meer DM, Vloon AP, Essahsah F, Fathers LM, Offringa R, Drijfhout JW, et al: **Vaccination against HPV-16 oncoproteins for vulvar intraepithelial neoplasia.** *N Engl J Med* 2009, **361:**1838-1847.
99. Varsani A, Williamson AL, de Villiers D, Becker I, Christensen ND, Rybicki EP: **Chimeric human papillomavirus type 16 (HPV-16) L1 particles presenting the common neutralizing epitope for the L2 minor capsid protein of HPV-6 and HPV-16.** *J Virol* 2003, **77:**8386-8393.
100. Daayana S, Elkord E, Winters U, Pawlita M, Roden R, Stern PL, Kitchener HC: **Phase II trial of imiquimod and HPV therapeutic vaccination in patients with vulval intraepithelial neoplasia.** *Br J Cancer* 2010, **102:**1129-1136.
101. Novagene: **iFOLD® Protein Refolding System 1.** In *User Protocol*, vol. TB457. pp. 7: EMD Chemicals Inc; 2009:7.
102. Radulovic S, Brankovic-Magic M, Malisic E, Jankovic R, Dobricic J, Plesinac-Karapandzic V, Maciag PC, Rothman J: **Therapeutic cancer vaccines in cervical cancer: phase I study of Lovaxin-C.** *J BUON* 2009, **14 Suppl 1:**S165-168.
103. Magalhaes PO, Lopes AM, Mazzola PG, Rangel-Yagui C, Penna TC, Pessoa A, Jr.: **Methods of endotoxin removal from biological preparations: a review.** *J Pharm Pharm Sci* 2007, **10:**388-404.
104. invitrogen: **XCell II™ Blot Module - User Manual.** vol. IM9051, MAN0000740 edition; 2009.
105. Jochmus I, Schafer K, Faath S, Muller M, Gissmann L: **Chimeric virus-like particles of the human papillomavirus type 16 (HPV 16) as a prophylactic and therapeutic vaccine.** *ArchMedRes* 1999, **30:**269-274.
106. Kalof AN, Cooper K: **p16INK4a immunoexpression: surrogate marker of high-risk HPV and high-grade cervical intraepithelial neoplasia.** *AdvAnatPathol* 2006, **13:**190-194.
107. Mulvany NJ, Allen DG, Wilson SM: **Diagnostic utility of p16INK4a: a reappraisal of its use in cervical biopsies.** *Pathology* 2008, **40:**335-344.
108. Tsoumpou I, Arbyn M, Kyrgiou M, Wentzensen N, Koliopoulos G, Martin-Hirsch P, Malamou-Mitsi V, Paraskevaidis E: **p16(INK4a) immunostaining in cytological and histological specimens from the uterine cervix: a systematic review and meta-analysis.** *Cancer TreatRev* 2009, **35:**210-220.
109. Yildiz IZ, Usubutun A, Firat P, Ayhan A, Kucukali T: **Efficiency of immunohistochemical p16 expression and HPV typing in cervical squamous intraepithelial lesion grading and review of the p16 literature.** *PatholResPract* 2007, **203:**445-449.
110. Volgareva GM, Zavalishina LE, Andreeva I, Shtil' AA, Frank GA: **[Cell protein p16INK4a hyperexpression in epithelial malignancies induced by human papillomaviruses].** *ArkhPatol* 2008, **70:**57-61.
111. Reuschenbach M, Clad A, von Knebel Doeberitz C, Wentzensen N, Rahmsdorf J, Schaffrath F, Griesser H, Freudenberg N, von Knebel Doeberitz M: **Performance of p16INK4a-cytology, HPV mRNA, and HPV DNA testing to identify high grade cervical dysplasia in women with abnormal screening results.** *Gynecol Oncol* 2010, **119:**98-105.
112. Serrano M, Hannon GJ, Beach D: **A new regulatory motif in cell-cycle control causing specific inhibition of cyclin D/CDK4.** *Nature* 1993, **366:**704-707.
113. Kamb A, Gruis NA, Weaver-Feldhaus J, Liu Q, Harshman K, Tavtigian SV, Stockert E, Day RS, 3rd, Johnson BE, Skolnick MH: **A cell cycle regulator potentially involved in genesis of many tumor types.** *Science* 1994, **264:**436-440.
114. Guan KL, Jenkins CW, Li Y, Nichols MA, Wu X, O'Keefe CL, Matera AG, Xiong Y: **Growth suppression by p18, a p16INK4/MTS1- and p14INK4B/MTS2-related CDK6 inhibitor, correlates with wild-type pRb function.** *Genes Dev* 1994, **8:**2939-2952.

115. Chan FK, Zhang J, Cheng L, Shapiro DN, Winoto A: **Identification of human and mouse p19, a novel CDK4 and CDK6 inhibitor with homology to p16ink4.** *Mol Cell Biol* 1995, **15:**2682-2688.
116. Hirai H, Roussel MF, Kato JY, Ashmun RA, Sherr CJ: **Novel INK4 proteins, p19 and p18, are specific inhibitors of the cyclin D-dependent kinases CDK4 and CDK6.** *Mol Cell Biol* 1995, **15:**2672-2681.
117. Cho NH, Kim YT, Kim JW: **Alteration of cell cycle in cervical tumor associated with human papillomavirus: cyclin-dependent kinase inhibitors.** *Yonsei MedJ* 2002, **43:**722-728.
118. Serrano M: **The tumor suppressor protein p16INK4a.** *ExpCell Res* 1997, **237:**7-13.
119. Madej T, Addess KJ, Fong JH, Geer LY, Geer RC, Lanczycki CJ, Liu C, Lu S, Marchler-Bauer A, Panchenko AR, et al: **MMDB: 3D structures and macromolecular interactions.** *Nucleic Acids Res* 2012, **40:**D461-464.
120. Cuschieri K, Wentzensen N: **Human papillomavirus mRNA and p16 detection as biomarkers for the improved diagnosis of cervical neoplasia.** *Cancer EpidemiolBiomarkers Prev* 2008, **17:**2536-2545.
121. McLaughlin-Drubin ME, Park D, Munger K: **Tumor suppressor p16INK4A is necessary for survival of cervical carcinoma cell lines.** *Proc Natl Acad Sci U S A* 2013, **110:**16175-16180.
122. Munger K, Phelps WC: **The human papillomavirus E7 protein as a transforming and transactivating factor.** *BiochimBiophysActa* 1993, **1155:**111-123.
123. Reuschenbach M, Waterboer T, Wallin KL, Einenkel J, Dillner J, Hamsikova E, Eschenbach D, Zimmer H, Heilig B, Kopitz J, et al: **Characterization of humoral immune responses against p16, p53, HPV16 E6 and HPV16 E7 in patients with HPV-associated cancers.** *IntJCancer* 2008, **123:**2626-2631.
124. Reuschenbach M, von Knebel DM: **p16INK4a peptide vaccination trials.** 2010.
125. VicOryx S486: **Phase I/IIa Study of Immunization With a p16INK4a Peptide Combined With MONTANIDE ISA-51 VG in Patients With Advanced HPV-associated Cancers. EUDRACT2011-000948-18.** 2011.
126. Yu L, Wang L, Zhong J, Chen S: **Diagnostic value of p16INK4A, Ki-67, and human papillomavirus L1 capsid protein immunochemical staining on cell blocks from residual liquid-based gynecologic cytology specimens.** *Cancer Cytopathol* 2010, **118:**47-55.
127. Huang MZ, Li HB, Nie XM, Wu XY, Jiang XM: **An analysis on the combination expression of HPV L1 capsid protein and p16(INK4a) in cervical lesions.** *DiagnCytopathol* 2009.
128. Yoshida T, Sano T, Kanuma T, Owada N, Sakurai S, Fukuda T, Nakajima T: **Immunochemical analysis of HPV L1 capsid protein and p16 protein in liquid-based cytology samples from uterine cervical lesions.** *Cancer* 2008, **114:**83-88.
129. Murata Y, Lightfoote PM, Rose RC, Walsh EE: **Antigenic presentation of heterologous epitopes engineered into the outer surface-exposed helix 4 loop region of human papillomavirus L1 capsomeres.** *VirolJ* 2009, **6:**81.
130. Schadlich L, Senger T, Kirschning CJ, Muller M, Gissmann L: **Refining HPV 16 L1 purification from E. coli: reducing endotoxin contaminations and their impact on immunogenicity.** *Vaccine* 2009, **27:**1511-1522.
131. Ljunggren HG, Ohlen C, Hoglund P, Franksson L, Karre K: **The RMA-S lymphoma mutant; consequences of a peptide loading defect on immunological recognition and graft rejection.** *Int J Cancer Suppl* 1991, **6:**38-44.
132. Ljunggren HG, Karre K: **Host resistance directed selectively against H-2-deficient lymphoma variants. Analysis of the mechanism.** *J Exp Med* 1985, **162:**1745-1759.
133. Lin KY, Guarnieri FG, Staveley-O'Carroll KF, Levitsky HI, August JT, Pardoll DM, Wu TC: **Treatment of established tumors with a novel vaccine that enhances major histocompatibility class II presentation of tumor antigen.** *Cancer Res* 1996, **56:**21-26.

134. Feltkamp MC, Smits HL, Vierboom MP, Minnaar RP, de Jongh BM, Drijfhout JW, ter Schegget J, Melief CJ, Kast WM: **Vaccination with cytotoxic T lymphocyte epitope-containing peptide protects against a tumor induced by human papillomavirus type 16-transformed cells.** *Eur J Immunol* 1993, **23:**2242-2249.
135. Speidel K, Osen W, Faath S, Hilgert I, Obst R, Braspenning J, Momburg F, Hammerling GJ, Rammensee HG: **Priming of cytotoxic T lymphocytes by five heat-aggregated antigens in vivo: conditions, efficiency, and relation to antibody responses.** *Eur J Immunol* 1997, **27:**2391-2399.
136. Gey GO, Bang FB, Gey MK: **Responses of a variety of normal and malignant cells to continuous cultivation, and some practical applications of these responses to problems in the biology of disease.** *Ann N Y Acad Sci* 1954, **58:**976-999.
137. Ohlschlager P, Osen W, Dell K, Faath S, Garcea RL, Jochmus I, Muller M, Pawlita M, Schafer K, Sehr P, et al: **Human papillomavirus type 16 L1 capsomeres induce L1-specific cytotoxic T lymphocytes and tumor regression in C57BL/6 mice.** *JVirol* 2003, **77:**4635-4645.
138. Rammensee HG, Bachmann J, Emmerich NPN, Bachor OA, Stevanović S: **SYFPEITHI: database for MHC ligands and peptide motifs.** *Immunogenetics* 1999, **50:**213-219.
139. Vaccarella S, Lortet-Tieulent J, Plummer M, Franceschi S, Bray F: **Worldwide trends in cervical cancer incidence: Impact of screening against changes in disease risk factors.** *European Journal of Cancer* 2013, **49:**3262-3273.
140. Harper DM: **Currently approved prophylactic HPV vaccines.** *Expert Review of Vaccines* 2009, **8:**1663-1679.
141. Aida Y, Pabst MJ: **Removal of endotoxin from protein solutions by phase separation using Triton X-114.** *J Immunol Methods* 1990, **132:**191-195.
142. Garland SM, Skinner SR, Brotherton JM: **Adolescent and young adult HPV vaccination in Australia: achievements and challenges.** *Prev Med* 2011, **53 Suppl 1:**S29-35.
143. Schiller JT, Castellsagué X, Villa LL, Hildesheim A: **An update of prophylactic human papillomavirus L1 virus-like particle vaccine clinical trial results.** *Vaccine* 2008, **26, Supplement 10:**K53-K61.
144. Schädlich L: **Development of prophylactic and therapeutic second generation vaccines against the human papillomavirus type 16.** University of Heidelberg, 2009.
145. Oganesyan N, Ankoudinova I, Kim SH, Kim R: **Effect of osmotic stress and heat shock in recombinant protein overexpression and crystallization.** *Protein Expr Purif* 2007, **52:**280-285.
146. Amersham Pharmacia Biotech: **Protein Purification Handbook.** 2001.
147. Petsch D, Anspach FB: **Endotoxin removal from protein solutions.** *J Biotechnol* 2000, **76:**97-119.
148. Waheed MT, Thones N, Muller M, Hassan SW, Razavi NM, Lossl E, Kaul HP, Lossl AG: **Transplastomic expression of a modified human papillomavirus L1 protein leading to the assembly of capsomeres in tobacco: a step towards cost-effective second-generation vaccines.** *Transgenic Res* 2011, **20:**271-282.
149. Yuan H, Estes PA, Chen Y, Newsome J, Olcese VA, Garcea RL, Schlegel R: **Immunization with a pentameric L1 fusion protein protects against papillomavirus infection.** *J Virol* 2001, **75:**7848-7853.
150. McCarthy MP, White WI, Palmer-Hill F, Koenig S, Suzich JA: **Quantitative disassembly and reassembly of human papillomavirus type 11 viruslike particles in vitro.** *J Virol* 1998, **72:**32-41.
151. Kling M, Zeichner JA: **The role of the human papillomavirus (HPV) vaccine in developing countries.** *IntJDermatol* 2010, **49:**377-379.
152. Maciag PC, Radulovic S, Rothman J: **The first clinical use of a live-attenuated Listeria monocytogenes vaccine: a Phase I safety study of Lm-LLO-E7 in patients with advanced carcinoma of the cervix.** *Vaccine* 2009, **27:**3975-3983.

153. de Vos van Steenwijk PJ, Ramwadhdoebe TH, Lowik MJ, van der Minne CE, Berends-van der Meer DM, Fathers LM, Valentijn AR, Oostendorp J, Fleuren GJ, Hellebrekers BW, et al: **A placebo-controlled randomized HPV16 synthetic long-peptide vaccination study in women with high-grade cervical squamous intraepithelial lesions.** *Cancer Immunol Immunother* 2012, **61:**1485-1492.
154. Zhang W, Carmichael J, Ferguson J, Inglis S, Ashrafian H, Stanley M: **Expression of human papillomavirus type 16 L1 protein in Escherichia coli: denaturation, renaturation, and self-assembly of virus-like particles in vitro.** *Virology* 1998, **243:**423-431.
155. Thones N, Herreiner A, Schadlich L, Piuko K, Muller M: **A direct comparison of human papillomavirus type 16 L1 particles reveals a lower immunogenicity of capsomeres than viruslike particles with respect to the induced antibody response.** *J Virol* 2008, **82:**5472-5485.
156. Lai WB, Middelberg AP: **The production of human papillomavirus type 16 L1 vaccine product from Escherichia coli inclusion bodies.** *Bioprocess Biosyst Eng* 2002, **25:**121-128.
157. Bian T, Wang Y, Lu Z, Ye Z, Zhao L, Ren J, Zhang H, Ruan L, Tian H: **Human papillomavirus type 16 L1E7 chimeric capsomeres have prophylactic and therapeutic efficacy against papillomavirus in mice.** *Mol Cancer Ther* 2008, **7:**1329-1335.
158. Khan RH, Rao KB, Eshwari AN, Totey SM, Panda AK: **Solubilization of recombinant ovine growth hormone with retention of native-like secondary structure and its refolding from the inclusion bodies of Escherichia coli.** *Biotechnol Prog* 1998, **14:**722-728.
159. Kim MJ, Park HS, Seo KH, Yang HJ, Kim SK, Choi JH: **Complete solubilization and purification of recombinant human growth hormone produced in Escherichia coli.** *PLoS One* 2013, **8:**e56168.
160. Govind CK, Gahlay GK, Choudhury S, Gupta SK: **Purified and refolded recombinant bonnet monkey (Macaca radiata) zona pellucida glycoprotein-B expressed in Escherichia coli binds to spermatozoa.** *Biol Reprod* 2001, **64:**1147-1152.
161. Panda AK: **Bioprocessing of therapeutic proteins from the inclusion bodies of Escherichia coli.** *Adv Biochem Eng Biotechnol* 2003, **85:**43-93.
162. Mukhopadhyay A: **Inclusion bodies and purification of proteins in biologically active forms.** *Adv Biochem Eng Biotechnol* 1997, **56:**61-109.
163. Jaganaman S, Pinto A, Tarasev M, Ballou DP: **High levels of expression of the iron-sulfur proteins phthalate dioxygenase and phthalate dioxygenase reductase in Escherichia coli.** *Protein Expr Purif* 2007, **52:**273-279.
164. Esposito D, Chatterjee DK: **Enhancement of soluble protein expression through the use of fusion tags.** *Curr Opin Biotechnol* 2006, **17:**353-358.
165. Fernando GJ, Murray B, Zhou J, Frazer IH: **Expression, purification and immunological characterization of the transforming protein E7, from cervical cancer-associated human papillomavirus type 16.** *Clin Exp Immunol* 1999, **115:**397-403.
166. Stanley M, Gissmann L, Nardelli-Haefliger D: **Immunobiology of human papillomavirus infection and vaccination - implications for second generation vaccines.** *Vaccine* 2008, **26 Suppl 10:**K62-K67.
167. Li M, Cripe TP, Estes PA, Lyon MK, Rose RC, Garcea RL: **Expression of the human papillomavirus type 11 L1 capsid protein in Escherichia coli: characterization of protein domains involved in DNA binding and capsid assembly.** *J Virol* 1997, **71:**2988-2995.
168. Muller M, Zhou J, Reed TD, Rittmuller C, Burger A, Gabelsberger J, Braspenning J, Gissmann L: **Chimeric papillomavirus-like particles.** *Virology* 1997, **234:**93-111.
169. Rizk RZ, Christensen ND, Michael KM, Muller M, Sehr P, Waterboer T, Pawlita M: **Reactivity pattern of 92 monoclonal antibodies with 15 human papillomavirus types.** *J Gen Virol* 2008, **89:**117-129.

170. Rietschel ET, Schade U, Jensen M, Wollenweber HW, Luderitz O, Greisman SG: **Bacterial endotoxins: chemical structure, biological activity and role in septicaemia.** *Scand J Infect Dis Suppl* 1982, **31:**8-21.
171. Opal SM: **Endotoxins and other sepsis triggers.** *Contrib Nephrol* 2010, **167:**14-24.
172. Beutler B, Rietschel ET: **Innate immune sensing and its roots: the story of endotoxin.** *Nat Rev Immunol* 2003, **3:**169-176.
173. US Food and Drug Administration: **Guideline for Validation of Limulus Amebocyte Lysate Test as an End-Product Endotoxin Test for Human and Animal Parenteral Drugs, Biological Products, and Medical Devices.** (US Department of Health and Human Services ed.; 1998.
174. Schafer K, Muller M, Faath S, Henn A, Osen W, Zentgraf H, Benner A, Gissmann L, Jochmus I: **Immune response to human papillomavirus 16 L1E7 chimeric virus-like particles: induction of cytotoxic T cells and specific tumor protection.** *IntJCancer* 1999, **81:**881-888.
175. Chen W, McCluskey J: **Immunodominance and immunodomination: critical factors in developing effective CD8+ T-cell-based cancer vaccines.** *Adv Cancer Res* 2006, **95:**203-247.
176. Palena C, Schlom J: **Vaccines against human carcinomas: strategies to improve antitumor immune responses.** *J Biomed Biotechnol* 2010, **2010:**380697.
177. Corradin GdG, G: **Novel Adjuvants for Vaccines.** *Curr Med Chem – Anti-Inflammatory & Anti-Allergy Agents* 2005, **4**.
178. Tefit JN, Serra V: **Outlining novel cellular adjuvant products for therapeutic vaccines against cancer.** *Expert Rev Vaccines* 2011, **10:**1207-1220.
179. Aucouturier J, Dupuis L, Ganne V: **Adjuvants designed for veterinary and human vaccines.** *Vaccine* 2001, **19:**2666-2672.
180. Bijker MS, van den Eeden SJ, Franken KL, Melief CJ, Offringa R, van der Burg SH: **CD8+ CTL priming by exact peptide epitopes in incomplete Freund's adjuvant induces a vanishing CTL response, whereas long peptides induce sustained CTL reactivity.** *J Immunol* 2007, **179:**5033-5040.
181. Capron A, Capron M, Dombrowicz D, Riveau G: **Vaccine strategies against schistosomiasis: from concepts to clinical trials.** *Int Arch Allergy Immunol* 2001, **124:**9-15.
182. Capron A, Riveau G, Capron M, Trottein F: **Schistosomes: the road from host-parasite interactions to vaccines in clinical trials.** *Trends Parasitol* 2005, **21:**143-149.
183. Siddiqui AA, Siddiqui BA, Ganley-Leal L: **Schistosomiasis vaccines.** *Hum Vaccin* 2011, **7:**1192-1197.
184. McManus DP, Loukas A: **Current status of vaccines for schistosomiasis.** *Clin Microbiol Rev* 2008, **21:**225-242.
185. Da Silva DM, Pastrana DV, Schiller JT, Kast WM: **Effect of preexisting neutralizing antibodies on the anti-tumor immune response induced by chimeric human papillomavirus virus-like particle vaccines.** *Virology* 2001, **290:**350-360.
186. Da Silva DM, Schiller JT, Kast WM: **Heterologous boosting increases immunogenicity of chimeric papillomavirus virus-like particle vaccines.** *Vaccine* 2003, **21:**3219-3227.
187. Ikuerowo SO, Kuczyk MA, von WR, Shittu OB, Jonas U, Machtens S, Serth J: **p16INK4a expression and clinicopathologic parameters in renal cell carcinoma.** *EurUrol* 2007, **51:**732-737.
188. Jarrard DF, Modder J, Fadden P, Fu V, Sebree L, Heisey D, Schwarze SR, Friedl A: **Alterations in the p16/pRb cell cycle checkpoint occur commonly in primary and metastatic human prostate cancer.** *Cancer Lett* 2002, **185:**191-199.
189. Milde-Langosch K, Riethdorf S: **Role of cell-cycle regulatory proteins in gynecological cancer.** *J Cell Physiol* 2003, **196:**224-244.

190. Herschkowitz JI, He X, Fan C, Perou CM: **The functional loss of the retinoblastoma tumour suppressor is a common event in basal-like and luminal B breast carcinomas.** *Breast Cancer Res* 2008, **10:**R75.
191. Kommoss S, du Bois A, Ridder R, Trunk MJ, Schmidt D, Pfisterer J, Kommoss F: **Independent prognostic significance of cell cycle regulator proteins p16(INK4a) and pRb in advanced-stage ovarian carcinoma including optimally debulked patients: a translational research subprotocol of a randomised study of the Arbeitsgemeinschaft Gynaekologische Onkologie Ovarian Cancer Study Group.** *Br J Cancer* 2007, **96:**306-313.
192. Andujar P, Wang J, Descatha A, Galateau-Salle F, Abd-Alsamad I, Billon-Galland MA, Blons H, Clin B, Danel C, Housset B, et al: **p16INK4A inactivation mechanisms in non-small-cell lung cancer patients occupationally exposed to asbestos.** *Lung Cancer* 2010, **67:**23-30.
193. Romagosa C, Simonetti S, Lopez-Vicente L, Mazo A, Lleonart ME, Castellvi J, Ramon y Cajal S: **p16(Ink4a) overexpression in cancer: a tumor suppressor gene associated with senescence and high-grade tumors.** *Oncogene* 2011, **30:**2087-2097.
194. Burd Christin E, Sorrentino Jessica A, Clark Kelly S, Darr David B, Krishnamurthy J, Deal Allison M, Bardeesy N, Castrillon Diego H, Beach David H, Sharpless Norman E: **Monitoring Tumorigenesis and Senescence In Vivo with a p16INK4a-Luciferase Model.** *Cell* 2013, **152:**340-351.
195. Bueter M, Gasser M, Lebedeva T, Benichou G, Waaga-Gasser AM: **Influence of p53 on anti-tumor immunity (review).** *Int J Oncol* 2006, **28:**519-525.
196. Moudgil KD, Sercarz EE: **The self-directed T cell repertoire: its creation and activation.** *Rev Immunogenet* 2000, **2:**26-37.
197. Li X, Wang Y, Zhao Y, Yang H, Tong A, Zhao C, Shi H, Li Y, Wang Z, Wei Y: **Immunotherapy of tumor with vaccine based on basic fibroblast growth factor-activated fibroblasts.** *J Cancer Res Clin Oncol* 2014, **140:**271-280.
198. Keijzer C, van der Zee R, van Eden W, Broere F: **Treg inducing adjuvants for therapeutic vaccination against chronic inflammatory diseases.** *Front Immunol* 2013, **4:**245.
199. Wigren M, Nilsson J, Kolbus D: **Lymphocytes in atherosclerosis.** *Clin Chim Acta* 2012, **413:**1562-1568.
200. Fedoseyeva EV, Boisgerault F, Anosova NG, Wollish WS, Arlotta P, Jensen PE, Ono SJ, Benichou G: **CD4+ T cell responses to self- and mutated p53 determinants during tumorigenesis in mice.** *J Immunol* 2000, **164:**5641-5651.
201. Petersen TR, Buus S, Brunak S, Nissen MH, Sherman LA, Claesson MH: **Identification and design of p53-derived HLA-A2-binding peptides with increased CTL immunogenicity.** *Scand J Immunol* 2001, **53:**357-364.
202. Zwaveling S, Vierboom MP, Ferreira Mota SC, Hendriks JA, Ooms ME, Sutmuller RP, Franken KL, Nijman HW, Ossendorp F, Van Der Burg SH, et al: **Antitumor efficacy of wild-type p53-specific CD4(+) T-helper cells.** *Cancer Res* 2002, **62:**6187-6193.
203. Stanley MA: **Progress in prophylactic and therapeutic vaccines for human papillomavirus infection.** *ExpertRevVaccines* 2003, **2:**381-389.
204. Paz De la RG, Monroy-Garcia A, Mora-Garcia ML, Pena CG, Hernandez-Montes J, Weiss-Steider B, Gomez-Lim MA: **An HPV 16 L1-based chimeric human papilloma virus-like particles containing a string of epitopes produced in plants is able to elicit humoral and cytotoxic T-cell activity in mice.** *VirolJ* 2009, **6:**2.
205. Slupetzky K, Shafti-Keramat S, Lenz P, Brandt S, Grassauer A, Sara M, Kirnbauer R: **Chimeric papillomavirus-like particles expressing a foreign epitope on capsid surface loops.** *JGenVirol* 2001, **82:**2799-2804.
206. Fausch SC, Da Silva DM, Kast WM: **Heterologous papillomavirus virus-like particles and human papillomavirus virus-like particle immune complexes activate human Langerhans cells.** *Vaccine* 2005, **23:**1720-1729.

207. Klamp T, Schumacher J, Huber G, Kuhne C, Meissner U, Selmi A, Hiller T, Kreiter S, Markl J, Tureci O, Sahin U: **Highly specific auto-antibodies against claudin-18 isoform 2 induced by a chimeric HBcAg virus-like particle vaccine kill tumor cells and inhibit the growth of lung metastases.** *Cancer Res* 2011, **71:**516-527.
208. Xie M, Li S, Shen W, Li Z, Zhuang Y, Mo X, Gu Y, Wu T, Zhang J, Xia N: **[Expression, purification and immunogenicity analysis of HPV type 18 virus-like particles from Escherichia coli].** *Sheng Wu GongCheng XueBao* 2009, **25:**1082-1087.
209. Melief CJ, Van Der Burg SH, Toes RE, Ossendorp F, Offringa R: **Effective therapeutic anticancer vaccines based on precision guiding of cytolytic T lymphocytes.** *Immunol Rev* 2002, **188:**177-182.
210. **A therapeutic HPV vaccine candidate: ProCervix** [http://www.genticel.com/products/procervix/]
211. Garcia-Hernandez E, Gonzalez-Sanchez JL, Andrade-Manzano A, Contreras ML, Padilla S, Guzman CC, Jimenez R, Reyes L, Morosoli G, Verde ML, Rosales R: **Regression of papilloma high-grade lesions (CIN 2 and CIN 3) is stimulated by therapeutic vaccination with MVA E2 recombinant vaccine.** *Cancer Gene Ther* 2006, **13:**592-597.

VI. Abbreviations

aa	amino acid
AC	affinity chromatography
Amp	ampicillin
APC	antigen-presenting cell
aqua bidest.	bidestilled water
AU	absorption units
bp	base pairs
BPV	bovine papillomavirus
BSA	bovine serum albumin
CDK	cyclin dependent kinase
cDNA	complementary DNA
CIN	cervical intraepithelial neoplasia
ConA	concavalin A
COPV	canine oral papillomavirus
CRPV	cotton-tail rabbit papillomavirus
CTL	cytotoxic T lymphocytes
CV	column volumes
CVLP	chimeric virus like particle
DC	dendritic cell
DMSO	Dimethylsulfoxide
DNA	deoxyribonucleic acid
dNTP	deoxynucleotide triphosphate
DTT	Dithiothreitol
E. coli	Escherichia Coli
ECL	enhanced chemiluminescence
EDTA	ethylenediaminetetraacetic acid
ELISA	enzyme-linked immuno sorbent assay
ELISpot	enzyme-linked immunosorbent spot assay
EM	electron microscopy
EtBr	ethidium bromide
EV	epidermodysplasia verruciformis
FBS	fetal bovine serum
Ger	Germany
GST	glutathione S-transferase

GuHCl	guanidine hydrochloride
HNSCC	head and neck squamous cell carcinoma
HPV	human papillomavirus
HRP	horse raddish peroxidase
IB	inclusion bodies
IEX	ion exchange chromatography
IFNγ	interferon gamma
IPTG	Isopropyl β-D-1-thiogalactopyranoside
Kan	kanamycin
LB	Luria-Bertani broth or lysogeny broth
LC	Langerhans cell
LCR	long control region
LPS	lipopolysaccharides
MDM	murine double minute
MHC	major histocompatibility complex
MPL	monophosphoryl lipid A
MWCO	molecular weight cut-off
NK cell	natural killer cell
NMSC	nonmelanoma skin cancer
OD	optical density
ORF	open reading frame
PAGE	Polyacrylamid gel electrophoresis
Pap test	Papanicolau test
PBS	phosphate-buffered saline
PCR	polymerase chain reaction
Rb	retinoblastoma
RNA	ribonucleic acid
Ros	E. coli Rosetta
rpm	rounds per minute
RT	room temperature
SCC	squamous cell carcinoma
SDS	sodium sodecyl sulfate
SDS-PAGE	denaturing SDS polyacrylamide gel electrophoresis
SEC	size exclusion chromatography
SIL	squamous intraepithelial lesion
SV40	simian virus type 40
Taq	thermophilus aquaticus

TB	terrific broth
TBE	Tris-Borate-Edta Buffer
TBS	Tris-buffered saline
TEM	transmission electron microscopy
TLR	toll-like receptor
TMB	3,3',5,5' tetramethylbenzidine
TNF	tumor necrosis factor
Tris	Tris (hydroxymethyl) aminomethane
tRNA	transfer ribonucleic acid
US	United States
VLP	virus like particle
w/v	weight per volume
x-gal	5-bromo-4-chloro-3-indolyl b-galactoside

Short notations for chimeric proteins consisting of the modified L1 and $p16^{INK4a}$:

#1	L1ΔN10Δh4ΔC29-$p16^{INK4a}$	L1-$p16^{INK4a}$	L1p16
#2	$p16^{INK4a}$ -L1ΔN10Δh4ΔC29	$p16^{INK4a}$-L1	p16L1
#3	L1ΔN10Δh4-$p16^{INK4a}$-ΔC29	L1-$p16^{INK4a}$-L1	L1p16L1

VII. Appendix

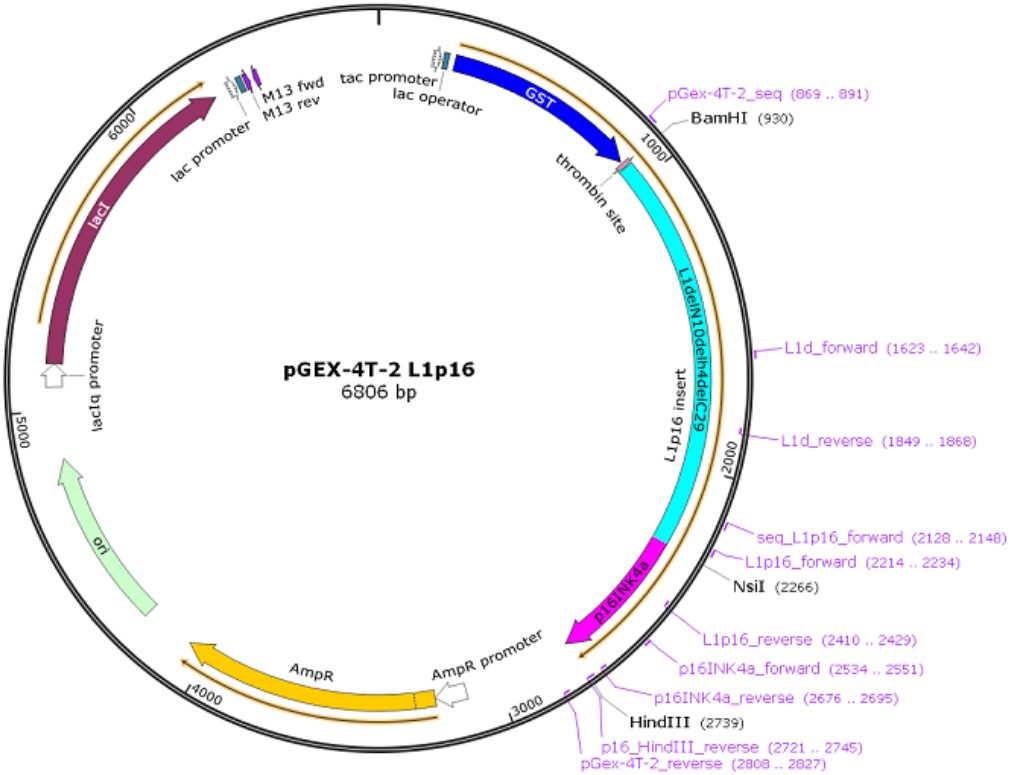

Figure 63: Plasmid map pGex-L1ΔN10Δh4ΔC29-p16^{INK4a} with restriction sites BamHI, NsiI and HindIII. Primers and their binding positions within the plasmid are indicated in pink. Translated ORFs are marked with a yellow arrow (genproducts: AmpR → β-lactamase; lacI → lac repressor; GST-L1p16 insert → GST-L1-p16^{INK4a} chimeric protein, 92.4 kDa); Created with SnapGene.

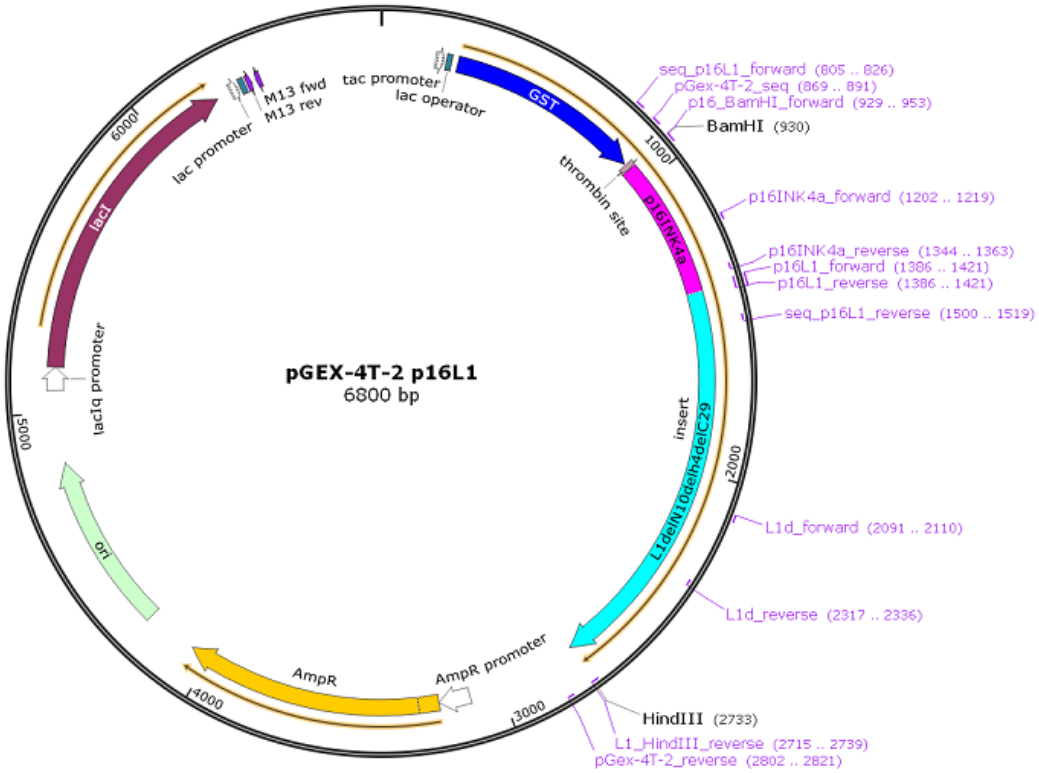

Figure 64: Plasmid map pGex-p16^{INK4a}-L1ΔN10Δh4ΔC29 with restriction sites BamHI and HindIII. Primers and their binding positions within the plasmid are indicated in pink. Translated ORFs are marked with a yellow arrow (genproducts: AmpR → β-lactamase; lacI → lac repressor; GST-p16L1 insert → GST-p16^{INK4a}-L1 chimeric protein, 92.1 kDa); Created with SnapGene.

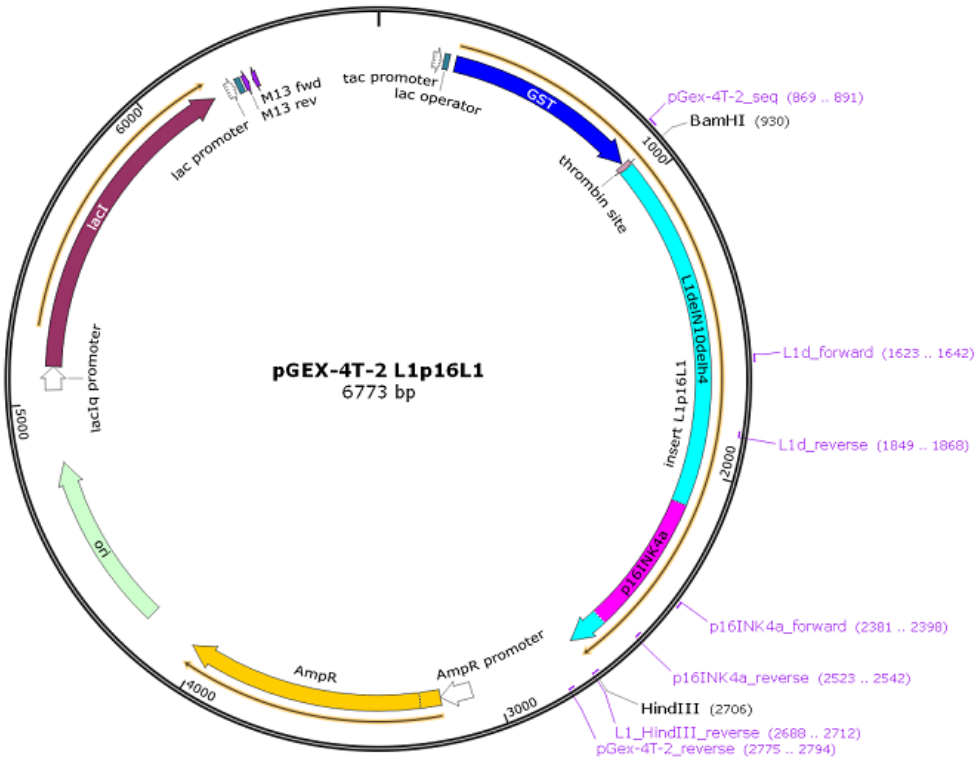

Figure 65: Plasmid map pGex-L1ΔN10Δh4-p16^{INK4a}-L1ΔC29 with restriction sites BamHI and HindIII. Primers and their binding positions within the plasmid are indicated in pink. Translated ORFs are marked with a yellow arrow (genproducts: AmpR → β-lactamase; lacI → lac repressor; GST-L1p16L1 insert → GST-L1-p16^{INK4a}-L1 chimeric protein, 91.2 kDa); Created with SnapGene.

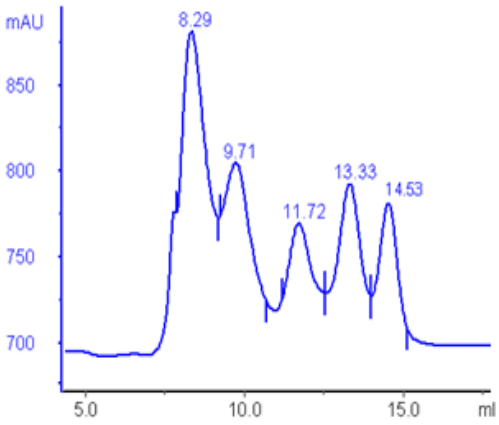

Peak name / marker protein	Retention (ml)	MW (kDA)
Blue Dextran (void volume)	7.0	> 2000
Thyroglobulin	8.29	669
Ferritin	9.71	440
Aldolase	11.72	158
Conalbumin	13.33	75
Ovalbumin	14.53	43

Figure 66: Calibration of the Superdex200® gel filtration column using the high molecular weight calibration kit (GE Healthcare). 100 µl of the marker proteins (0.3 - 5 mg/ml) were loaded on the column and eluted in buffer L_{mod} (5.4.2). The proteins were detected by measuring the absorbance at 280 nm during elution. The void volume of the column (> 850 kDa) was determined using Blue Dextran.

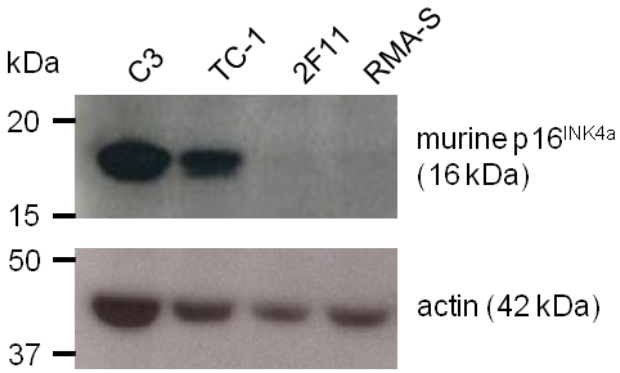

Figure 67: Murine $p16^{INK4a}$ expression in different mouse cell lines. The anti-p16 western blot (F-4) of Ripa cell lysates reveals similar $p16^{INK4a}$ expression levels in C3 and TC-1 cells whereby no expression could be detected in 2F11 and RMA-S cells.